FLUXES OF SOIL ORGANIC CARBON FROM ERODING PERMAFROST COASTS, CANADIAN BEAUFORT SEA

NICOLE J. COUTURE

Department of Geography, McGill University, Montreal
January 2010

A thesis submitted to McGill University in partial fulfillment of the requirements of the degree of Doctor of Philosophy

© Nicole J. Couture 2010

The Earth is strong. You learn this. Not that you ever suspected it wasn't. You just get the opportunity to get blown around and swayed more, working with it.

- Rick Bass, *Oil Notes*

ABSTRACT

Resolving uncertainties about the cycling of organic carbon in the world's oceans is particularly crucial in the Arctic because it is the locus of deep water formation, as well as rapid environmental change. The specific goal of this thesis was to quantify the flux of soil organic carbon (SOC) to the Arctic Ocean due to erosion along the Yukon Coastal Plain. Ground ice and SOC within coastal sediments, and the current and future fluxes of carbon were examined in detail.

An evaluation of the volume of ground ice showed it to be a significant constituent of coastal bluffs. The amount of it was related to surficial material and geomorphic history, being lowest in coarse-grained marine deposits and highest in lacustrine materials. It made up almost half the soil volume in formerly glaciated areas where bluffs are high, but only one third the volume in unglaciated portions with low bluffs.

Overlooking ground ice resulted in overestimates of SOC and mineral sediment of up to 20%. Corrections were especially important in the upper ice-rich soil layers. Organic carbon contents were related to surficial material and bluff height, and 57% of carbon was located at depths greater than 1 m. SOC fluxes were up to three times higher than previously thought, but comparable to other parts of the Arctic. Eleven per cent of the carbon eroded annually was buried in nearshore sediments, and the carbon in those sediments was overwhelmingly terrigenous.

A morphodynamic model of coastal evolution was used to evaluate future coastal retreat. Low bluffs will retreat more rapidly than higher ones. Ground ice controls the amount of sediment in coastal bluffs and therefore the retreat rates, since bluffs with high ice contents have a lower effective cliff height. SOC fluxes from low coastal bluffs will increase by 29%, but will be offset by a 13% decrease from high bluffs. Regions of low cliffs could become sources of carbon flux to the atmosphere.

By providing insight into the origins and fate of organic matter in a sensitive section of the Arctic coastal system, this study offers valuable input for both current and future studies of regional carbon dynamics.

RÉSUMÉ

LES FLUX DE CARBONE ORGANIQUE DU SOL PROVENANT DE L'ÉROSION DES CÔTES PERGÉLISOLÉES, MER DE BEAUFORT CANADIEN

Le cycle du carbone organique dans les océans est d'une importance primordiale, spécialement dans l'Arctique puisqu'ils sont le lieu de formation des eaux abyssales et subissent des changements environnementaux rapides. L'objectif de cette thèse est de quantifier le flux de carbone organique du sol (COS), provoqué par l'érosion, entre la plaine côtière du Yukon et l'Océan arctique. Cette étude examine en détail la teneur en glace et en COS des sédiments côtiers, ainsi que les flux de carbone actuels et projetés.

Une évaluation du volume de la glace de sol révèle qu'elle est une composante importante des falaises côtières. La teneur en glace est liée à la géologie des dépôts de surface et à l'histoire géomorphologique de la région. En effet, cette teneur est plus basse dans les dépôts marins à grain grossier et plus élevée dans les matériaux lacustres. La glace de sol représente presque la moitié du volume du sol dans les zones de hautes falaises antérieurement englacées, mais seulement un tiers du volume dans les régions qui n'ont jamais été englacées et où les falaises sont plus basses.

Le fait de ne pas tenir compte de la glace de sol entraîne des surestimations de la quantité de COS et de sédiment minéral qui atteignent jusqu'à 20%. Les corrections relatives à la glace de sol sont particulièrement importantes, surtout dans les couches riches en glace près de la surface. La teneur en carbone organique dépend de la géologie des dépôts de surface et de la hauteur des falaises. Les résultats montrent que 57% du carbone est situé à des profondeurs supérieures à 1 m. Le flux de carbone organique est trois fois plus élevé que ce qui avait été estimé antérieurement, mais est toutefois comparable aux valeurs calculées pour d'autres régions de l'Arctique. Onze pourcent de la matière organique érodée annuellement est enfouie dans les sédiments marins littoraux et le carbone retrouvé dans ceux-ci est d'origine principalement terrigène.

L`érosion côtière future a été évaluée à l'aide d'un modèle d`évolution côtière morphodynamique. Le modèle démontre que les falaises basses reculeront plus rapidement que celles qui sont plus

hautes. Puisque les falaises qui possèdent une teneur en glace de sol élevée ont une hauteur effective moindre, cette glace de sol a un impact sur le montant de sédiment et sur le taux de recul des falaises. Le flux de COS des falaises basses augmentera de 29%, mais sera atténué par une baisse de 13% dans le flux de COS des falaises hautes. Les régions où les falaises sont basses pourraient devenir des sources de dioxyde de carbone pour l'atmosphère.

Cette recherche apporte une contribution importante aux études actuelles et futures de la dynamique régionale du carbone; elle offre de nouvelles perspectives sur les origines et le sort de la matière organique dans une région sensible du système côtier arctique.

TABLE OF CONTENTS

PAGE

APPENDICES

LIST OF TABLES

PAGE

LIST OF FIGURES

PAGE

ACKNOWLEDGEMENTS

I am deeply indebted to my thesis supervisor, Wayne Pollard, for his steadfast guidance, thoughtful advice and continued support throughout the research and writing of this thesis. It is doubtful that I would have undertaken this project without his initial prodding. Along the way, he has provided numerous opportunities that have helped me to develop as a scholar, and I am very grateful. He pushed me forward and allowed me to recognize what I was capable of accomplishing, and his unwavering belief in me helped me to believe in myself when I needed it.

I would also like to thank my committee members from the McGill Geography Department – Profs. Michel Lapointe, Jonathan Seaquist, and George Wenzel – as well as Prof. Michel Allard of Laval University, all of whom provided useful comments and suggestions, and helped me to frame my research. My work was further advanced by fruitful and interesting discussions with Steve Solomon and Don Forbes of the Geological Survey of Canada, Hugues Lantuit, Paul Overduin and Volker Rachold of the Alfred Wegener Institute for Polar and Marine Research, Md. Azharul Hoque, and the members of the Arctic Coastal Dynamics Project. Thanks also to Hugues Lantuit, Michael Fritz, Lutz Schirrmeister, and Md. Azharul Hoque for kindly allowing me to use their data. Derek Mueller provided helpful advice about R programming.

Financial support was provided by the Fonds québécois de la recherche sur la nature et les technologies (FQRNT), the ArcticNet Network of Centres of Excellence of Canada, and the Eben Hobson Fellowship in Arctic Studies. Prof. Pollard also supplied generous assistance in the form of research assistantships and NSERC funds for research expenses. Fieldwork would not have been possible without support from the Polar Continental Shelf Project and the Northern Scientific Training Program. I received graduate student stipends and a networking grant from McGill University's Global Environmental and Climate Change Centre (GEC3), as well as young scientist travel grants from the International Arctic Science Committee.

I appreciate the help and assistance I received from all the staff and faculty of the McGill Geography Department. An especially big thanks to Paula Kestleman who always helped me get whatever was needed, and to Maria Marcone who always answered my questions, and then reanswered my questions. Prof. Gail Chmura allowed me access to her laboratory and equipment. I'm grateful to my fellow Geography students who shared the fun and the agony of a doctoral degree, especially Hugues, Tim, and Dolly… what would I have done without you?

I am grateful to the Potsdam Research Unit of the Alfred Wegener Institute for Polar and Marine Research (AWI) for hosting me as a visiting scientist and paying my expenses during my stay. AWI also graciously allowed me access to their laboratories and analytical resources, and I am grateful for technical assistance from Ute Bastian, Hanno Meyer, and Antje Eulenburg. A special "Danke schön!" to all the other staff and students who made my visits to Potsdam so enjoyable.

Fieldwork was a large part of this project and would not have been possible without able assistance from Hugues Lantuit, Tim Haltigin, Greg De Pascale, and Casey Johnson of the McGill Geography Department; Gavin Manson of the Geological Survey of Canada; Lutz Schirrmeister and Hanno Meyer of the Alfred Wegener Institute for Polar and Marine Research, Eli Nasogaluak of Inuvik, and Jordan MacLeod of Aklavik. The expertise and experience of Danny C. Gordon, Dennis Arey, and Lawrence Rogers were invaluable. I'd like to thank the staff of the Aurora Research Institute, the Polar Continental Shelf Project, Canadian Helicopters, Aklak Air, and Parks Canada (Western Unit) for logistical support. I'm especially appreciative of the support and friendship provided by Richard Gordon and the park rangers of Herschel Island (Qikiqtaruk) Territorial Park.

Finally, I'd like to thank my mother and the rest of my family for their love and support. I could not have done it without you.

CONTRIBUTIONS OF AUTHORS

Manuscript 1 **"Quantifying ground ice volumes in permafrost along the Yukon Coastal Plain"** by Nicole Couture and Wayne Pollard. As my thesis supervisor, Wayne Pollard contributed intellectually and financially to the research for this and subsequent manuscripts and is a co-author on all of them. He provided help in developing the conceptual model for this first manuscript, and read and provided editorial comments on the text. I developed the model scenarios and equations, gathered the input data, performed the analyses, and wrote the manuscript.

Manuscript 2 **"Organic carbon in soils of the Yukon Coastal Plain and fluxes to the Beaufort Sea"** by Nicole Couture and Wayne Pollard. I designed the field program, gathered the data, performed the laboratory work, analyzed the data, and wrote the manuscript. Prof. Pollard helped in constructing the framework and several of the ideas presented in the research, and gave valuable feedback on the manuscript.

Manuscript 3 **"Predicting future fluxes of organic carbon from the Yukon Coastal Plain to the Beaufort Sea"** by Nicole Couture, Wayne Pollard and Md. Azharul Hoque.
Dr. Hoque (Manitoba Water Stewardship, Winnipeg) proposed the use of the Leont'yev model and supplied data on the nearshore wave climate. Prof. Pollard provided intellectual guidance and constructive comments on the manuscript. I performed all analysis and wrote the text.

CHAPTER 1
THESIS INTRODUCTION AND OBJECTIVES

1.1 Thesis structure

This thesis is comprised of three manuscripts (Chapters Three through Five) that will be submitted for publication in peer-reviewed journals. Each of the manuscripts is focussed on a specific theme, but together, they address a larger set of objectives which are presented in the introductory chapter (Chapter One). The manuscripts are preceded by a section that explains their context within the thesis. The concluding chapter (Chapter Six) summarizes the research project's findings. Tables and figures for each manuscript are grouped at the end of the corresponding chapter, following formatting standards for scientific journals. A complete list of all references cited is included at the end of the thesis.

1.2 Introduction

Despite the fact that carbon (C) is a primary building block of life, our understanding of its cycling through the Earth's systems is incomplete. The need for a better grasp of the dynamics of carbon is underscored by the role of carbon dioxide (CO_2) as a greenhouse gas and the influence that changes in atmospheric CO_2 levels have on global climate.

Unlike most other gases, carbon dioxide is highly soluble and, as a result, the vast majority of CO_2 is found in the ocean. Although the world's largest store of carbon is locked up in the lithosphere, the oceans are the largest near-surface pool of carbon, containing approximately 38,000 petagrams (10^{15} grams), which is over 50 times as much as the atmosphere (Schlesinger, 1997). The oceanic uptake of atmospheric carbon dioxide, however, is a function of the partial pressures of CO_2 in the air and in the sea, so an increase in anthropogenic emissions of CO_2 to the atmosphere will affect this uptake, as will any changes to the carbon balance of the ocean. It has been estimated that about 27% of the CO_2 added to the atmosphere by humans has been absorbed by the oceans (Prentice et al., 2001) which are in essence buffering greenhouse warming. The oceans' continued capacity to mitigate the atmospheric buildup of carbon dioxide is not clear, though, because there are still uncertainties in our understanding of global carbon cycling.

The carbon balance of high latitude oceans, in particular, is of special importance for a number of reasons. Firstly, carbon dioxide is more soluble in cold water so a greater proportion of the drawdown of CO_2 from the atmosphere occurs in colder regions (Marinov and Sarmiento, 2004). Secondly, there is a strong seasonality in biological activity in surface waters so transformations of carbon from inorganic (such as dissolved CO_2) to organic forms are different from those in more temperate waters (Sakshaug, 2004). Thirdly, this colder water sinks to form the deep water portion of the thermohaline circulation and because of its long residence time, much of the carbon it contains can be isolated from the global cycle for as long as a thousand years (Chester, 2000). Fourthly, the effects of climate change will be more dramatic and more rapidly felt in the polar areas, with significant alterations to carbon cycling and resulting feedbacks to the climate system (Friedlingstein et al., 2001; Chen et al., 2003). And finally, sources, sinks and transformations of carbon between inorganic and organic forms are relatively well quantified for more temperate oceans, but are much less well delineated for the Arctic Ocean (Stein and MacDonald, 2004c). Although recent studies are helping to refine the organic carbon cycle in the Arctic Ocean (Jorgenson and Brown, 2005, Grigoriev and Rachold, 2003), questions still remain particularly with regard to coastal vs. riverine C fluxes, regional differences in the proportion of organic carbon supplied from each of the various sources (Rachold et al., 2000), and how they might be affected by environmental changes.

Climate warming is predicted to be greatest in the polar regions and evidence of change there has already been well documented (Serreze et al., 2000; Hinzman et al., 2005). Although many environmental systems in the Arctic are affected by climate warming, Arctic coastal regions may experience disproportionally large transformations since they are at the interface of the land, the ocean and the atmosphere and are impinged on from three different fronts. For instance, warmer air and sea temperatures will increase sensitivity to erosion, as will expected rises in sea level and the thermal expansion of the oceans (Shaw et al., 1998). Storms have been shown to be highly correlated with coastal erosion in some regions (Solomon et al.,1994) and an increase in their frequency is predicted (Lambert, 1995), as well as an increase in the open water period during which they exert the strongest influence on coastal retreat (McGillvray et al., 1993). For these reasons, it is expected that changing environmental forcings in the Arctic will intensify coastal erosion and therefore increase the amount of soil organic carbon being input into the Arctic Ocean from coastal sources.

The exact extent of the current flux and future changes is highly dependent on the composition and properties of the coastal permafrost and its ground ice content. These factors govern not only the amount of carbon contained within the sediments, but also the susceptibility of the coast to erosion and how likely it is to be affected by a changing environment. This is the result not only of structural differences due to phase change, but also how mechanical properties such as shear strength and cohesion are dependent on the amount of ground ice within the permafrost (Williams and Smith, 1989). Ice within soil is very close to its melting point, so small changes in temperature can result in very different responses to coastal processes.

This work is a contribution to the Arctic Coastal Dynamics (ACD) project. ACD is a circum-Arctic study that seeks to develop not only a better understanding of the processes at work in Arctic coastal regions, but also how material fluxes are affected. The present study will help answer many of these questions for the Yukon Coastal Plain region along the Canadian Beaufort Sea.

1.3 On the location of research and study sites

The Yukon Coastal Plain was chosen as a region for study because little data is available on organic carbon flux, yet much of its carbon stores are vulnerable to erosion, The Beaufort Sea is one of seven regional water bodies that, together with a central deep basin, constitute the Arctic Ocean. Along the Canadian Beaufort Sea, sediment fluxes are largely controlled by discharge from the Mackenzie River (Hill et al., 1991; Macdonald et al., 1998), the fourth largest in the Arctic. As a result, little focus has been placed on the contribution of organic carbon from coastal erosion in the region and therefore uncertainties about the flux of carbon still remain. Nevertheless, it has been shown that in some regions a significant amount of sediment can be supplied by coastal degradation (Rachold et al., 2000; Reimnitz et al., 1988), and Are (1988) has documented that even where rivers supply more sediment than coasts, the flux of carbon from coasts can exceed that of rivers.

The Yukon Coastal Plain, is located along the Beaufort Sea west of the Mackenzie Delta (Figure 1.1). It is a lowland of dissected and hilly tundra about 300 km long and 10-30 km wide, and straddles the Wisconsinan glacial limit. Most of the flat or gently sloping landscape is covered by organic deposits, and peat beds are common, particularly in lacustrine basins (Rampton, 1982). These landscape types have been shown to constitute significant stores of soil organic carbon (Bockheim et al., 2004; Ping et al., 2008). This region is classified as having a low arctic climate, with a mean annual temperature of –11°C and mean annual precipitation between 200 and 300 mm. It is in the continuous permafrost zone, so permafrost is present everywhere except for beneath large lakes and rivers. This part of the Canadian Arctic is one of the most ice-rich areas of the country and, volumetrically, ground ice can constitute up to 70% of the upper portion of permafrost (French et al., 1986). Two factors considered to be important in the formation of ground ice are aggradation of permafrost into coastal sediments during marine regression, and proximity to the margin of continental ice sheets (Mackay, 1971; 1989; Mackay and Dallimore, 1992; Rampton 1974, 1991). Both of these help to explain the high ground ice content of the Yukon Coastal Plain. Beaches along the coast are generally narrow and are backed by coastal bluffs up to 90 m high, many of them comprised of unconsolidated and easily erodible sediments. In addition to the climatic changes that are expected to affect erosion rates, the Yukon Coastal Plain is considered to be in a submergent area (Forbes, 1980), with current rates of relative sea level rise for the region estimated to be approximately 3.5mm/a (Manson et al., 2002). These increases in sea level will contribute to the region's sensitivity to erosion (Shaw et al., 1998).

Offshore, the continental shelf slopes gently to the shelf break located at about 80 m water depth (Hill et al., 1991). Although the shelf is over 150 km wide at the front of the Mackenzie River, it narrows to about 40 km along the coastal plain and is bisected by the Mackenzie Trough, a deep submarine canyon that is located less than 10 km from the coast in certain sections and which is a site with strong upwelling of nutrient-rich waters (Carmack and Kulikov, 1998; Carmack and

Macdonald, 2002). Carbon which is released by erosion can be either buried on the shelf, remineralized in the water column, or transported to the deep ocean. The proximity of the shelf break to the Yukon coast therefore has a strong influence on the fate of the SOC and what role it plays in the carbon cycle.

It is the combination of these factors – the paucity of data, the high ground ice and soil organic carbon contents of the sediments, the sensitivity to erosion of those sediments, and the narrowness of the continental shelf – that make the Yukon Coastal Plain a region warranting investigation.

1.4 Thesis objectives

The specific goal of this thesis is to narrow the uncertainties related to carbon flux to the Arctic Ocean by quantifying the amount of organic carbon being added to the Canadian Beaufort Sea from erosion along the Yukon Coastal Plain. The amount of ground ice and soil organic carbon (SOC) within coastal sediments and the current and future fluxes of this carbon are examined in detail. The Yukon coast is especially sensitive to climatic change and, as such, the central hypothesis of the research is that the flux of terrigenous organic carbon from this region will increase in the coming decades as a result of escalating permafrost degradation and shoreline erosion.

1.5 Summary of subsequent chapters

Chapter Two reviews permafrost and ground ice conditions along the Yukon Coastal Plain, the distribution of soil organic carbon in Arctic sediments (both onshore and offshore), previous work on coastal erosion rates, and expected climatic changes in the Arctic with an emphasis on environmental controls that govern or influence coastal erosion.

Chapter Three quantifies the volume of ground ice in permafrost along the Yukon coast. This is done by developing a morphological model that evaluates the proportions of different types of ground ice in the various geologic and geomorphic terrain units along the coast. Determining the amount of ground ice is a necessary first step for the research developed in subsequent chapters because it governs the relative volume of sediment and organic carbon in the soils, influences the ground thermal response to changing climatic conditions, and dictates how susceptible these coastal terrain units are to erosion.

Chapter Four assesses how much soil organic carbon is found in different terrain units and how much of it is currently being eroded into the Beaufort Sea. The flux of soil organic carbon depends not just on the carbon content of eroding coastal sediments, but also on the rates at which erosion occurs. Spatial variations in erosion rates arising from differences in environmental variables such as shore morphology and materials, wave energy, and exposure to wave attack are explored. Conclusions are drawn about the fate of the eroded carbon based on isotopic analyses of coastal and nearshore marine sediments. The significance of the current C flux in relation to regional and circum-Arctic values is also considered.

Chapter Five examines how changes in environmental forcings will influence future wave climate and erosion rates. Based on these data, the resulting SOC fluxes to the Beaufort Sea are projected. Conclusions are drawn about how these fluxes will impact the global carbon cycle and about their possible role in climatic feedbacks.

Chapter Six provides a summary of the overall thesis and revisits how each manuscript was able to address the original thesis objectives.

Figure 1.1 Location map of the study area showing several of the sites mentioned in the text, as well as the limits of glaciation (Smith et al., 1989 p. 6; adapted from Rampton, 1982 and Dyke & Prest, 1987).

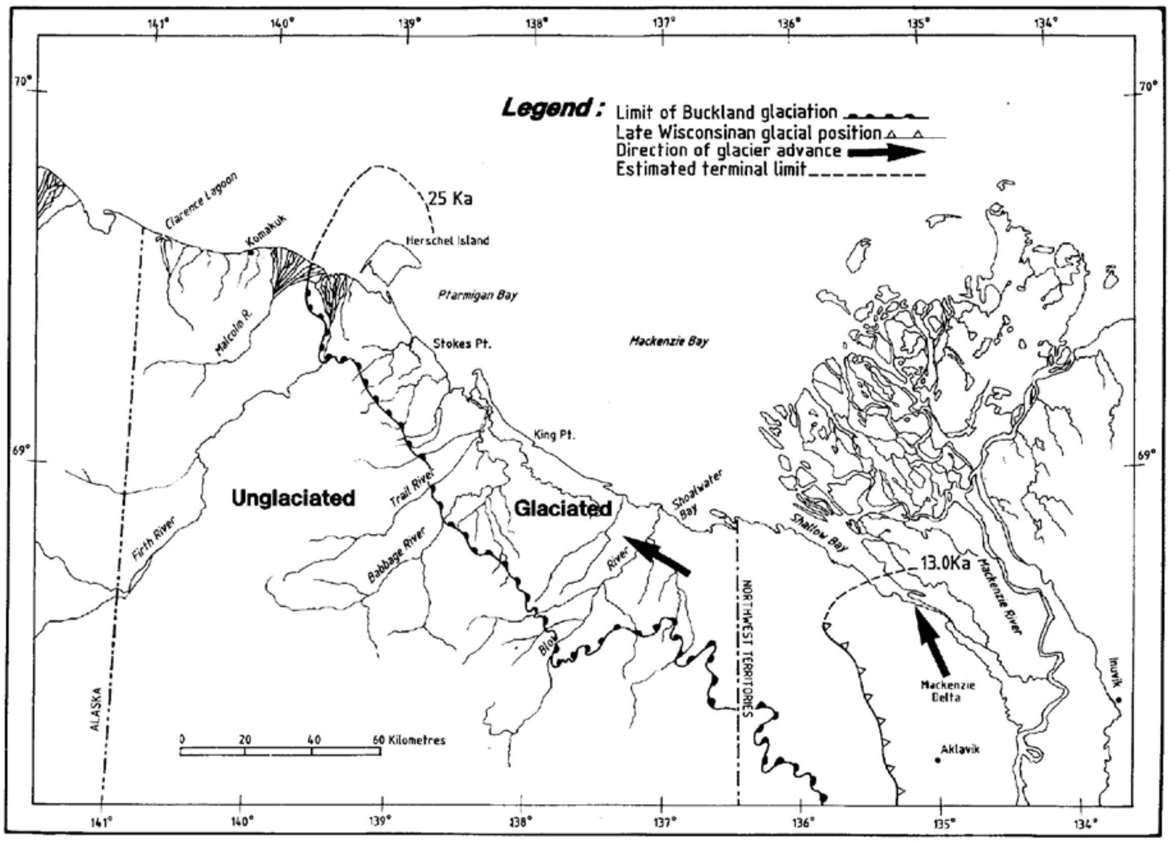

CHAPTER 2
BACKGROUND

2.1 Introduction

One of the goals of this chapter is to provide an overview of some of the major constituents of permafrost. Emphasis is placed on ground ice and soil organic carbon, in light of their importance in an erosional environment. The factors influencing Arctic coastal dynamics and the important controls on erosion are also examined in order to provide a context for understanding how they may change in the future.

2.2 Permafrost and ground ice

Permafrost is ground that remains at or below 0°C for at least two consecutive years (International Permafrost Association, 1998). It is overlain at the ground surface by a layer that thaws and freezes seasonally, known as the active layer. Active layer thickness is variable both spatially and temporally, depending on such factors as temperature, snow cover, vegetation, parent material, aspect, and soil moisture. It can range from 10-20 cm in areas of the high Arctic to well over 1 m in the sub-Arctic. Permafrost itself may be dry, consisting only of soil or rock, but this is rare (Bockheim and Tarnocai, 1998a), and some form of ice is usually present. The more common forms of ground ice include those which are part of the soil structure itself such as pore ice, or thin lenses of segregated ice that form when water migrates to the freezing front. However, ground ice can also occur as large discrete bodies such as pingos, ice wedges, or beds of massive ice (Figure 2.1).

Pingos are ice-cored domes which are initiated when water under pressure freezes and uplifts overlying sediments (Mackay, 1985). Ice wedges are one of the more visible geomorphic features associated with permafrost and are widespread in areas of continuous permafrost. They form when surface meltwater trickles into thermal contraction cracks in the ground and freezes to form an ice veinlet. Over the years, the cracks occur at the same place and the veinlets build up to form an ice wedge (Dostovalov and Popov, 1966; Leffingwell, 1915; Lachenbruch, 1962). The size of ice wedges is related to the age of the wedge and the availability of water. In regions of Siberia, ice wedges can grow to several tens of metres wide (French, 1996; Romanovskii, 1985). North American ice wedges are generally smaller, usually 1.5 - 2 m wide and approximately 4.5 - 6 m high (Brown, 1968; Mackay, 1974; Harry et al., 1985; Péwé, 1963), although most data comes from wedges in formerly glaciated areas, and there is little information about wedge morphologies outside the glacial limit. Ice wedges tend to be roughly triangular in shape, although changes in environmental conditions can result in a different geometry (Mackay, 1988; 1990). Seasonal thawing at the top of an ice wedge often results in a trough running along its length and, in plan view, these troughs form a network of polygons on the tundra. Massive ice takes the form of large tabular bodies having an ice content greater than 250% on an ice-to-dry-soil weight basis (van Everdingen, 1998). They form when pressurized water is intruded or injected into existing sediments, or as a result of ice segregation, particularly when there is an abundant water supply at the freezing front. Commonly several metres thick, massive ice beds can be up to 30 m thick and can extend for hundreds of metres (Harry et al., 1985; 1988; Pollard and Dallimore, 1988; Pollard, 1990; Rampton, 1982; Mackay, 1972; de Krom 1990). Until bodies of massive ice are exposed, detecting them can be problematic. However, most occurrences do tend to be within or near the glacial limit, and their presence has been shown to be associated with certain geomorphic features such as scars from thaw slumping (Mackay, 1963b; Aylsworth et al., 2000; Wolfe et al., 2001) known as retrogressive thaw slumps, involuted hills (Rampton, 1974), and marine deposits in terrace-like structures (Pollard, 2000). A knowledge of surficial geology can also help in locating bodies of massive segregated ice since Mackay (1973) has shown that such ice is most commonly found at the interface where fine-grained sediments overlie coarse-grained ones. Geophysical techniques such as ground penetrating radar have also been used to delineate massive ice beds (Robinson et al., 1993). Drill logs from seismic and geotechnical investigations provide another source of data about subsurface conditions and the location of ice bodies (Rampton and Mackay, 1971; Pollard and French, 1980; Smith et al., 2005).

Determining the amount and location of ground ice is important because it is the only earth material that is at or near its melting point under natural environmental conditions and, as such, holds tremendous potential for change. A number of previous North American studies have focussed on making regional determinations of all types of ground ice (Brown, 1968; Brown, 1974; Pollard and French, 1980; French et al., 1986; Couture and Pollard, 1998). Several studies have provided general descriptions of ground ice contents along the Yukon Coastal Plain (Rampton, 1974; 1982; Harper, 1990; Harper et al., 1985), and a number of others have provided detailed assessments of ground ice volumes for specific sites (Dallimore et al., 1996; O'Connor and Associates, 1986; Harry et al., 1985; 1988; Pollard, 1990, 1991; Pollard and Dallimore, 1988; de Krom, 1990; McDonald and Lewis, 1973). Most of these focussed on the top 5-10 m of permafrost only. The research presented here enables a detailed survey to be made of ground ice conditions for the entire Yukon Coastal Plain.

2.3 Soil organic carbon in the Arctic

The world's store of soil carbon is approximately twice as large as that of the atmosphere and almost three times that of vegetation (Schlesinger, 1997). Estimates of the global stock of soil organic carbon vary considerably, ranging from ~700 to ~3000 Pg (1 Pg = 10^{15} g), but it was generally considered to be approximately 1500 Pg (Post et al., 1982; Batjes, 1996; Tarnocai et al., 2009 and references therein). The depth of soil considered affects this value, however. Earlier estimates only examined the near-surface, but more recent studies have shown that considerable amounts of carbon are found to depths of 3 m or more (Batjes, 1996; Jobbágy and Jackson, 2000; Schurr et al., 2008; Tarnocai et al., 2009; Zimov et al., 2006), and the total SOC pool is now considered to be approximately 2400 Pg C.

In permafrost soils, organic matter originates primarily from surface litter and root biomass which decompose slowly because of limited biological activity due to cold temperatures (Hobbie et al., 2000; Tarnocai et al., 2007; McGuire et al., 2009). Impeded drainage from a frozen substrate contributes to water-logging and the development of peat in areas of low relief. Much of the SOC occurs close to the surface since the active layer limits rooting depth, but significant amounts of SOC can also be found in the top of permafrost as a result of changes in the active layer thickness over time (Tarnocai et al., 2007; Schuur et al., 2008). In addition, the process of cryoturbation (frost-churning) acts to transfer a considerable amount of organic matter deeper into the soil profile where colder temperatures further enhance preservation (Bockheim, 2007; Bockheim and Tarnocai, 1998b). Organic matter may also be buried in river deltas or loess deposits -- although the latter are limited to unglaciated regions -- with cold temperatures once again contributing to preservation of the SOC (Zimov et al., 2006; Tarnocai et al., 2009).

The tundra climate region was long thought to contain 13.7% of the world`s total SOC (191.8 Pg C), second only to wetlands which contain 14.5% (Post et al., 1982). This estimate, however, was based on a limited number of samples in the tundra region (Ping et al., 2008) and examined only the top of the soil column. Using a larger database of sites, but still looking at the top 1 m, Tarnocai et al. (2003) calculated that cryosols (permafrost-affected soils) contain approximately 16% (268 Pg) of the world's SOC. The total figure is affected not only by the depth considered, but by the actual content of carbon in the soils. More detailed and wider analyses of the carbon contents of tundra soils (to 1 m depth) indicate that the values used in early estimates were under-reported (Michaelson et al., 1996; Bockheim et al., 1998; Bockheim et al., 1999; Bockheim et al., 2003; Bockheim et al., 2004; Ping et al., 2008) and that SOC values in tundra are likely twice as large as originally thought. Recognizing the importance of deeper carbon in permafrost regions, several recent studies have examined SOC contents to greater depths (Zimov et al., 2006; Bockheim and Hinkel, 2007; Schuur et al., 2008; Tarnocai et al, 2009). Current evaluations of the stock of SOC in permafrost regions now place it between 1400 and 1850 Pg C, or more than 50% of the world's pool of soil organic carbon (Schuur et al., 2008, Tarnocai et al., 2009; McGuire et al., 2009). In Canada, cryosols account for 35% of the country's soils and contain 103 Pg C, or almost 40% of the SOC (Tarnocai, 1998; Tarnocai et al., 2007).

At the scale of the pedon or terrain unit, soil organic carbon contents are usually reported as a percentage of soil dry weight (%wt), or as a function of area (kg C/m^2). In the latter case, this effectively equates to a carbon density when the top 1 m of soil is reported (kg C/m^3). The concept of organic carbon density can be a useful comparative tool when different soil volumes (i.e., depths) are considered. There is wide variability of organic carbon contents reported in the literature. In North American permafrost soils, Tarnocai et al. (2003) suggest values of 26-137 kg C/m^2, but caution that it could be twice that value if deeper values are considered. Bockheim et al. (1999) report numbers from 2.5 to 109 kg C/m^2 for various soils near Barrow, Alaska, with several other studies arriving at intermediary values. Average values of SOC density for the top

1 m of soils in Arctic North America are provided in Table 2.1. Most are much higher than the average value for the tundra life-zone of 21.8 kg C/m^2 which was used by Post et al. (1982) in their early assessment of global SOC stores. The amount of SOC present within the permafrost to a depth of 1 m underscores how important transfers of carbon from the active layer can be. Although only a limited amount of data is available for deeper permafrost, Table 2.2 emphasizes that considerable amounts of carbon do exist below 1 m.

Studies of SOC along the Yukon coast are relatively sparse. Rampton (1982) has mapped out organic deposits at the 1:125,000 scale, stating only that they are 0.5 to 3.5 m thick. The Soil Organic Carbon Digital Database of Canada includes values for six representative pedons (although measurements were made at only four of them) with organic carbon contents ranging from 0.9 to 40.7% or 2.9 and 99.2 kg C/m^2 (Tarnocai and Lacelle, 1996). Yunker et al. (1991) reported TOC contents of 22.9 to 29.8% for peat at three sites along the Yukon Coastal Plain. Studies at ten sites on Herschel Island have TOC values between 1.9 and 25% (Kokelj et al., 2002; Smith et al., 1989). Although most of these measurements were limited to the top 1 metre of soil, some do penetrate deeper, with a maximum depth of 1.63 m.

The presence of ground ice reduces the amount of soil and therefore the amount of SOC it contains. Calculations of soil organic carbon density rely on measurements or estimates of the dry bulk density, so the volume taken up by structural ground ice such as pore ice or thin lenses of ice is normally accounted for. Other types of ground ice such as ice wedges can reduce carbon contents considerably. For instance, Bockheim et al. (1999) note that average SOC values declined from 61 kg C/m^3 at sites without ice wedges, to 27 kg C/m^3 at sites where ice wedges were encountered. It is not always clear how ground ice is treated when extrapolating to larger scale estimates of SOC, although most studies appear to rely on broad qualitative estimates of ground ice content (i.e., Brown et al., 2003), which are sometimes varied with depth (Tarnocai and Lacelle, 1996; Jorgensen and Brown, 2005).

2.4 Erosion and material fluxes

Considerable research has focussed on Arctic coastal systems in Canada (Dallimore et al., 1996; Forbes and Frobel, 1985; Forbes and Taylor, 1994; Lewis and Forbes, 1974; Mackay, 1959, 1986; McDonald and Lewis, 1973; Wolfe et al., 1998). Many studies concerning shoreline sensitivity and coastal hazards in the southern Beaufort Sea were undertaken as a result of engineering and regulatory requirements associated with offshore hydrocarbon exploration during the 1970's and 1980's, but more recent work has focused on the threat to heritage sites or community infrastructure (Forbes, 1997; Johnson et al., 2003).

Some of the earliest work on erosion in the Beaufort Sea region was done by Mackay (1963a, 1986) who noted the importance of ground ice in erosional processes. Detailed erosion rates for the entire Yukon coast were first provided by McDonald and Lewis (1973) and Lewis and Forbes (1974). Data on retreat rates were subsequently updated using air photos from the 1950s and 1970s (Harper et al., 1985; Harper, 1990). They found widescale regional retreat, with an average erosion rate of approximately 1 m/year. Maximum retreat at some sites was over 18m. More recent work by Solomon (2005) determined that the average coastal retreat rate for the southern Mackenzie Delta area was 0.6 m/year over the 28-year period between 1972 and 2000. He also noted, however, that the change rates ranged from 15.33 m/year of erosion to 3.84 m/year of accretion, depending on the site. A study by Lantuit and Pollard (2008) examined coastal retreat rates around Herschel Island over a 50-year period. During that time, the total horizontal change in the shoreline varied from a loss of 59 m at one site to a gain of 20 m at one of the few sites where accumulation was occurring. However, almost all sites on the island are erosional. The annual rate of coastal retreat varied over time, but averaged 0.61 m/year during the 1952-1970 period, and 0.45 m/year during the 1970-2000. Despite the widespread occurrence of ground ice in eroding coastal and nearshore sediments, only a few investigations have attempted to calculate the importance of ground ice contribution to sediment budgets and predictions of nearshore settlement in the region (Mackay 1986; Reimnitz and Barnes, 1987; Harry and Dallimore, 1989; Dallimore et al., 1996; Wolfe et al., 1998). Kobayashi et al. (1999) investigated how ground ice affects the thermal-mechanical processes at the base of coastal cliffs.

The first material flux calculations for the Beaufort Sea region were done by Harper and Penland (1982). They used the erosion rates from McDonald and Lewis (1973) and cliff heights estimated from video recordings to evaluate sediment fluxes, which they determined to be 2.9 x 10^6 m^3/year for the entire Canadian Beaufort Sea coast and 1.5 x 10^6 m^3/year for the Yukon coast. Hill et al. (1991) calculated an annual sediment flux of 3.5 x 10^6 m^3 which they converted to 5.6 Mt/year of sediment for the entire Beaufort Sea coast (1Mt = 10^6 tonnes). Of that, 2.5 Mt/year of sediment was being eroded from the Yukon coast. The total annual flux of terrigenous organic carbon to the Arctic Ocean is estimated to be 40.8 Mt/year, with 80% of that being delivered by river discharge (Rachold et al. 2004). The Mackenzie River supplies 2.1 Mt of particulate organic carbon (POC), and about half of that is deposited within the delta, so approximately 1.2 Mt of C per year is delivered to the continental shelf (Macdonald et al, 1998). The first gross estimates of the flux of organic material from coastal erosion to the Beaufort Sea were carried out by Yunker et al. (1990; Yunker et al., 1991). Using erosion rates from previous studies, regional estimates of organic matter coverage by Rampton (1982), and peat samples from three locations along the Yukon coast, they determined that 1298 x 10^3 m^3/year of peat were being eroded from the entire Beaufort coast, which included 85.6 x 10^3 m^3/year from the Yukon coast. MacDonald et al. (1998) determined that this amounted to a flux of organic carbon of approximately 0.06 Mt/year (with an absolute maximum of 0.3 Mt), and this is the value that has been used in all subsequent regional and global C flux studies (Macdonald et al., 2004; Rachold et al., 2000; Rachold et al., 2004; Stein and Macdonald, 2004c). No other assessment of SOC flux for the region has been conducted until now.

2.5 Fate of organic carbon in the ocean

The significance of organic carbon to the ocean carbon cycle depends on how much of it is being mineralized by bacteria in the water column, how much is being buried in sediments, or how much is exported off the continental shelf to the deeper ocean. The fate of carbon often depends on its source. Up to 90% of the marine organic matter produced by photosynthesis is recycled in the water column on short time scales. Most terrestrial organic matter, on the other hand, is derived from vascular plant material which contains refractory biomolecules such as lignin and tannin (Hedges et al., 1997). Since marine organic matter is more labile than terrestrial organic matter, it can more easily and more rapidly be mineralized by bacteria. Estimates show that 25% of riverborne POC (Ittekott, 1988) and 15-30% of dissolved organic carbon (DOC) is readily oxidized (Spitzy and Ittekot, 1991 cited in Smith and Hollibaugh, 1993). The material derived directly from coastal erosion contains a higher proportion of POC than riverine inputs, and is therefore more reactive. Additionally, the cold and often wet conditions under which Arctic soils form serve to limit oxidation, so the organic matter they contain is more available than it would be in soils of more temperature zones (Shaver et al., 1992). Although a terrigenous source might imply that preservation of organic matter in the ocean is more likely, surprisingly there is often very little evidence of a terrestrial origin for the organic matter found in the marine environment (Hedges et al., 1997); this suggests that our understanding of the mineralization processes affecting terrigenous material is incomplete.

The fate of particulate organic matter depends strongly on sediment dynamics in the local riverine and marine environment. Bottom sediments in the coastal zone are more likely than deeper deposits to be affected by dynamic near-surface processes such as the action of waves, tides, or more episodic ones such as storms. Resuspension back into the water column provides an additional opportunity for organic carbon that has been deposited to be mineralized and/or transported to the deep ocean. Some organic matter in the top layers of the sediment may be mineralized after deposition, so even simple turbation of the bottom can enhance the likelihood of degradation of the organic carbon within the sediments (Canfield, 1994). In addition to tides, currents, and storms, resuspension by ice scouring is significant in Arctic settings (Héquette et al., 1995; Hill et al., 1991). Reimnitz et al. (1977) have shown that the entire seafloor of the Alaskan Beaufort Shelf has been reworked by scouring over a 50-year period. Depending on the environment, the timescale for resuspension and reworking can range from daily to decadal.

Material that is permanently buried is not available for transport to the deep ocean or for remineralization and is essentially lost to the system for geological time scales. As much as 70% of POC delivered by rivers can be buried in deltas and estuaries (Blair et al., 2004; Dittmar and Kattner, 2003). MacDonald et al. (1998) figure that 50% is intercepted in the delta of the

Mackenzie River, 40% of it is deposited on the continental shelf, and 10% is transported to the deeper ocean. Berner (1982) reckons that 85% of organic carbon is buried in deltaic and shelf sediments, with 20% of it later being mineralized during diagenesis. He estimates that 126 Mt C per year is therefore permanently sequestered in shelf sediments. The rate of sedimentation has been shown to be a strong determinant of preservation through burial (Blair et al., 2004; Dittmar and Kattner, 2003; Stein, 1991), so sequestration in sediments on geological timescales is more likely in environments with high sediment loads, frequent flooding episodes, or highly seasonal discharge, as in the Arctic (Hill et al., 2001).

The export of organic carbon away from shallow coastal areas is important to global carbon cycling in that there is a much greater likelihood of remineralization as the material sinks down the water column in the open ocean. This transformation at depth increases the chances that the carbon will be sequestered in deep water circulation and isolated from the atmosphere for long periods of time. The transport of material offshelf is effected by often complex circulation patterns, including jets, filaments, various currents, and tides. It can also occur via episodic events such as storms (Héquette et al., 2001; Hill et al., 1991). In the Arctic, sea ice is an important transport agent of particulate matter (Rearic et al., 1990; Belicka et al., 2002; Eicken, 2004). Sea ice takes on even more importance, though, because it stabilizes surface water when it melts and generates brine when it forms (Chen et al., 2003), and this has important implications for offshelf water transport and mixing. The amount of organic carbon that is exported from the shelves to the deeper ocean is not well quantified. Export is generally recognized to happen more readily along narrow rather than wide continental shelves, but it is known to be highly episodic, and estimates vary by an order of magnitude, ranging from 5 to 50% of particles reaching the shelf floor (Ducklow and McCallister, 2004).

One way to help narrow down the fate of organic matter supplied to the ocean is to examine the sources of the carbon in nearshore sediments. Organic geochemical bulk parameters can be used to distinguish between terrigenous (higher plants) and marine (algal) sources of organic carbon in sediments. The source of carbon used for photosynthesis by algae and terrestrial plants varies, and the fractionation of stable carbon isotopes during the photosynthetic process does as well.

As a result, the ratio of stable isotopes (expressed as $\delta^{13}C_{org}$) will be different. The isotope ratio can also be affected by the pathway terrestrial plants used to fixate carbon (C_3 vs. C_4), although Teeri and Stowe (1976) show that most of the plants in the North American Arctic fixate carbon using the C_3 pathway. The $\delta^{13}C_{org}$ values for terrestrial C_3 plants are relatively "light" and are commonly considered to be in the -26 to -28‰ range. Previous studies for the Beaufort Sea have used values of -26.5 to -27‰ (Goñi et al., 2000; Naidu et al., 2000). The δ^{13} of marine organic matter is usually "heavier" than that of C_3 plants, and is generally about -20 to -22‰ (Meyers, 1994 and references therein). At high latitudes, however, it can vary widely for a number of reasons, and values ranging from -16.7 to -30.4‰ have been reported (Stein and MacDonald, 2004b and references therein; Belicka and Harvey, 2002). The C/N ratios of marine organic matter are generally between 4 and 10, whereas those for terrigenous plants are typically much higher (>15) and show a much wider range (Meyers, 1994; 1997; Hedges et al., 1986).

2.6 Environmental forcing of coastal processes

Waves are the result of winds acting on a water surface and transferring energy to the water. As waves approach shore, they begin to interact with the sea bed and they slow down. Successive waves begin to pile up, and the height of the waves increase until they steepen to the point that they break on the shore. The energy they contain is thereby liberated to effect sediment transport and erosion. If a wave approaches the shore at an angle, the portion of the wave closer to shore will slow first, while the deeper portion remains unaffected. As a result, the wave is refracted, or bent, so that the wave crest more closely parallels the shore. In examining the generation of waves, there are three important wind-related aspects to consider: the distance over which the wind blows (i.e., the fetch), the wind speed, and the length of time for which it blows (i.e., the duration).

The Arctic Ocean's seasonal ice cover means that fetch is often limited for a large part of the year and the presence of sea-ice makes the coastal dynamics there distinctive from other parts of the world. In the Canadian Beaufort Sea, coastal areas are ice-covered for eight to nine months of the year, with breakup normally starting in June and freeze-up beginning in October. The amount of open water can reach several hundred kilometres (McGillvray, 1993), but the location of the edge of the pack ice will vary from year to year. The ice edge is often much closer along the western part of the Yukon Coastal Plain, and in some years may remain onshore at Herschel Island and to the west of it. Although sea ice inhibits wave formation, some waves can still form and propagate under limited ice conditions. In their analysis of the variables affecting coastal erosion, Solomon et al. (1994) considered that it was only when the ice coverage was 3/10 or greater that wave formation was limited. Squire (1983, cited in Eid and Cardone, 1992) found that 5/10 ice coverage will damp out waves with a period of less than 10 seconds, so 5/10 coverage can be considered to be the ice edge when discussing fetch lengths. The transition zone between solid ice and completely ice-free water is approximately 55 km (Eid and Cardone, 1992).

Beyond its role in controlling wind fetch and dampening or halting wave action, sea ice also plays a role in coastal dynamics by scouring the sea bottom and by transporting sediments onshore and offshore (Forbes and Taylor, 1994; Ogorodov et al., 2005; Taylor and McCann, 1976). Scouring in shallow water may occur due to ice pile up in the nearshore and may supply significant sediment to beaches and barriers through bulldozing or ice-push events, particularly west of Herschel Island (Harper, 1990; Hequette et al., 1995; Hume and Schalk, 1976; Kovacs, 1983; Mahoney et al., 2004; Short, 1976). Scouring farther offshore appears to drive erosion at the coast by disturbing the equilibrium of the shoreface profile (Héquette and Barnes, 1990; Héquette et al., 1995; Ogorodov, 2003; Reimnitz and Barnes, 1974; Reimnitz et al., 1990). Offshore sediment transport can occur at breakup when sediment incorporated into bottom fast ice is rafted away, or when material slumped from bluffs is deposited on top of drift ice (Macdonald et al., 1998; Reimnitz and Barnes, 1974; Reimnitz et al., 1994).

The meteorological data available for the Beaufort Sea comes from a small number of onshore stations, supplemented by some data from offshore platforms. The oldest records extend back to 1957; although the data has some gaps, most storm studies for the region have pre-processed the data to account for inconsistencies. The origin and general nature of the storm systems in the southern Beaufort Sea over a 40-year period (1957-1995) is documented by Hudak and Young (2002). A comprehensive storm database compiled by Eid and Cardone (1992) provides detailed wind data for offshore storms likely to produce extreme waves. Solomon et al. (1994) developed an index of storm intensity for the southern Beaufort Sea based on data from Tukotyaktuk and demonstrated that shoreline recession at several points along the coast was strongly correlated with storm intensity. General information on the spatial and temporal variability of storminess is provided by Atkinson (2005) in a circum-Arctic study, whereas a more detailed examination of these elements for the southeastern part of the Beaufort Sea is provided by Manson et al. (2005). The definition of a storm is somewhat variable, but generally thresholds of wind speed and duration are used. Several studies defined storms as having windspeeds of at least 10 m/s (~37 km/h) which are sustained for at least 6 hours (Solomon et al., 1994; Atkinson, 2005; Manson et al., 2005; Hudak and Young, 2002). Eid and Cardone (1992) used a slightly different approach, basing their definition on a combination of pressure gradients along the coast and the length of time those gradients lasted. Manson et al. (2005) determined that over a 50-year period, Tuktoyaktuk experienced 262 storms, ranging in number from 2 to 14 per year, with August being the stormiest month. Sachs Harbour, farther to the east, had only 161 storms during that period, with most of them occurring in October. For the entire Beaufort Sea sector, Atkinson (2005) found that over that same period, storm counts increased steadily through the open water season, starting from an average of 3.2 storms in June and reaching a maximum average of 4.5 in October. He notes that these storms are generated by systems moving up from the Pacific Ocean. The amount of open water also influences storm activity in each month because of the thermal gradients established either between the water and the ice, or between the water and land.

The Canadian Beaufort Sea has a very small tidal range with heights of 0.5 m or less. The tidal zone is therefore almost negligible and it is storms which are of particular interest because of their ability to generate large, high energy waves and to increase water levels due to surges. Positive storm surges are increases in the mean water level as a result of strong winds blowing from the sea towards the coast, whereas negative ones are associated with onshore winds. Low air pressure may also increase the water level slightly, but this effect is only secondary. Storm surges require a fetch of open water in order for the wind to generate the energy that will drive the resulting waves forward. In the Beaufort Sea, the largest surges (>1.6 m) are associated with winds from the west and northwest and wind speeds greater than 15 m/s. Using log debris lines near Tuktoyaktuk, Harper et al. (1988) documented a maximum positive storm surge of 2.4 m, although farther west along the Yukon coast, the maximum recorded storm surge is under 2 m (Forbes, 1989). Surges during full ice cover have been recorded in 1974 and 2005, and although these may not contribute to direct coastal retreat, changes to the nearshore profile are likely as a result of lifting off of bottomfast ice. Generally such surges are exceptional and occur on a decadal scale, however, their frequency appears to have increased over the past 20 years. Minor surges are common and occur frequently.

The process of coastal erosion in a permafrost region is described extensively by Are (1988). Erosion is both a mechanical and a thermal process, which he terms thermal abrasion. This results in rates of erosion that are three to four times higher than along similar coasts in temperate regions. As noted by Nairn et al. (1998), this is due to three factors: 1) the melting of frozen sediments by warm seawater, 2) the lower volume of sediment available in the littoral zone since ice formed part of the initial bluff volume, and 3) the subsidence of the nearshore due to melting of submerged permafrost. As such, once would expect that areas with higher ground ice contents would experience greater erosion. Overall, the ground ice content of the deposits along the Yukon Coastal Plain is high due to the presence of pore ice and thin ice lenses, abundant ice wedges, and massive ice which can be up to 30 m thick and can extend for hundreds of metres (Rampton, 1982; Mackay, 1972; Pollard 1990; Pollard and Dallimore, 1988; Harry et al., 1985, 1988). Several studies in the Beaufort Sea have shown a strong relationship between ground ice volume and erosion (Lantuit and Pollard, 2008; Dallimore et al., 1996; Wolfe et al., 2001). Coastal composition in terms of grain size can also play a role in erosion in two ways: firstly, finer-grained silts and clays along the Yukon Coastal Plain are often ice-rich (Rampton, 1982); secondly, they are also more likely to be quickly washed away to the offshore zone so are not able to protect the base of bluffs from further wave action as easily as coarser material might. The combination of morphology and composition may play another part in erosive action as well. For instance, Owens and Harper (1983, cited in Trenhaile, 1997) suggest that, because there is often more ground ice in the upper part of the soil profile, erosion will be more rapid on low bluffs because they tend to be more ice-rich. The main landforms along the

Canadian Beaufort Sea are coastal cliffs, which represent 52% of the shoreline (Harper 1990). These cliffs are fronted by narrow sand and gravel beaches and are mostly low-lying, generally <10 m in height, although they can be up to 90 m high. Flats and deltaic deposits are found at the mouth of small rivers. Aggradation is occurring along some portions of the Canadian Beaufort Sea coastline, but overall, the coast is an erosional one with average annual retreat rates of about 1 m/a and maximum annual retreat of 22.5 m/a (Solomon, 2005; Harper, 1990; Lantuit and Pollard, 2008).

Waves generally break in water depth that is equal to wave height, so the steepness of the nearshore zone will influence how close they are to shore when they break. Along the Yukon Coastal Plain, wave energy is dissipated somewhat by the gentle bottom slope and fine-grained sediments in the eastern part near the Mackenzie Delta, but tends to be higher farther west in the study area where the shoreface is steeper (Forbes, 1997; Forbes et al., 1995). Changes as a result of wave action on the shore combine with changes in the offshore zone (i.e., ice scouring) to alter the nearshore profile, as will changes in sea level. Current rates of relative sea level rise for the overall Canadian Beaufort Sea region are not well defined, but tide-gauge data from Tuktoyaktuk indicate statistically significant relative sea level rise of 3.5mm/a (Manson et al., 2002). Long terms changes in sea level and short term ones due to storm surges are significant in that they raise the mean water level and allow waves to more directly attack backshore sediments. This process will be more pronounced in areas with little or no beach and/or steep backshore bluffs.

Coastal exposure to wind and waves is a strong determinant in how vulnerable that shoreline is to erosion. The orientation of a coast with respect to prevailing wind and waves is therefore important. In his analysis of coastal retreat rates in the Mackenzie Delta region, Solomon (2005) found coastal change rates were strongly influenced by exposure to northwest winds, with low retreat rates along east and south facing shorelines. The northwestern coast of Herschel Island shows much higher rates of erosion than other sites on the island (Lantuit and Pollard, 2008). Landmasses can also serve to protect the shore from wave attack. Forbes (1997) notes that both Herschel Island and Kay Point exhibit strong sheltering effects. There is a series of long linear barrier islands west of Herschel Island, although their role in protecting the coast landward of them is unclear; the islands appear to be quite stable and are likely fed by an offshore sediment supply (Harper, 1990; Forbes, 1997). Offshore bathymetry also plays a role in coastal morphology. Due to wave refraction, wave energy is dissipated by submarine depressions and concentrated by ridges. Wave action is therefore greater on headlands than in bays. On a large scale, general wave action is likely directed somewhat by the Mackenzie Trough to the east of Herschel Island. On a smaller scale, wave refraction has been shown to play a strong role in shoreline erosion and development (Ruz et al., 1992; Hill and Solomon, 1999).

It is the interplay of a number of different site specific properties which appears to govern erosion rates. Héquette and Barnes (1990) conducted statistical analyses to try and determine which coastal parameters might be most important in governing erosion. They found that sediment texture, cliff height, and nearshore gradient had only minor effects on retreat rates. Wave action and ground ice content were found to have moderate effects, but they concluded that changes to the nearshore profile was the main driver as the shoreface profile attempted to return to equilibrium. Nevertheless, Solomon et al. (1994) did find a strong correlation between storm intensity and erosion rates.

2.7 Impacts of predicted climate change

In the next century, climate warming is expected to be twice as high in the Arctic as in other parts of the world. Projections call for increases of up to 4.5ºC in summer and as much as 16.0ºC in winter (Meehl et al., 2007). Besides increased air temperatures, other changes in environmental parameters such as precipitation and sea level pressure are expected. Some of the more important variables in terms of their effects on coastal dynamics are discussed in the following sections.

Satellite data show that since 1978, the annual extent of Arctic sea ice has declined by about 10% per decade (Serreze et al., 2003; Serreze et al., 2007). The decreases are most pronounced in September and there have been reductions of up to 50% in some parts of the Beaufort Sea (Johannessen et al., 2002). Modelling shows that this trend is expected to continue, with some projections showing almost complete loss of summer ice cover by 2037 (Wang and Overlord, 2009). The exact distribution of future sea ice is difficult to predict because climate models that incorporate sea ice do not appear to model its circulation very well (Bitz et al., 2002). As a result, determining the precise location of the ice edge is speculative. Nevertheless, due to the overall decrease in the extent of the pack ice, fetch will likely be greater in all Arctic coastal regions and result in larger waves and increased wave power at the coast. In addition to changes in the pack ice, the duration and extent of landfast ice will be affected by changing conditions. McGillvray et al. (1993) estimated that the open water season in the Beaufort Sea could increase by 60 to 150 days. Solomon et al. (1994) calculated that this would result in a 22 to 39% increase in deep water wave height. Dumas et al. (2005) modelled how ice thickness and duration in the Beaufort Sea would be affected by changes in the surface air temperature and precipitation. Their results examine a wide range of possible conditions and show that the largest decrease in the thickness would be 0.51 m (from the current 1.74 m to 1.23m). This would result in a 44 day reduction in the duration of the landfast ice. Given that the greatest temperature increases are expected in the fall and winter, this implies that freeze-up will be delayed, providing for more open water during the stormier months.

One aspect of future climate that is not entirely clear is how the pattern of storms may change. Lambert (1995) had concluded that there would be a slight decrease in the number of storms, but that their intensity would increase, particularly in the Northern Hemisphere. McCabe et al. (2001) examined changes in northern hemisphere storminess over the period from 1959 to 1997. They found that although mid-latitude storms decreased in frequency, high latitude ones showed a significant increase and were correlated with the Arctic Oscillation index. In addition, the high-latitude storms increased in intensity. These results only apply to winter storms (November to March) however. They would therefore only be expected to impact wave climate in the Beaufort Sea if they are concurrent with a delay in the freeze-up period. A more recent study in the Northeast Atlantic and the North Sea (Weisse et al., 2005) shows that although there was an initial increase in storms in these regions beginning in 1958, their number decreased in the 1990's. Hinzman et al. (2005) see no evidence for changes in cyclonic activity around Alaska, but they do report an increase in high wind events since the 1960's. Cassano et al. (2006) examined how ten different climate models treated Arctic circulation patterns. Although the models showed slight differences in results for the 1991-2000 period, they were in general agreement for trends in 21st century storminess. Overall they show an increase in Arctic low pressure systems in both summer and winter, with the largest changes occurring in the first half of the century.

Relative sea levels along the Beaufort Sea coast are already increasing due to submergence. Sea level rise due to thermal expansion of the ocean and the addition of water from melting glaciers and icecaps is predicted to be 0.40 m by 2090 (Church et al., 2001). The isostatic submergence will result in a further 0.21 m of change, for a total rise in relative sea level of 0.61 m in the coming century. The implications for coastal dynamics will be site specific and depend on the morphology of the backshore. Low coastal bluffs could be overtopped and higher ones subject to thermo-erosional niche formation. In lower lying coastal areas, spits and barrier island would migrate landwards, and the breaching of thermokarst lakes would result in the formation of bays and headlands (Hill and Solomon, 1999; Ruz et al., 1992).

Manson and Solomon (2007) extracted data for the Beaufort Sea region from the Canadian Centre for Climate Modelling and Analysis which show increases in 21st century surface air temperatures of up to 4ºC for the June to October period and up to 16ºC for the November to May timeframe. Noting the importance of site specific factors and snow cover, Zhang et al. (2005) nevertheless tied the past rise in 20th century air temperatures in Canada to a rise in ground temperatures. As such, permafrost temperatures are likely to rise in the coming century as air temperatures rise. Although increased ground temperatures have been recorded, to date there has been no firm evidence of an increase in the active layer thickness in Alaska (Hinzman et al, 2005), but such an increase is a distinct possibility. Ground warming and an increase in the active layer will reduce the strength of coastal permafrost and make it more susceptible to thermal abrasion (Are, 1988). Globally, sea surface temperatures have increased by approximately 1°C in the last century and recent surveys have shown a distinct warm layer in the Arctic Ocean (Meehl et al., 2007). Warmer water will increase the development of thermo-erosional niches in coastal bluffs and will lead to greater bluff erosion (Nairn et al., 1998). In addition, an increase in water temperature will result in thaw of subsea permafrost (Dyke, 1991) and a readjustment of the nearshore profile (Dallimore et al., 1996).

2.8 Conclusions

This review has shown that a number of questions still need to be addressed in order to be able to provide a comprehensive look at organic carbon dynamics along Canada's Yukon Coastal Plain. The first involves making a detailed assessment of the amount of ground ice in the coastal sediments, which I address in Chapter 3 of this thesis. The second involves examining the soil organic carbon content of those sediments through an analysis of materials from the various geomorphic and geologic terrain units in the study region. I determine the current fluxes of this SOC by building on the work on previous researchers who have established erosion rates for the different parts of the coastline. The amount of ground ice in permafrost soils is shown to be crucial in quantifying the soil carbon. An important element of the organic carbon work is establishing what role it plays in regional carbon dynamics. Carbon from terrestrial sources has been largely overlooked to date in the region. These questions are examined in Chapter 4 of this work. Finally, in Chapter 5, I seek to establish how carbon fluxes are likely to change in the coming decades as climate warming changes the environment in this sensitive part of the globe.

Table 2.1 Average density of soil organic carbon contents (kg C/m^3) in the top 1 m of various landcover and soil types in Arctic North America. Changes in the active layer over time and cryoturbation result in a considerable amount of carbon being stored in the permafrost.

	Category	n	kg C/m^3	Proportion in active layer (%)	Proportion in permafrost (%)
Michaelson et al., 1996	coastal plain moist	6	63	62	38
	coastal plain wet	6	60	38	62
	northern foothills moist	7	43	47	53
	northern foothills wet	3	45	62	38
Bockheim et al., 1998	barrens	6	11.5	100	0
	moist nonacidic	20	55.4	60	40
	moist acidic	10	48.7	39	61
	shrublands (nonacidic)	4	36.8	81	19
	shrublands (acidic)	4	33.1	68	32
	wet tundra (organic)	6	63	60	40
	wet tundra (mineral)	5	66.7	41	59
Ping et al., 2008	lowlands	54	55.1	53	47
	uplands	76	40.6	63	37
	rubblelands	5	3.4	85	15
	mountains	4	3.8	100	0
Tarnocai et al., 2009	Histels (organic cryosols)	87	66.6	---	---
	Turbels (turbic cryosols)	256	32.2	---	---
	Orthels (static cryosols)	131	33.6	---	---

Table 2.2 Average density of soil organic carbon (kg C/m^3) for different depth classes of permafrost soils in North America.

Soil type	n	C density per depth class (kg C/m^3)			Proportion in 0 - 1 m (%)	Proportion > 1 m (%)
		0 - 1 m	1 – 2 m	2 – 3 m		
Histels [a]	11	55.9	29		66	34
[b]	13	67.2	62	42	39	61
Turbels [a]	11	53.2	28		66	34
[b]	8	61	53.1	45	38	62
Orthels all [a]	7	44.4	32		58	42
w/alluvium [b]	2	142.6	142.5	67	40	60
w/out alluvium [b]	4	4.5	1.6	0	74	26

[a] Bockheim and Hinkel, 2007
[b] Tarnocai et al., 2009

Figure 2.1 Different types of ground ice, including a) and b) pore ice and thin lenses of segregated ice. A small ice wedge is shown in c); the ice axe to the left of it is approximately 70 cm high. A body of massive ice, approximately 20 m high is shown in d); note the person on the top of the bluff for scale.

a)

b)

c)

d)

CHAPTER 3

QUANTIFYING GROUND ICE VOLUMES IN PERMAFROST ALONG THE YUKON COASTAL PLAIN

3.1 Context within the thesis

This chapter presents an assessment of the volumes of all different types of ground ice within terrain units. The ground ice content of coastal soils must be determined because it affects the sediment and organic carbon content of the soils, and governs the coast's susceptibility to erosion. This is an important first step in order to frame the work in Chapters Four and Five because although soil sampling at the pedon level can provide an accurate assessment of soil constituents such as organic carbon, it is necessary to relate those point measurements to other elements in the terrain in order to apply them at a larger, landscape level. As will be demonstrated, ground ice is often the most important component of the soil in permafrost regions, but the forms it takes are not always directly incorporated into traditional soil pedons. Similarly, given the thermal and structural sensitivity of ice to environmental changes, its presence has to be considered when examining changing rates of coastal erosion. The primary objective of this chapter is therefore to examine the different types of ground ice, and based on their morphology and relationship to other ground ice types, calculate an overall volume for each of the terrain units in the region under study.

3.2 Introduction and background

Ice within permafrost occurs when water freezes within the sediment or when surface ice is buried, and the exact nature of the ground ice is a reflection of a region's geologic, hydrologic, and climatic history. A commonly used classification of North American ground ice developed by Mackay (1972) includes ten different types of intra-sedimental ice alone, reflecting the diversity of ways in which ground ice can originate and the various forms it can take. Some of the more common forms include pore ice (water freezes within soil pores), segregated and intrusive ice (water migrates or is pushed towards the freezing front), and wedge ice (water infiltrates thermal contraction cracks in the ground). Regardless of the ice's origin, it is often the actual volume of ground ice that is of interest, since that is what governs how permafrost will change in response to environmental shifts or human development.

Permafrost often contains significant amounts of ground ice and the Canadian western Arctic is one of the country's most ice-rich areas. The ice content of these soils is high due to the presence of pore ice and thin segregated ice lenses, abundant ice wedges, and beds of massive ice –- defined as large tabular ice bodies with a gravimetric ice content greater than 250% (van Everdingen, 1998). Pingos, ice-cored hills which are made up of several ice types, are also quite common in the Mackenzie Delta region (Mackay 1963b, 1985). Subsea ice-bonded permafrost is present below the Beaufort Sea in water depths up to 100 m (Mackay, 1972; Dallimore et al., 1988; Dyke, 1991). Although there has been some debate about the origin of some of the ground ice, much of it appears to result from a combination of pore water expulsion during permafrost aggradation and high hydraulic gradients from meltwater supplied by the degrading Laurentide Ice Sheet (Mackay, 1971; 1989; Mackay and Dallimore, 1992; Rampton, 1974; 1991; Harris and Murton, 2005). Buried glacier and snowbank ice has also been documented (French and Harry, 1990; Murton et al., 2005; Pollard, 1991; Sharpe, 1992; Dyke and Savelle, 2000).

The goal of this work is to develop a method for quantifying ground ice at the landscape level, which is important in order to properly assess how a permafrost region will respond to changes in the environment, whether natural or anthropogenic. The area selected for study is the Yukon Coastal Plain, located to the west of the Mackenzie Delta along the Beaufort Sea. Previous work on coastal conditions has been conducted on general coastal dynamics and erosional processes (e.g. , Harper et al. 1985, Solomon et al., 1994), or in relation to specific interests such as industrial development (O'Connor and Associates, 1986; McDonald and Lewis, 1973; Lewis and Forbes, 1974) or protection of archeological sites (Forbes, 1997). Permafrost along the Yukon coast is continuous and reaches depths of approximately 300 m (Smith and Burgess, 2000). Much of the coastline consists of unconsolidated, ice-bonded material forming low to moderate bluffs, although some range as high as 90m. Many are fringed by narrow beaches and spits, and barrier islands are also found protecting lagoons and small inlets. Much of this area was covered by a lobe of the Laurentide ice sheet known as the Buckland Glaciation in the early Wisconsinan, as well as by a later stillstand or re-advance known as the Sabine Phase (Duk-Rodkin et al., 2004; Dyke and Prest, 1987). Surficial deposits reflect this history, with the coast east of

Herschel Island being covered by glacial outwash plains and fans, moraines, and fine-grained lacustrine sediment. Moraines make up ice-pushed ridges, or else blanket rolling to hummocky topography likely resulting from thermokrast activity (Rampton, 1982). West of Herschel Island, the plain was unaffected by the Buckland Glaciation and is made up of coastal lagoons, coalesced deltas and alluvial fans (Rampton, 1982).

Several studies have provided general descriptions of ground ice contents along the Yukon Coastal Plain (Rampton, 1974, 1982; Harper, 1990; Harper et al., 1985) and a number of others have provided detailed assessments of ground ice volumes for specific sites (O'Connor and Associates, 1986; Harry et al., 1985, 1988; Pollard, 1990, 1991; Pollard and Dallimore, 1988; de Krom, 1990; McDonald and Lewis, 1973). The research presented here enables a detailed survey to be made of ground ice conditions for the entire Yukon Coastal Plain. To assess ice content along the Yukon Coastal Plain, a morphological model has been developed, based on a method first presented by Pollard and Couture (1999). Specific objectives of this study include 1) determining different terrain units for the study areas based on geology, coastal morphology, and the presence of different types of ground ice, 2) quantifying the different types of ground ice within each terrain unit, and 3) quantifying the overall volume of ground ice within a terrain unit based on the stratigraphic relationships between the different ice types.

3.2.1 Significance of the findings

Ground ice has a high degree of spatial variability. When considering terrain units that cover areas of tens to thousands of square kilometers, an accurate measure of ice content would require establishing an incredibly dense sampling network, made all the more difficult to achieve by the cost and logistical constraints of operating in an Arctic setting. This study does not attempt to present highly accurate estimates of ground ice contents. Instead, its goal is to provide a first approximation of ground ice for different terrain units in a region where such estimates are lacking, filling the gap between the overly general and the limited site-specific. The data used comes from a variety of sources, and there is a range of associated errors. While uncertainties in measured values were assessed where sampling density was high enough, several variables were estimated based on field observations, or were drawn from sources which did not specifically report error. The calculations of ice content include the different data sources; a detailed error analysis is therefore not possible and would misrepresent the level of detail. Accounting for uncertainties inherent in the method, the results are likely accurate to within 10% (W. Pollard, pers. comm.). Although these results may not be absolute, they can be considered representative. Section 3.5 provides a discussion of the uncertainties and potential errors associated with the assumptions that are made. This work goes beyond previous regional studies conducted in other areas in that the different possible stratigraphic relationships between the types of ground ice are considered in detail, so more confidence can be placed in the overall results. The model can be applied to other regions, but will be particularly valuable in locations with complex ground ice stratigraphies, especially where massive ice is present.

3.3 Methods

3.3.1 Description of the model

The model calculates the total volume of ground ice for different terrain units along the coast by determining how much of each different type of ground ice is contained within that segment. As part of the Arctic Coastal Dynamics (ACD), a detailed segmentation of the Canadian Beaufort Sea coastline was conducted based on predominant landforms, surficial materials, permafrost conditions, and coastal processes. Details on the segmentation procedure are given in reports from a series of ACD workshops (Overduin and Couture, 2008; Rachold and Cherkashov, 2004; Rachold et al. 2002; Rachold et al., 2003; Rachold et al., 2005). This initial segmentation (resulting in 21 terrain units) was based on data included in the Coastal Information System (CIS) compiled by the Geological Survey of Canada (Atlantic). It was then refined to account for massive ground ice occurrence (resulting in 44 terrain units), using direct field observations as well as data from Rampton (1982), Wolfe et al. (2001), and Harper et al. (1985). Because of the different factors considered in the coastal segmentation, the length of each segment is variable. Four types of ground ice are considered in the calculations: 1) pore ice and thin lenses of segregated ice, 2) wedge ice, 3) beds of massive ice, and 4) pingo ice. The percentage of ice content for each ice type is first established, then the volume of each ice type in a terrain unit is determined. Finally, the percentages of ice content by volume for each terrain unit are calculated. Although the total volume of ground ice is important to document in process studies, the volume of excess ice within permafrost can be critical, so it is also quantified. Excess ice is defined as “ice in excess of the fraction which would be retained in the soil voids upon thawing” (Pihlainen and Johnston, 1963). It is significant in that it provides an indication of how much ground subsidence can be expected upon melting of the permafrost.

For each terrain unit analysed, 17 input variables are needed. They are:

A	total surface area of a terrain unit
AL	thickness of the active layer
D_1	thickness of the uppermost layer of soil
e	soil porosity
D_{BM}	depth to the bottom of massive ice
D_M	mean depth to the top of massive ice
D_W	depth of ice wedge
H_C	height of coastal segment
N_G	number of pingos
P_G	volumetric ice content of pingo ice
P_M	volumetric ice content of massive ice
P_{P1}	volumetric ice content due to pore ice and thin segregated lenses in layer 1
P_{P2}	volumetric ice content due to pore ice and thin segregated lenses in layer 2
P_W	volumetric ice content of wedge ice
R	mean pingo radius
W_S	mean ice wedge spacing
W_T	mean ice wedge width

Values for these inputs come from a variety of sources and are detailed below and in Appendix A. The input data are used to generate derived variables and volumes which are needed to obtain a total ground ice volume. The equations used to obtain the derived variables and volumes are found in Appendix B.

3.3.2 Extent of permafrost

The thickness of material considered depends on the height of the coastal bluffs. Heights are based on direct measurement or mean values from the CIS database. Ground ice contents are typically higher near the ground surface (Pollard and French, 1980), with excess ice commonly found just below the active layer (Mackay, 1970). Because the upper part of the soil profile typically contains more ice, two layers are considered for the purposes of determining ice content of pore and segregated ice. The thickness of a layer is based on stratigraphic data and layer 1 generally extends down to the most obvious sedimentary break. Layer 2 extends from the base of layer 1 to the base of the bluff. Since the estimates concern only the volume of perennially frozen materials, the average active layer thickness for the terrain unit is subtracted to arrive at the actual thickness of materials used in calculations. In order to properly consider three dimensional variations in ice types, each segment is considered to extend 100 m back from the coast. This buffer size was selected both to allow proper representation of different size ice wedge polygons, and yet to not overestimate the size of ground ice bodies.

3.3.3 Pore ice and thin segregated ice lenses

Ice contents due to pore ice and thin lenses were measured in shallow cores for upper soil layers, and from bluff exposures for lower layers. Coring was carried out in 2004 and 2005 at 20 representative sites along the Yukon coast using a modified CRREL 7.5 cm corer. Cores depths ranged from 0.90 m to 1.70 m below the active layer, which itself varied between 0.28 and 0.83 m in thickness. The cores were sub-sampled for ice content at approximately 5 cm intervals. For terrain units which could not be sampled, ice contents are extrapolated from units with similar characteristics or, where available, data from previously published site-specific reports are used. For each terrain unit considered, mean percentages of ice content for the two horizontal layers are computed. The volume of frozen material in each layer is then multiplied by the ice content to arrive at a volume of ice. This assumes that the permafrost materials consist only of sediments containing pore ice and thin segregated ice lenses. The volume taken up by ice wedges and massive ice therefore needs to be accounted for; this is discussed further in the section on total ice content.

3.3.4 Ice wedge ice

The amount of wedge ice is quantified by estimating the length of wedges in a terrain unit based on the size of the polygons and therefore the spacing of the wedges (Equation B11 in Appendix B). The calculations assume that the wedges meet at right angles and form a tetragonal network in plan view, which is a common geometry per French (1996). The wedges are assumed to be triangular in cross-section and their volume is calculated geometrically (Equation B12) using measured wedge dimensions. Where not available, conservative values for the region are used based on values provided by Rampton (1982). Because of the triangular shape of the wedges, they occupy different volumes in each of the horizontal layers being considered, so Equation B12 is modified for each layer (Equations B13 and B14). Limited data exists on volumetric ice content of wedges (Pw), so a default of 88% is used, based on a measurement at one location within the study area. The calculations of wedge ice volume assume that all wedges in the study area have a surface expression, and they are therefore conservative estimates.

3.3.5 Massive ice

Massive ice is considered to underlie a terrain unit only if it or a significant number of retrogressive thaw slumps have been positively identified in a coastal unit, either by observation or from remote sensing imagery. Retrogressive thaw slumps are distinctly shaped landforms caused by the melting out of portions of a massive ice bed. The mean depth to the top (D_M) and bottom (D_{BM}) of massive ice beds is from direct measurement or estimated from published values. Because the thickness of massive ice beds is difficult to determine since the lower part of exposures is normally buried in slumped debris, in several cases the massive ice is considered to extend to the base of the terrain unit. The calculated volume occupied by massive ice is shown in Equation B21, but is adjusted to account for the fact that ice wedges may extend down into the bed (Equations B15 through B18). Ice content of massive ice (P_M) is from direct measurement or site-specific published values, with a default of 80% where no values are available.

3.3.6 Pingo ice

According to Mackay (1979), there are eight pingos on the Yukon Coastal Plain, but none are located in the region selected for study. This ice type is included for the sake of completeness of the model, but all values for pingo ice are set to zero for this study. If the model were to be applied to other areas, however, the number of pingos identified on air photos and from ground observations would need to be multiplied by a volume based on a semi-spherical shape and a mean pingo radius (Equation B22). Although pingos often contain sediment, their volumetric ice content (P_G) is assumed to be 100%, barring any measured values.

3.3.7 Total ice volume

The total ice volume for a terrain unit is given by the following equation:

[3.1, see also B23] $$TIV = P_{P1} V_{P1} + P_{P2} V_{P2} + P_W V_{WT} + P_M V_{MT} + P_G V_G$$

where P is the volumetric ice content, V is the volume occupied by a given ice type, with the subscripts $_{P1}$ and $_{P2}$ for pore ice and thin segregated lenses in layers 1 and 2, $_{WT}$ for total wedge ice, $_{MT}$ for total massive ice, and $_{G}$ for pingo ice. As mentioned earlier, ice volumes need to be adjusted to reflect the presence of wedge ice and massive ice. This is best done by considering each horizontal layer separately. Several scenarios are considered which account for the depths and stratigraphic relationships of the different ice types. For instance, a terrain unit may have a pingo on the surface and may contain two layers of pore and lens ice, along with an ice wedge that penetrates both layers (Figure 3.1). Descriptions of the most likely scenarios are listed in Appendix C; expanded equations for total ground ice volumes are included for illustrative purposes only. The equations for derived variables and volumes in Appendix B take all these scenarios into consideration so that the basic equation for total ground ice volume listed above will apply no matter what the scenario.

3.4 Results

3.4.1 Parameterization

Based on surficial geology data provided by Rampton (1982), coastal morphology, and locations of massive ice, the Yukon coastline was divided into 44 different terrain units, ranging from 0.8 to 33.2 kilometers in length (Figure 3.2). Thirty five of the units are within the limit of the Buckland Glaciation. Massive ice was documented in 15 units in either lacustrine or morainic materials, and had an average thickness of 4 m. All but two of the massive ice units are within the Wisconsinan glaciation limit. Cliff heights for the coastal segments ranged from 0.9 to 60 m. They were generally much lower in the western, unglaciated section of the coast, averaging 3 m high as compared to 15 m in the eastern sector. This difference in topography can be accounted for by the presence of glaciogenic deposits (<5 m per Rampton, 1982) and massive ice beds, and by the relief generated by ice thrusting. Active layers thicknesses were between 0.28 and 1.50 m. Several input variables showed a relationship with grain size. The percentage of pore ice and thin segregated lenses ranged from 10 to 95%, with the higher values in fine-grained material. As expected, percentages were higher in layer 1 (mean of 46%) than in layer 2 (mean of 37%). Ice wedge dimensions were smallest in lacustrine deposits. Overall, ice wedge depths ranged from 3.0 to 7.0 m, with a mean of 5.3 m. The widths of the wedges were between 1.5 and 2.3 m, averaging 2.0 m, while the mean spacing was 13 m.

3.4.2 Ground ice volumes

Model results show that over 180 million m^3 of ground ice is present in sediments along the Yukon Coastal Plain. This represents 46% of all earth materials. In unglaciated areas, ground ice accounts for 35% of materials. Three of the terrain units in this study contained no ground ice (Clarence Lagoon E, Malcolm River fan, Malcolm River fan with barriers). Figure 3.3 shows the actual volumes of the different types of ground ice and how they vary between terrain units, listed from west to east.

The percentage of ground ice for each terrain unit is shown in Table 3.1. Ice volumes range from 0 to 74% and are a function of surficial material. They are lowest in the coarser grained marine deposits in bars and spits (3%), while the highest ice volumes are found in more finely grained lacustrine deposits (54%). The distribution of the total ground ice and the excess ice for the different coastal segments is shown in Figure 3.4. Four of the 9 non-glaciated units contained excess ice, all of them lacustrine. None of the fluvial or marine units in the glaciated portion of the coast contained excess ice. Of the 18 terrain units that did contain excess ice, half were underlain by massive ice. There does not appear to be any correlation between excess ice and cliff heights (mean height for cliffs with excess ice is 15 m (st. dev. 18 m).

When considering the breakdown of ice types, pore ice and thin segregated lenses account for 76% of the total ground ice, wedge ice accounts for 3%, and massive ice for 21%. Figure 3.5 shows the percentage of each ice type for all terrain units. Given that ice wedges take up a greater proportion of the upper parts of the soil column, the percentage of wedge ice shows a relatively strong inverse correlation with cliff height ($r = -0.64$).

3.5 Discussion

This study provides a means of assessing ground ice volumes that accounts for the varying morphology and stratigraphy of terrain units along the Yukon Coastal Plain. The percentage of ground ice found here (46%) is similar to that calculated by other nearby regional studies. Pollard and French (1980) reported 47.5% ground ice in the top 10 m of permafrost on Richards Island, NWT to the east of the study region, while Brown (1968) found that ground ice comprised 46.6% in the upper 8 m of permafrost along the Alaskan Coastal Plain to the west. The slightly lower values reported here can be accounted for by the fact that over a third of the Yukon coastline has bluffs higher than 10m; since ground ice volumes decrease with depth, more ice-poor material is included in this work. Although the difference in ice content between the studies is not that large, it nevertheless underlines the importance of considering morphology in such assessments. This is particularly true in coastal areas, where environmental processes act on the entire bluff face, rather than just the near-surface portions. Note that this study only considers the sub-aerial portion of coastal bluffs. Observations show that ground ice does extend below sea level, so if the shoreface is to be considered in process studies below the waterline, the method presented here should be modified to account for the additional ground ice which can be easily done by increasing the thickness of layer 2.

In considering the results, it is important to recognize how estimation of input parameters and extrapolation between the units can affect the values obtained. A number of the estimated inputs used conservative values, so some of the ground ice values provided here may be somewhat low. The largest discrepancy is likely in the thickness of massive ice beds. The thickest massive ice layer used in the calculations was 9 m, yet a study of several hundred shotholes in the Mackenzie

Delta which penetrated massive ice shows a mean thickness of 13 m (Mackay, 1971); that is considered a minimum thickness since not all the holes reached the bottom of the massive ice. Along the Yukon Coastal Plain, exposures with headwalls up to 25 m high have been observed. However, because the exposures did not extend the length of the terrain unit and the model calculations assume that massive ice underlies the entire unit, minimum values were used. So in some units, massive ice could potentially be up to three times as much as the values presented here.

The volume of wedge ice was based on their spacing seen in natural exposures, or in most cases, on the size of the polygons as seen at the ground surface. Since an exposure does not necessarily cut across the widest part of the polygons, the spacing of the wedges is usually underestimated (Mackay, 1977), and they appear to be denser than they are in fact. This would result in a slight overestimation of wedge ice volume. If polygon size is measured at the surface, this assumes that all ice wedges have a surface expression, however, field observations have shown that this is not always the case. Wedges therefore appear to be more widely spaced and less dense. Most of the wedge spacings in the study are based on surface measurements and, as a result, overall wedge ice volume is likely underestimated. Because of the correlation between cliff height and wedge ice volume, this underestimation is more important in low bluffs.

An overestimation of ice volumes could result if the assumption that massive ice underlies entire terrain units is not valid. However, Rampton (1982) has attributed the topographic relief in areas of rolling and hummocky moraine to thermokarst caused by the melting of massive ice, so this assumption is particularly valid for these units. Furthermore, the terrain units were segmented based on the evidence of massive ice occurrence to ensure that areas with no massive ice were parameterized differently. In two terrain units where retrogressive thaw slumps were observed only sporadically (Herschel Island S and Running River), the units were classified as not containing massive ice.

Another possible source of overestimation is the assignment of ice content values to the top layer of soil based on core measurements taken in the top 2 m of permafrost. As noted earlier, ice content values are generally higher just below the active layer (Pollard and French, 1980; Mackay, 1970). In this study, ice content values based on core measurements were used in 18 of the 44 terrain units. The average thickness of Layer 1 for these units was 4 m, with a mean volumetric ice content of 60%. This is slightly higher than the value of 52% for the upper 4.5 m found by Pollard and French (1980) in their study of over 500 drill holes from the Mackenzie Delta. However, ice wedges take up 22% of the volume of the upper layer, reducing the pore ice volume under consideration. Considering that only a portion of the layer may be overestimated, the resulting error in the ice volume for the entire layer would be 3%.

Although the percentage of ground ice is high in some of the unglaciated terrain units, this is due to the fact that the bluffs are lower, therefore a greater proportion of the total volume is made up of the more ice-rich layer 1 and ice wedges. Absolute ice contents, however, are higher in the formerly glaciated regions. The geographic distribution is obvious if massive ice is, in fact, buried glacier ice. If the ice is of segregated origin (whether as thin lenses or massive ice beds), the high volumes of it near the glacial limit are explained by high pore water pressures generated by permafrost aggrading as the ice sheet receded, or glacier meltwater driven by hydraulic gradients from the ice overburden (Mackay, 1971, 1989; Mackay and Dallimore, 1992; Rampton, 1974, 1991; Harris and Murton, 2005).

3.6 Conclusions

The model developed in this work demonstrates how ground ice can be quantified for terrain units with different geologies, coastal morphologies, and ground ice types. It considers the potential stratigraphic relationships between the different ice types and accounts for a variety of possibilities. The results allow us to draw the following conclusions:

1. Ground ice is an important component of sediments along the Yukon Coastal Plain, accounting for over 46% of earth materials. More than three quarters of this ice is pore ice and thin segregated lenses.

2. There is nevertheless considerable variation in both total ground ice content and excess ice among terrain units in the same region, much of it the result of differing surficial geology. Ice contents are lowest in marine deposits and highest in morainal and lacustrine materials.

3. Wedge ice constitutes a greater percentage of the ground ice in low bluffs.

2. Although a history of glaciation does not increase the percentage of ground ice in a terrain unit, it does appear to increase the absolute amount.

Table 3.1 Ground ice volumes and excess ice volumes for different terrain units along the Yukon Coastal Plain. Units were distinguished on the basis of surficial geology, coastal morphology and permafrost conditions.

Terrain unit	Surficial material	Ice volume (%)	Ice volume by material type (%)	Excess ice (%)	Massive ice
Kay Point spit	marine	1	3 ± 1		
Avadlek Spit	marine	2			
Whale Cove	marine	2			
King Point lagoon	marine	2			
Clarence Lagoon	marine	2			
Phillips Bay W	marine	2			
Simpson Point	marine	2			
Nunaluk Spit	marine	3			
Catton Point	marine	4			
Stokes Point	marine	6			
Malcolm River fan	fluvial	0	13 ± 19		
Malcolm River fan w/ barrier isl.	fluvial	0			
Babbage River Delta	fluvial	28			
Clarence Lagoon E	fluvial	0			
Running River	fluvial	39			
Kay Point	glacial outwash	42	46 ± 10		
Workboat Passage E	glacial outwash	40		2	
Whale Cove W	glacial outwash	57		17	
Kay Point SE	ice-thrust moraine	38	52 ± 9		y
Herschel Island N	ice-thrust moraine	50		2	y
Herschel Island W	ice-thrust moraine	51		5	y
Herschel Island E	ice-thrust moraine	56		13	y
Herschel Island S	ice-thrust moraine	63		35	
Shingle Point E	rolling moraine	40	52 ± 7		
Shingle Point W	rolling moraine	46			y
King Point NW	rolling moraine	48			y
Roland Bay W	rolling moraine	52			y
Stokes Point W	rolling moraine	53.			y
Whale Cove E	rolling moraine	53		15	y
Workboat Passage W	rolling moraine	55		27	
Sabine Point	rolling moraine	60		20	y
Phillips Bay NW	rolling moraine	62		33	y
Sabine Point W	lacustrine	30	54 ± 13		
Sabine Point E	lacustrine	32			y
Phillips Bay	lacustrine	47			
King Point	lacustrine	52			
Komakuk Beach W2	lacustrine	52		12	
Roland Bay E	lacustrine	54		1	
Stokes Point SE	lacustrine	56		17	
Komakuk Beach	lacustrine	57		22	
Clarence Lagoon W	lacustrine	58		22	y
Roland Bay NW	lacustrine	65		10	
Komakuk Beach W1	lacustrine	66		39	y
King Point SE	lacustrine	74		40	y

Figure 3.1 Diagram demonstrating the possible stratigraphic relationship between different ice types in a terrain unit. This unit has a pingo, layers with differing amounts of pore ice and thin lenses of segregated ice, plus ice wedges which penetrate into the bottom layer. See text for explanation of symbols used. Additional stratigraphic scenarios are shown in Appendix C.

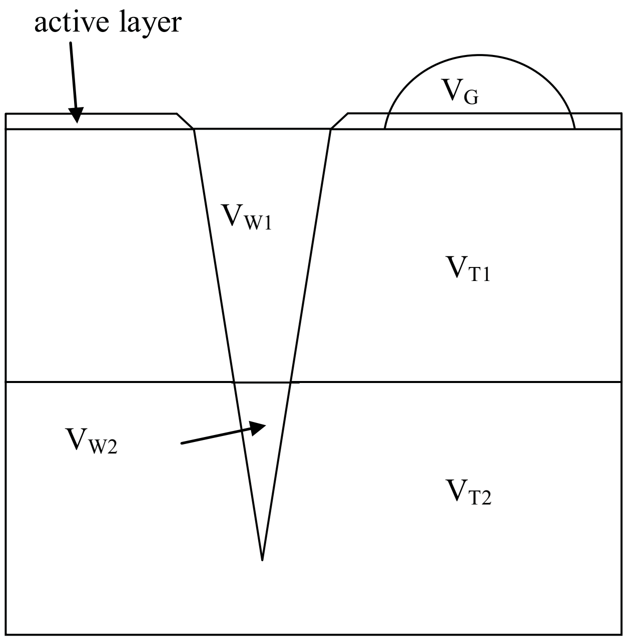

Figure 3.2 Surficial geology of terrain units along the Yukon Coastal Plain. Yellow dots indicate retrogressive thaw slumps generated by thawing of massive ice. (Terrain unit numbers are keyed to graphs in Figures 3.3 and 3.5).

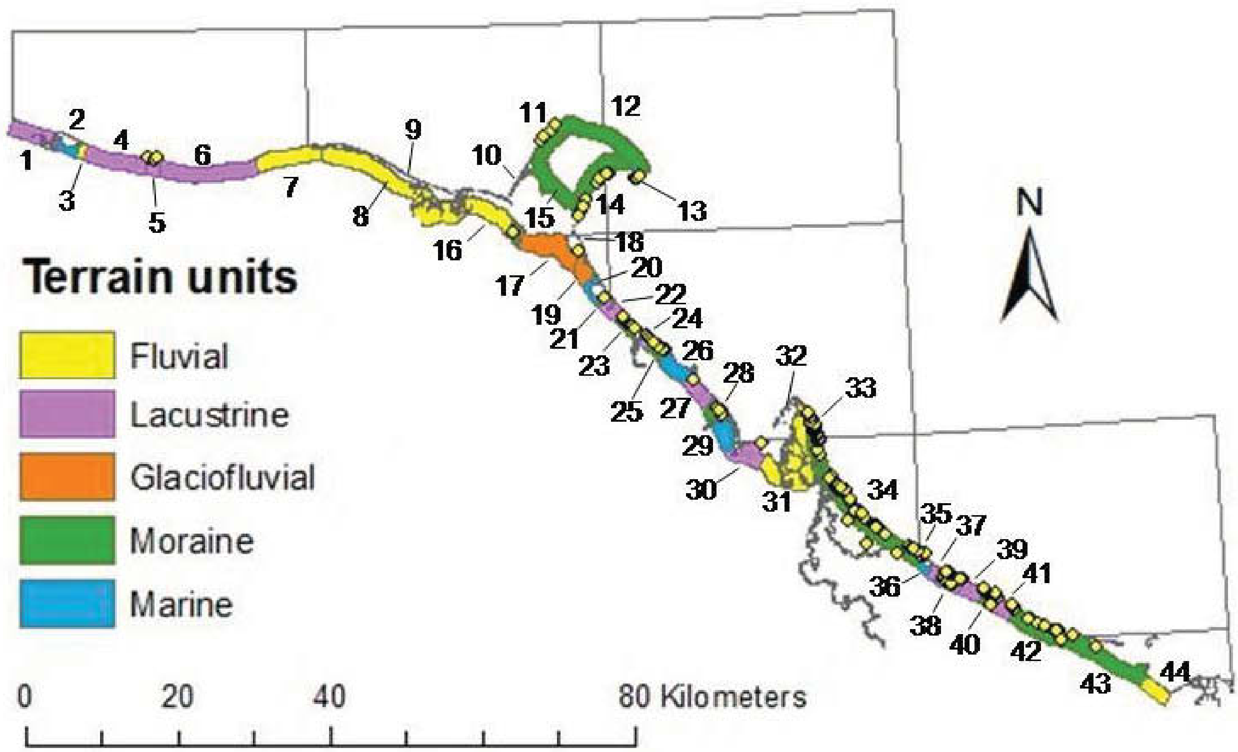

Figure 3.3 a) Actual volumes and type of ground ice for all terrain units, shown from west to east, and b) volume of ground ice per meter of coastline. The approximate limit of glaciation is indicated. (Terrain unit numbers are keyed to map in Figures 3.2).

a)

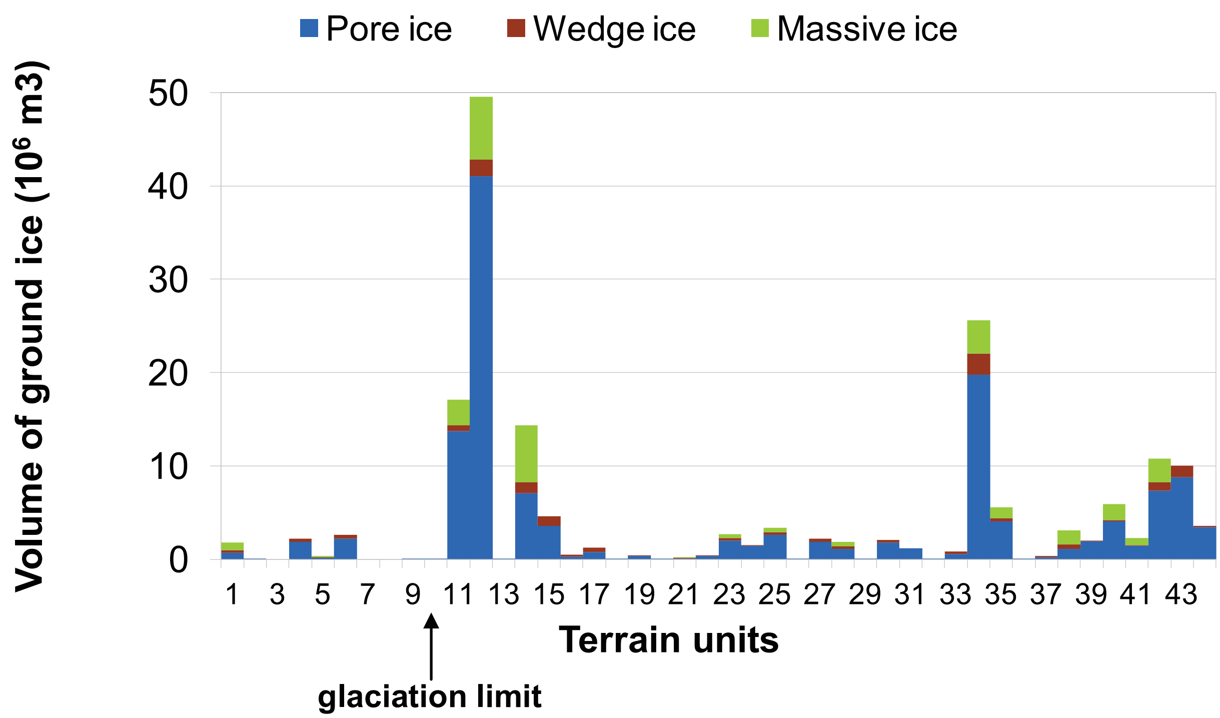

b)

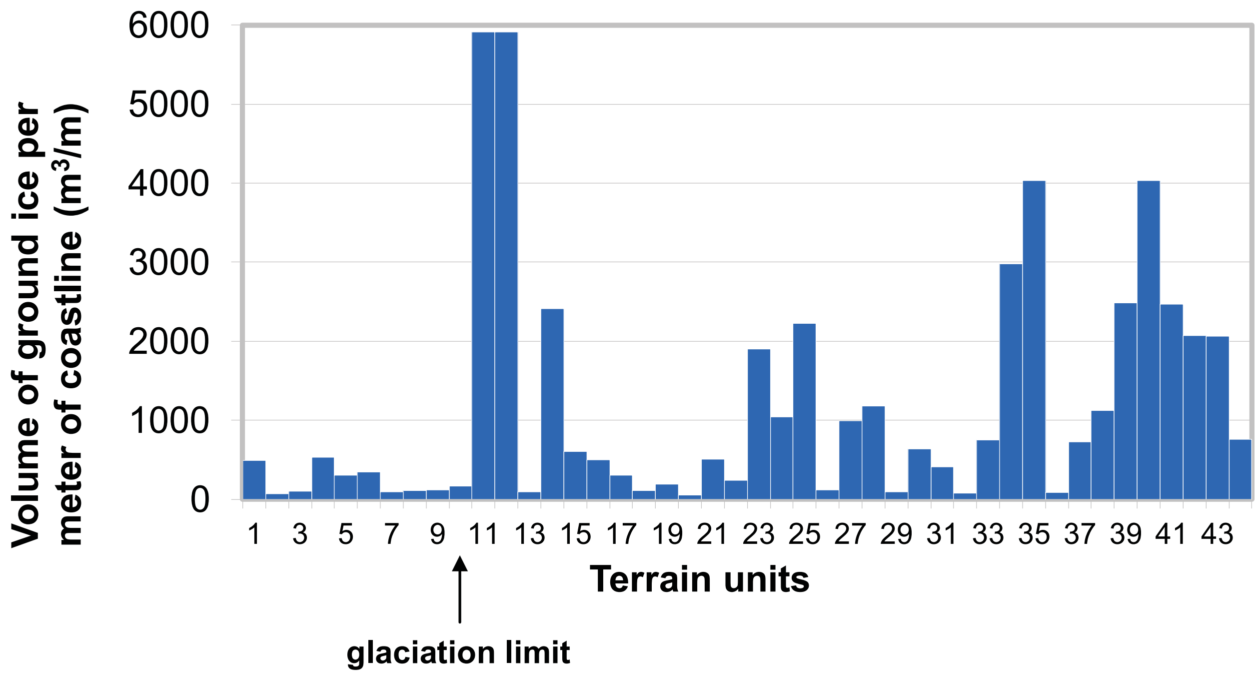

Figure 3.4 a) Ground ice as a percentage of the total volume of materials for different terrain units along the Yukon Coastal Plain. b) Excess ice as a percentage of the total volume of materials.

a)

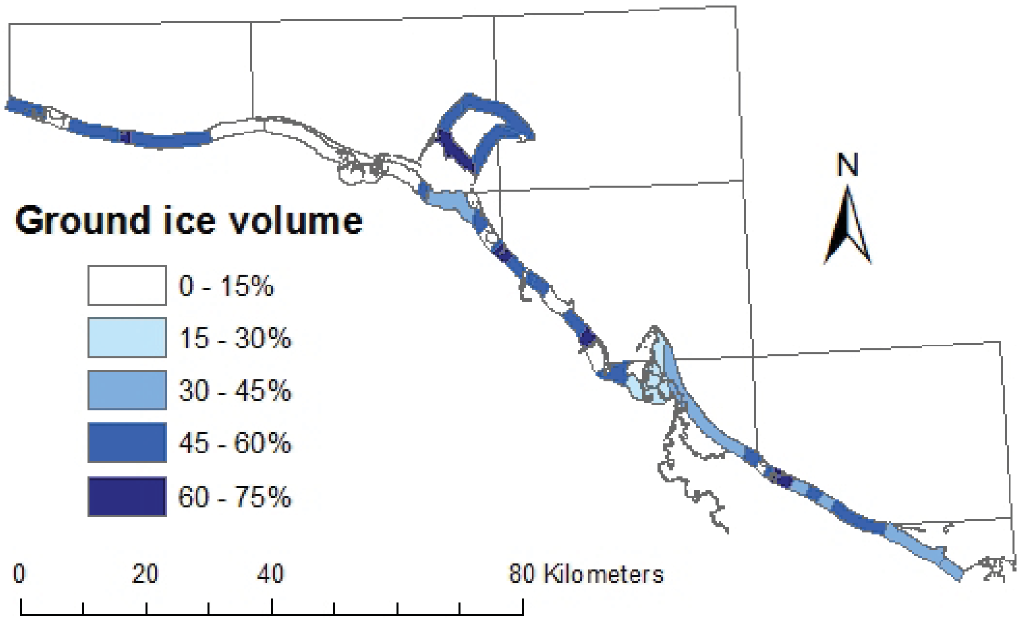

b)

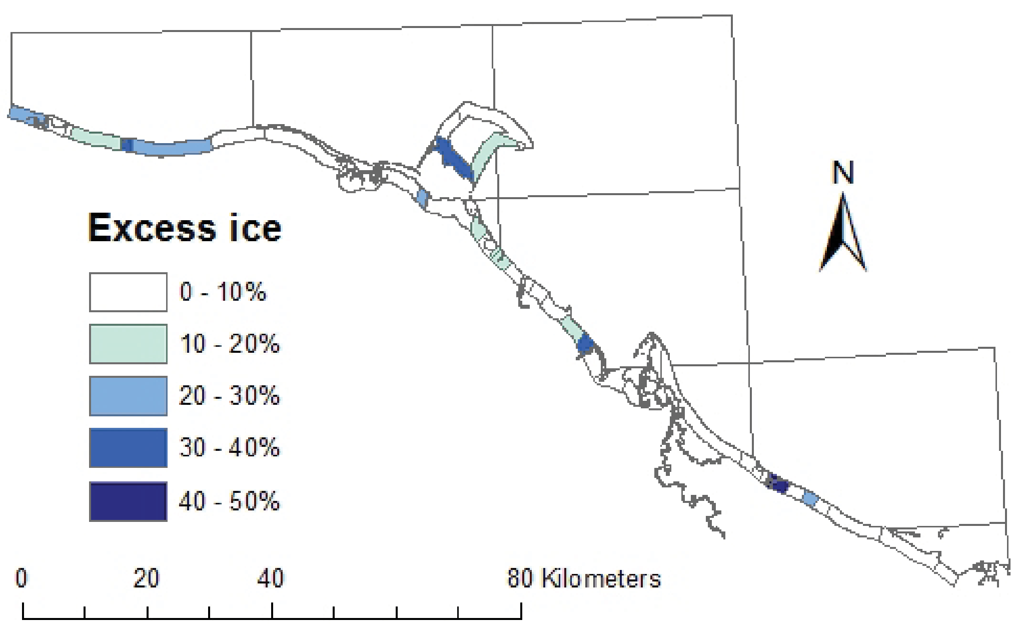

Figure 3.5 Different ground ice types as a percentage of the total volume of ice for all terrain units, shown from west to east. (Terrain unit numbers are keyed to map in Figures 3.2).

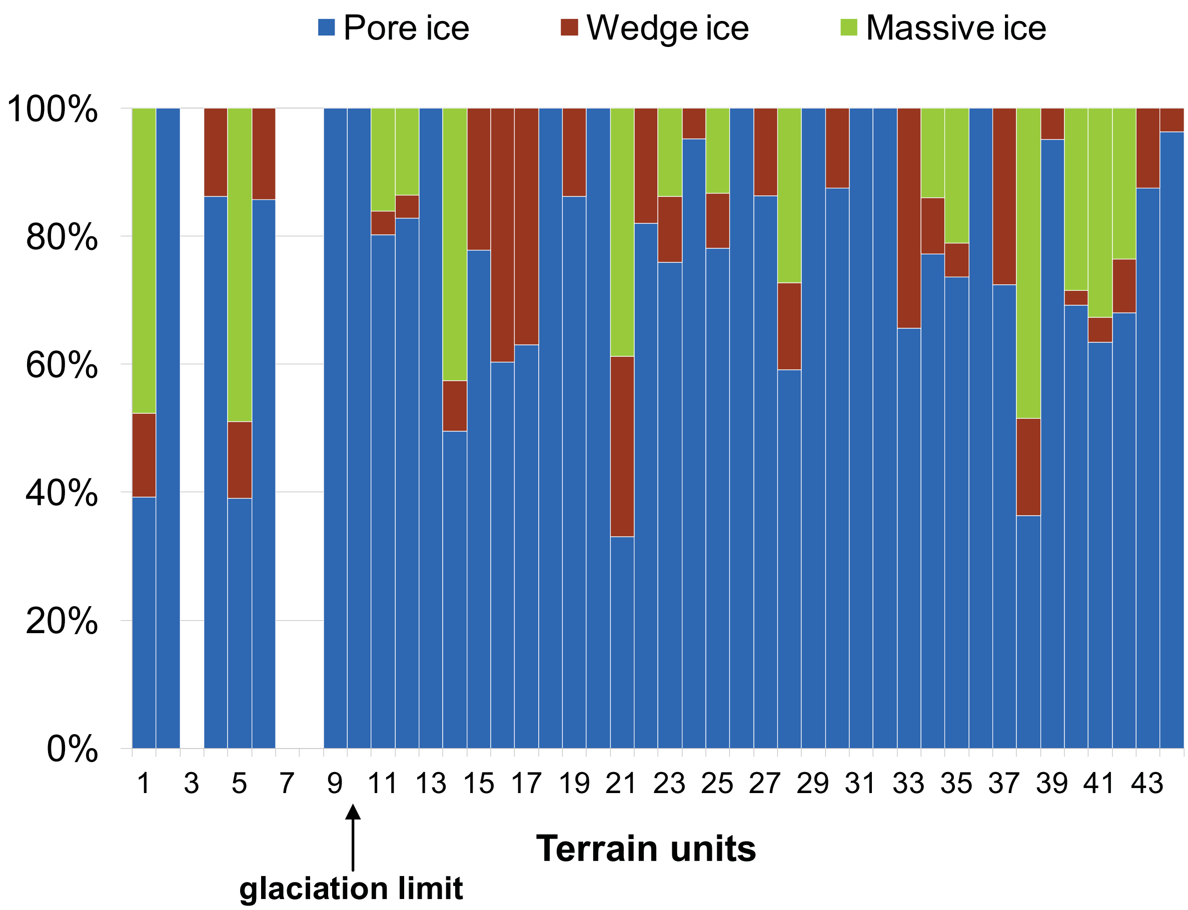

CHAPTER 4

ORGANIC CARBON IN SOILS OF THE YUKON COASTAL PLAIN AND FLUXES TO THE BEAUFORT SEA

4.1 Context within the thesis

The rate of organic carbon flux from an eroding coastline depends on the soil organic carbon content in the coastal sediments, and how rapidly those sediments are eroding. This chapter examines both of these elements for a permafrost coast along the Canadian Beaufort Sea. The work presented here builds on results from Chapter 3 in that the carbon contents are strongly influenced by the amount of ground ice contained within the sediments and its stratigraphic position within the coastal bluffs. Larger ground ice volumes mean smaller volumes of sediment and therefore less carbon. This is particularly important in the more carbon-rich horizons closer to the ground surface. While acknowledging the importance of ground ice, previous investigations for the region have not attempted to determine the magnitude of its influence on C fluxes. In addition to ascertaining the actual carbon flux, the implication of the C transfer is investigated by attempting to establish where the eroded carbon is deposited and therefore what role it might potentially play in the oceanic carbon cycle.

4.2 Introduction and background

Understanding the carbon dynamics of the world's oceans is important because of the ocean's capacity to buffer increases in atmospheric carbon dioxide (CO_2) and because of the impact on marine ecosystems (Dunton et al, 2006). Uncertainties remain about the fluxes to and from the system, and narrowing those uncertainties is especially critical in regions such as the Arctic, where rapid environmental changes are likely to increase the cycling of carbon (McGuire et al., 2009; Schuur et al., 2008). Studies of the overall cycling of organic carbon in the Arctic Ocean have progressed towards elucidating the processes involved and highlighting the knowledge gaps (Stein and Macdonald, 2004a; Vetrov and Romankevich, 2004). On a volume basis, the Arctic Ocean receives higher levels of terrestrially-derived organic matter than any other ocean (Dittmar and Kattner, 2003). Terrestrial inputs of sediment and organic carbon to the Arctic Ocean come from both riverine and coastal sources, with the proportion varying by region (Rachold et al., 2000; Rachold et al., 2004). Inputs to the Canadian Beaufort Sea -- one of the regional seas of the Arctic Ocean – are largely dominated by discharge from the Mackenzie River (Macdonald et al., 1998). However, although several studies have provided estimates of material fluxes to the Beaufort Sea from coastal sources (Harper and Penland, 1982; MacDonald et al., 1998; Hill et al., 1991; Yunker et al., 1990; Yunker et al., 1991; Yunker et al., 1993), organic carbon inputs are still not very well defined. A major goal of the International Arctic Science Committee's Arctic Coastal Dynamics (ACD) project was to develop circum-Arctic estimates of the coastal contribution of sediment and carbon (Rachold et al., 2005). Organic carbon coastal inputs from some areas are fairly well-constrained (Rachold et al, 2004; Jorgenson and Brown, 2005; Streletskaya et al., 2009) but uncertainty still exists for other regions. This paper seeks to quantify the fluxes of organic carbon to the Beaufort Sea from eroding permafrost along the Yukon Coastal Plain.

4.3 Study area

The Yukon Coastal Plain, located west of the Mackenzie River, is a pediment surface which slopes gently from a series of inland mountain ranges to the Canadian Beaufort Sea. It is covered by a variety of unconsolidated materials, including fluvial and alluvial deposits, morainic and glaciofluvial material, and lacustrine sediments (Rampton, 1982). Permafrost is found everywhere except under large lakes, and contains considerable ground ice in the form of pore ice and thin lenses, ice wedges, and beds of massive ice. Previous investigations have found that, regionally, ground ice can account for 46% of earth materials along this coast (Couture and Pollard, Chapter 3, this work). The sediments are also quite rich in organic material and a layer up to 3.5 m thick blankets many of the deposits along the coastal plain (Rampton, 1982). Much of this accumulated in thermokarst basins -- caused by melting of ground ice -- that subsequently drained. This accumulation of organic matter was further promoted by poor drainage and low regional slope gradients, particularly in the western part of the plain.

Measurements of total organic carbon (TOC) in soils have been conducted at only a few sites along the Yukon Coastal Plain (Kokelj et al., 2002; Smith et al., 1989; Tarnocai and Lacelle, 1996; Yunker et al., 1990), yielding values between 2.9 and 99.2 kg C/m^3. In North America, TOC contents of permafrost soils have been shown to vary considerably depending on soil type and landcover, with average values between 30 and 60 kg C/m^3 (Michaelson et al., 1996; Bockheim et al., 1998; Bockheim et al., 1999; Bockheim et al., 2003; Bockheim et al., 2004; Bockheim and Hinkel, 2007; Ping et al., 2008; Tarnocai, 1998; Tarnocai et al., 2003; Tarnocai et al., 2007; Tarnocai et al., 2009). Most measurements of SOC in permafrost have been confined to the top 1 m of soil, although some recent studies have examined deeper deposits (Bockheim and Hinkel, 2007; Tarnocai et al., 2009; Zimov et al., 2006). In Arctic soils in general, most soil organic matter originates in the seasonally unfrozen active layer near the ground surface, so organic matter tends to decrease with depth. The thickness of the active layer can vary both temporally and spatially depending on surface conditions, however, and if this layer thins, organic matter remains in the upper part of permafrost. Current active layers along the Yukon coast range in depth from approximately 0.3 to 1.5 m, although during the Holocene warm period 9000 BP, active layer thicknesses in the region were up to 2.5 times present-day ones (Burn, 1997; Kokelj et al., 2002). A considerable amount of organic matter can also be transferred into the upper part of permafrost through cryoturbation (Bockheim and Tarnocai, 1998b). In addition, organic material along the Yukon Coastal Plain can be found at depth in pre-glaciation floodplain and deltaic sediments, and where surface organic matter appears to have been buried by glacial deformation (Rampton, 1982).

Comprehensive erosion rates for the Yukon coast were first provided by McDonald and Lewis (1973) and have been updated based on remotely sensed imagery (Harper et al., 1985; Harper, 1990; Lantuit and Pollard, 2008) and a number of site specific studies (Lewis and Forbes, 1974; Gillie, 1987; Forbes and Frobel, 1985; Solomon et al., 1994; Forbes et al., 1995; Forbes, 1997). Total volumetric losses due to erosion along the Canadian Beaufort Sea coast have been estimated at 3.51×10^6 m^3 annually (Harper and Penland, 1982). Hill et al. (1991) converted this to a gravimetric sediment flux of 5.62 Mt/yr. Yunker et al. (1990; Yunker et al., 1991) used Harper's updated retreat rates and estimated the flux of hydrocarbons associated with peat erosion. Based on these flux values and only a few TOC measurements, Macdonald et al. (1998) derived preliminary values of organic carbon flux from coastal erosion of between 0.055 and 0.3

Mt/yr. These studies did not consider ground ice in their calculations, although bulk densities used in calculation would have implicitly accounted for pore ice.

Once it reaches the ocean, the fate of terrestrially-derived organic carbon is important to an understanding of carbon sequestration and cycling. It is generally more refractory than marine organic matter and therefore has a greater likelihood of being buried in shelf sediments or exported off-shelf, rather than being re-mineralized in the water column (Hedges et al., 1997). Potential off-shelf transport is especially important because, unlike most other shelves of the Arctic Ocean which are quite wide, the shelf along the Yukon coast is only about 40 km wide, and narrows to 10 km in some places. Fairly comprehensive databases exist of organic carbon in offshore sediments of the Alaska Beaufort Sea (Naidu et al, 2000) and of the Mackenzie Shelf (Macdonald et al., 2004), but only a few samples have been taken from the Yukon coastal area. Several different methods have been used to determine the source of the organic matter in marine sediments including geochemical bulk parameters such as stable carbon isotopes or C/N ratios (i.e., Hedges et al., 1986; Meyers, 1997; Naidu et al., 2000), biomarkers (Yunker et al., 1991; Yunker et al., 1993; Goñi et al., 2000; Belicka et al., 2002), or a combination of methods (Belicka and Harvey, 2009; Drenzek et al., 2007).

With the overarching goal of developing a more robust assessment of carbon fluxes from the Yukon Coastal Plain, this paper has three specific objectives: 1) to measure total organic carbon in different surficial materials along the coast, to as great a depth as possible; 2) to determine annual fluxes of TOC using published retreat rates, ensuring that ground ice volumes at different depths are taken into consideration; and 3) to estimate the amount of terrestrially-derived organic matter being sequestered in shelf sediments.

4.4 Methods

The Yukon coast was segmented into different terrain units on the basis of landforms, surficial material, permafrost conditions, and coastal processes, since each of these factors influences the amount and flux of soil organic carbon. The flux of carbon was calculated from the measured carbon contents and the long-term erosion rates of each segment. The fate of the eroded carbon was determined by examining nearshore bottom sediments to see how much terrestrial organic carbon they contained.

4.4.1 Sample collection and laboratory analyses

Onshore soil sampling was carried out in August 2004 and 2005 at 26 locations along the coast (Figure 4.1). Sites were selected to represent terrain units from different parts of the coast. Sampling west of Herschel Island was restricted by ice conditions in 2005, and coarse grained units are not well represented due to difficulties associated with coring in gravelly and pebbly material. Samples from an additional 6 sites were collected in July and August 2006. Samples were collected from the side of soil pits in the unfrozen active layer. In the underlying permafrost they were obtained using a modified CRREL corer (7.5 cm i.d.) or, in a limited number of cases, using a hammer or an axe to cut samples (approximately 1000 cm^3) from the face of natural exposures. Active layer thicknesses ranged from 0.25 to 0.90 m. Cores began at the base of the active layer and penetrated to a maximum of 2.04 m below the ground surface. Natural exposures were sampled to a depth of 5.8 m from the surface. At several sites, samples were taken from the base of bluffs and are assumed to be representative of the entire lower portion of the bluff. The frozen cores were sub-sampled every 5 cm or where there was a distinct change in material composition. Samples were weighed in the field, then freeze-dried and re-weighed in the laboratory to determine ice content and bulk densities (based on frozen core volume or measurement of the sample block).

Offshore samples were obtained at 14 locations in July 2006. A Ponar sampler was used to obtain samples from bottom sediments along profiles perpendicular to the shore. Sample size varied due to differences in substrate and water depths, but averaged about 1000 cm^3. Samples were taken at distances of approximately 30 m, 50 m, 100 m, 250 m and 500 m from shore to assess how the composition of the organic carbon in the sediments might change.

Laboratory analyses were carried out at the Alfred Wegener Institute for Polar and Marine Research in Potsdam, Germany. Dried samples were ground to homogenize them, and then total carbon (TC), total organic carbon (TOC), and total nitrogen (TN) were measured using an Elementar Vario EL III elemental analyzer. Prior to TOC measurements, samples were treated with 10% HCl to remove carbonates. The samples are combusted in the analyzer, and the concentration of the resulting gases is measured and compared to standards of known composition to arrive at a weight. This is compared to the original sample weight to obtain a gravimetric percentage of the elements of interest. Samples were measured twice and their mean value is reported. Stable carbon isotopes were measured on carbonate-free samples using a Finnigan MAT Delta-S mass spectrometer equipped with a FLASH elemental analyser and a CONFLO III gas mixing system. Samples are oxidized, the gas is ionized, and the charged ions are deflected with a magnet, with heavier isotopes being deflected less. The mass spectrometer measures the weight of the different carbon isotopes in the sample and compares their ratio (^{13}C / ^{12}C) to a laboratory standard of known isotopic composition. The $\delta^{13}C_{org}$ of the sample is reported in ‰ relative to V-PDB. Isotopic ratios were measured twice and standard deviations are generally better than ±0.15‰.

4.4.2 Soil organic carbon determinations

For each terrain unit in the study area, the onshore TOC measurements were used to calculate the mass of soil organic carbon (M_C) for a 1 m^2 soil column equal in depth to the mean bluff height. For terrain units that did not contain a sampling site, values were extrapolated from areas with similar surficial geology and permafrost conditions. Where more than one sampling site occurred in a terrain unit, TOC values were averaged before calculating the carbon mass. A column's M_C is given by:

$$[4.1] \qquad M_C = \sum_{j=1}^{n} \rho_b \; X \; h \; X \; \%OC$$

where M_C is the mass of soil organic carbon in a soil column (kg), ρ_b is the dry bulk density based on the original frozen volume (kg/m^3), h is the thickness of the soil layer in question (m), and %OC is the percentage of TOC by weight in a unit layer. The layers are summed to arrive at a value for the entire soil column. A similar procedure is followed to obtain the mass of the mineral portion of the sediment:

$$[4.2] \qquad M_S = \sum_{j=1}^{n} (\rho_b \ \mathrm{X} \ h) - M_C$$

where M_S is the mass of mineral sediment (kg). For organic carbon, the lowermost soil layer, which generally comprises the largest percentage of the bluff, was assigned the lowest measured value for organic carbon. In cases where this value did not appear representative of the lowermost layer, a default value of 0.792 TOC (%wt) was assigned. This was one of the lowest values found in the study and came from a sample at the base of the highest cliff in the study area. Where no surface layer sample was available, a 10 cm-thick organic layer was assumed, with a TOC content of 25%. These are conservative estimates based on horizon data reported by Michaelson et al. (1996) and Bockheim et al. (1999; Bockheim et al., 2003). Sand and gravel beach deposits were assigned a value of 1.8% based on measurements by Smith et al. (1989) and Lawrence et al. (1984). For grab samples that had no volume measurements, bulk density was estimated from gravimetric ice contents according to the following equation:

$$[4.3] \qquad \rho_b = \frac{\text{mass of sediment}}{\text{vol. of ice + vol of sed.}} = \frac{100}{(\theta_i / \rho_i) + (100 / \rho_p)}$$

where θ_i is the gravimetric ice content of the sample (%wt) and the mass of the sediment is therefore assumed to be 100 g, ρ_i is the bulk density of ice (assumed to be 0.917 g/cm^3), and ρ_p is the particle density of the sediment (assumed to be 2.6 g/cm^3). There was a strong correlation (r^2 = 0.92) when values estimated using this method were compared to measured values (Figure 4.2).

Where gravimetric ice contents were not available, another method was used based on several studies that showed a significant relationship between organic carbon concentrations and bulk densities (Bockheim et al., 1998; Bockheim et al., 2003). In those cases, bulk density was estimated according to the following empirically derived equation (Bockheim et al., 1998):

$$[4.4] \qquad \rho_b = (1.374)\ 10^{-0.026x}$$

where x is the TOC (%wt).

All TOC values were corrected to account for the volume occupied by wedge ice and massive ground ice in each layer within the column. Percentages of these ice types for each terrain unit are given by Couture and Pollard (Chapter 3, this work). Corrections were not applied for pore ice and thin lenses of segregated ice, since it was already accounted for by the use of dry bulk density in the mass calculations.

4.4.3 Flux of soil organic carbon

Previous studies on coastal erosion have used shoreline length and bluff height to calculate the volume of material subject to erosion. However, the length of a shoreline will vary depending on the scale at which it was measured (Mandelbrodt, 1967). Because a large-scale map is more detailed, shoreline measurements will be longer than on a small-scale map with less detail. Lantuit et al. (2009) showed that scale-related errors of more than 30% can occur in some cases, and demonstrated that using area to calculate volumetric loss provides more robust results. In the current study, terrain units were originally delimited by establishing a buffer 100 m from the shoreline using a simple GIS routine; their area was calculated using only the landward side of the buffer. To calculate the TOC flux from shoreline erosion, the following equation was used:

$$[4.5] \qquad F_C = R\ (A / 100)\ (M_C/1000)$$

where F_C is the annual flux of organic carbon for a terrain unit (Mg/yr), R is the mean annual rate of erosion for a terrain unit, A is the area occupied by a terrain unit, and M_C is the total mass of organic carbon per soil column as defined above. Annual erosion rates for the terrain units are taken from Harper et al. (1985), except where more recent site-specific values are available.

4.4.4 Fate of the eroded soil organic carbon

In order to establish how much of the soil organic carbon from the Yukon Coastal Plain is being sequestered in nearshore sediments, two bulk identifiers were examined in the offshore marine sediments: stable carbon isotopes and carbon/nitrogen ratios. The amount of terrigenous organic carbon in the bottom samples was determined from the following equation, which assumes linear mixing between the terrigenous and marine sources of organic matter:

$$[4.6] \qquad TerrOC = \frac{\delta^{13}C_{sample} - \delta^{13}C_{marine}}{\delta^{13}C_{terrigenous} - \delta^{13}C_{marine}} \times 100$$

For the terrigenous end-member in the above equation, $\delta^{13}C_{org}$ was measured directly in the onshore samples. The marine end-member can be quite variable in the Arctic due to environmental effects on phytoplankton and contributions from sea-ice algae (Stein and Macdonald, 2004a and references therein). Here, we use a value of -20.75‰, as this is intermediary between the one proposed by Naidu et al. (2000) (-24‰) and that used by Belicka and Harvey (2009) (-17.5‰). The use of the C/N ratio helps to reduce uncertainty associated with the variability of the marine end-member.

4.5 Results

Of the 44 terrain units in the study area, TOC samples were collected directly from 17 units (Figure 4.1). Results were extrapolated to a further 16 units with similar characteristics, and in some cases, supplemented with stratigraphic information from previously published sources. For the marine units (i.e., beaches and spits) which we were unable to sample, TOC values reported in the literature were used.

4.5.1 Ground ice

As noted earlier, pore ice and thin lenses of ground ice are accounted for in SOC calculations by the use of dry bulk densities. The amount of wedge ice decreases with depth and ranges from a high of 53% of soil volume to less than 1%. Table 4.1 shows average values taken up by wedge ice in different depth ranges; it should be noted, however, that corrections to SOC contents were applied based on the specific depths of the sample layer. Massive ice, although not present everywhere, accounted for between 52 and 97% of the volume in soil layers where it did occur. Applying corrections for the volume taken up by wedge and massive ice reduces SOC values by an average of 19%, and sediment values by 16%. Table 4.2 shows the reductions for those terrain units that contained wedge ice or massive ice.

4.5.2. Organic carbon contents

The corrected organic carbon and sediment contents and fluxes for all units are shown in Table 4.3. Across all units, the mean TOC content in a 1 m^2 soil column is 223 kg. Values range from 30 to 919 kg C/m^2 and generally increase with bluff height, as the volume under consideration increases. Within the top 1 m, the mean value is 41 ± 15 kg C/m^2. Average values varied based on surficial materials and were highest in fluvial deposits (58 ± 10 C/m^2), followed by lacustrine (47 ± 13 C/m^2), glaciofluvial (44 ± 17 C/m^2), morainal (40 ± 15 C/m^2), and finally marine (27 ± 4 C/m^2). Analysis of variance (ANOVA) shows significant differences based on material type, but further testing (Tukey-Kramer HSD) reveals that only the marine unit shows a significant difference from all groups except the glaciofluvial one (Figure 4.3). On average, the top meter contains 43.2 ± 33.0% of the organic carbon in the soil column. At the site level, SOC contents generally decrease with depth. The mean percentage of organic carbon for individual samples was 9.3% by weight, with a low of 0.5% and a high of 49.4%. As a percentage of the entire soil column weighted by layer thickness, organic carbon averaged 4.9 ± 4.7%, with a range of 1.1 – 17.0%. The lowest values were seen in high bluffs with a significant mineral content (i.e., Herschel Island) and the highest values were seen in low bluffs with a thick organic cover (i.e., Komakuk Beach).

4.5.3 Material fluxes

The average erosion rate for the entire Yukon Coastal Plain is 0.7 m/yr. Thirty five of the terrain units (comprising 75% of the shoreline) are undergoing erosion, four are accreting (14%), and five are stable (11%). Although SOC fluxes from individual terrain units are provided in Table 4.3, it is the flux per meter of coastline that is important for comparison between different parts of the coast, and between the Yukon coast and other regions in the circum-Arctic. The average

SOC flux is 157 kg C/m/yr, with a maximum of 873 kg C/m/yr. The flux of sediment is 7.3 X 10^3 kg/m/yr on average, with a maximum value of 58.9 X 10^3 kg/m/yr. This results in a total flux of organic carbon from the Yukon coast of 0.04 Mt (1 Mt = 10^9 kg) per year and a flux of 2.66 Mt of sediment.

4.5.4 Organic carbon in nearshore sediments

Analysis of 50 onshore samples taken from different terrain units gives an average $\delta^{13}C_{org}$ value of - 27.12 ± -0.77‰ . This is the value used as the terrigenous end-member in the mixing model to determine the percentage of terrigenous organic carbon in the nearshore sediments. Twenty six samples of the nearshore samples were analyzed for $\delta^{13}C_{org}$ ‰. Three samples should be viewed with caution because they showed very little decomposition and their isotopic values were higher than that used for the terrigenous end-member. Samples were taken up to 500 m from shore and at water depths ranging from 0.9 to 14.5 m. Table 4.4 shows the results from isotopic analyses and from the mixing model. C/N ratios for the marine samples ranged from 11.3 to 25.9.

4.6 Discussion

4.6.1 Ground ice

As was seen from the reduction of SOC and sediment values in Table 4.2, failing to account for ground ice can result in significant overestimates of the total amount of material contained within a terrain unit and the annual flux of that material. Overall, this leads to errors of close to 19% and 16% in the assessment of total organic carbon and mineral sediments, respectively. However, in terrain units with a high proportion of ground ice, errors can be as high as 88% for SOC and 146% for sediment. This underscores the importance of properly identifying and quantifying massive ice bodies in coastal deposits. Although wedge ice has been shown to account for just 3% of frozen materials along the Yukon Coastal Plain (Couture and Pollard, Chapter 3, this work), it takes up 14% of the upper 7 m of soil, where the organic carbon-rich layers are found. Our values for wedge ice are approximately twice those of Jorgenson and Brown (2005) who use a slightly cruder ice wedge geometry in their calculations of OC contents for the Alaska Beaufort Sea coast. It is not just the overall volume of ground ice but the stratigraphic relationship between wedge ice and organic carbon, in particular, that is important since they both vary with depth. Some studies, while acknowledging the importance of ground ice, do not include it in their calculations of material fluxes (i.e. Harper and Penland, 1982; Hill et al., 1991). Others consider ground ice volumes in varying degrees of detail. Brown et al. (2003) use an average value of 50% for all ground ice types along the Alaskan Beaufort Sea. Rachold et al. (2000) use different values for different coastal types along the Laptev Sea; some are simple averages, while other are based on the various types of ground ice. Dallimore et al. (1996) provide an in-depth evaluation of all types of ice in their calculations of sediments fluxes from northern Richards Island in the Mackenzie Delta. In some cases, the importance of a detailed investigation depends on the geomorphology of the coast. For instance, Brown et al.'s (2003) use of an average ground ice value of 50% does not have a significant impact on potential stratigraphic differences because the mean elevation of bluffs they are looking at is only 2.5 m, so changes in ice content or in SOC content with depth are not as important. Considering the varied elevations along the Yukon Coast and the wide range of ground ice volumes with depth, our detailed approach is warranted.

4.6.2. Organic carbon contents

Given the sparseness of data on soil organic carbon for the Yukon Coastal Plain, this study provides a better picture of C stores in a region where carbon cycling is likely to increase. In addition to nearly tripling the number of pedons for which data is available, the results provide important information about deeper stores of organic carbon. The overall average SOC value reported here (223 kg C/m^2) is approximately 4 to 6 times higher than many previous estimates of total OC primarily because this study examines the entire soil column, whereas previous ones only looked at the upper portions. Our values are much closer to those reported by Tarnocai et al. (2009) who look at depths up to 3 m. Their study found organic carbon contents ranging as high as 352 kg C/m^2. When comparing the top 1 m of soil, our average value of 41 kg C/m^3 is consistent with the value reported by Bockehim et al. (1999) for the Alaska coast (50 kg C/m^3). As noted by those authors, this is less than other inland Arctic sites (62 kg C/m^3 reported in Michaelson et al., 1996 and 65 kg C/m^3 in Bockheim et al., 1998), but is likely due to higher ground ice contents in the coastal regions. Our results emphasize how important it is to include deeper carbon in calculations since only 43% of the SOC in our study was above 1 m, with 57% of it at greater depths. Bockheim and Hinkel (2007) found 64% of SOC above 1 m and 36% in the 1-2 m depth range. Tarnocai et al. (2009) had 48% above 1 m, and 52% between 1 and 3 m; when they included even deeper deposits, the ratio became 30% SOC above 1 m to 70% below. A number of different processes have contributed to the presence of organic carbon at depth in the sediments of the Yukon Coastal Plain including cryoturbation, alluvial deposition, ice-thrusting, accumulation in lacustrine basins, and possibly some aeolian deposition (Rampton, 1982). Coastal erosion involves the mobilization of all the carbon in the soil column relative to the sea level, so it is essential to consider deep SOC in flux calculations. In more inland regions, processes that affect carbon cycling (such as the thaw of the upper part of permafrost), are more likely to involve near-surface SOC only, so the consideration of carbon at greater depths may not be as critical. Several of the assumptions made in this study are conservative, particularly with regards to the 25% organic carbon content in the surface horizon and in extrapolating the values of 0.792% to the base of soil columns. In addition, the amount of carbon in the ice-thrust morainal units is likely underestimated since a minimum SOC value was used for most of the volume of the bluff, but glaciotectonic activity likely resulted in an interlayering of carbon-rich and carbon-poor layers.

4.6.3 Material fluxes

The results presented here give the fluxes of SOC (0.04 Mt/yr) and sediment (2.66 Mt/yr) from the Yukon Coastal Plain only. The sediment flux is 70% more than the value given by Harper and Penland (1982) for the Yukon (and later used by Hill et al., 1991). Those authors noted that their sediment flux was a first approximation only and was likely a maximum value since they were not accounting for ground ice volumes. The discrepancy with our results is partly due to the fact that their study considered less of the coastline to be erosive (150 km vs. the approximately 220 km considered here), and partly due to probable differences in bluff height estimation. The only other study of SOC flux for the region is based on the entire coastline of the Canadian Beaufort Sea (Macdonald et al., 1998) and provides a range of potential fluxes. Using data from Yunker et al. (1991), Macdonald et al. estimate annual flux to be 0.06 Mt/yr. Their value for the Yukon coast would be 0.015 Mt/yr, which is one third of the flux found in this study. Again, they consider a shorter length of coastline and only look at eroding peat, not other sediment contained in the coastal bluffs. Their maximum estimate is 0.3 Mt/yr based on data from Hill et al. (1991) and a presumed SOC content for all coastal sediments of 5% by weight. The value for the Yukon portion of the coast would be 0.12 Mt/yr, which is three times our result. As seen above, however, eroded volumes did not account for ground ice and so are likely too high. It is interesting to note that even though SOC values for our terrain units ranged from 1 to 17%, the value assumed by Macdonald et al. is the same as our average of 5% for all units. If our results from the Yukon Coastal Plain are applied to the other areas of peat erosion examined by Macdonald et al. (1998), the average flux of organic carbon from the Canadian Beaufort Sea would be 0.19 Mt/yr, which is more than three times the value used to date in Arctic Ocean budgets (Rachold et al., 2004). This is approximately 10% of the particulate organic carbon input by the Mackenzie River each year (MacDonald et al., 1998), which has the largest carbon input of any Arctic river (Rachold et al., 2004).

A comparison of flux rates of organic carbon per metre of coastline for the different terrain units shows a strong relationship between the flux rate and bluff height (r^2 = 0.68), and a slightly weaker one between C flux and erosion rate (r^2 = 0.42). The flux of SOC per metre of coast found in this study (157 kg C/m) is intermediate to the results of studies for other Arctic Seas. Along the Alaskan Beaufort coast, Jorgenson and Brown (2005) estimated an average annual flux of 149 kg C/m, while Streletskaya et al.'s (2009) results for the Kara Sea indicate a flux of 154 kg C/m. Rachold et al. (2004) found an average of 263 kg C/m for different coastal types along the Laptev Sea and 375 kg C/m for the East Siberian Sea. Sediment fluxes show similar trends for the different seas. The lower values for the Alaskan Beaufort and Kara Seas appear to be the result of lower bluffs and lower TOC contents, respectively. The higher fluxes from the Laptev and East Siberian are chiefly the result of higher erosion rates.

Finally, it should be noted that the calculations in this study only involve sub-aerial erosion. This is primarily due to the paucity of data available for the nearshore. Although, over time, a significant amount of material can be eroded below the waterline (Are, 1988; Reimnitz et al., 1988), the volume of freshly eroded material that is lost on an annual basis will not be that large and so carbon fluxes from these sources are likely to be quite small.

4.6.4 Organic carbon in nearshore sediments

Based on results from the isotopic mixing model, the organic carbon in the nearshore sediments is overwhelmingly terrestrial, with a mean terrigenous organic carbon content of 92%. The influence of the value for the marine end-member can be seen by examining the two values invoked in the literature. Had we chosen the heavier value of -17.5‰ proposed by Belicka and Harvey (2009), the proportion of terrigenous carbon would have been 95%. Using the lighter value (-24.00‰) for the marine end-member suggested by Naidu et al. (2000) would have resulted in a mean terrigeous OC value of 86%. Belicka and Harvey (2009) compared several different methods of estimating terrestrial organic carbon, including the isotopic mixing model. Although each of the four proxy methods they examined produced different results, the mixing model despite its sensitivity to the marine end-member, produced intermediate results. Because of the variability of the marine end-member, C/N ratios are used here to help in assessing the source of organic carbon in nearshore sediments. Figure 4.4 shows a plot of these two parameters for the nearshore samples. Although most samples are heavier than the terrigenous end-member, indicating a marine influence, the high C/N ratios help to confirm the strong contribution of terrigenous carbon to these samples. Previous studies of organic carbon in the Beaufort Sea (Figure 4.5) show a progressive decrease in the terrigenous component as distance from shore increases (Macdonald et al., 2004; Naidu et al., 2000). No obvious trend was seen in our data set when comparing terrigenous carbon contents with distance from shore, likely due to the fact that the maximum distance from shore was only 500 m. However, it is interesting to note that the two samples with the highest marine content (open circles in Figure 4.4) were taken north of Herschel Island in the area farthest from the mainland, and therefore most likely to be subject to marine influences. There is an overall shift towards heavier OC values from east to west in the Beaufort Sea, which is due to the greater importance of marine productivity in the more nutrient-rich waters in the west (Dunton et al., 2006; Naidu et al., 2000). The data presented here are consistent with that trend and are intermediate between values seen on the

Mackenzie Shelf to the east and the Alaskan Shelf to the west (Macdonald et al., 2004; Naidu et al., 2000).

Knowing how much of the organic carbon in the nearshore sediments is of terrestrial origin provides an indication of how much of the annual flux is being sequestered in those sediments and how much may be remineralized or exported off-shelf. Following Macdonald et al. (1998), we estimate organic carbon burial based on sedimentation rate and the proportion of OC in the marine sediments. Sedimentation rates for the area adjacent to the Mackenzie Delta are relatively well known, but there is much less information for the shelf area to the west. Based on data from Harper and Penland (1982), rates range from 2 mm/yr near the delta to less than 0.1 mm/yr in more distal areas. If we use the lower value of sedimentation and assume a solid density of 2600 kg/m^3 and a porosity of 60% for the marine sediments, then the annual flux of material to the seafloor for the entire shelf off the Yukon coast (3100 km^2 per Macdonald et al., 1998) would be 0.32 Mt/yr. Of this, 1.6% is organic carbon based on our measurements, 92% of which is of terrestrial origin. Therefore 0.005 Mt or 11.5% of the organic carbon eroded from the coastal sediments is sequestered in the nearshore sediments. This value is likely an upper limit since the sedimentation rate is probably even lower due to wave erosion and offshore transport of sediment (Macdonald et al, 1998; Reimnitz et al., 1988). The organic carbon not sequestered in the nearshore is presumably mineralized or transported off the shelf (de Haas et al., 2002). There is strong support that terrestrial TOC is involved in both processes. For instance, a considerable amount of terrigenous material has been found in sediment traps at the shelf edge (O'Brien et al., 2006) and beyond (Belicka et al., 2009; Belicka et al., 2002; Stein and Macdonald, 2004a), and Dunton et al. (2006) demonstrate that terrigenous organic carbon may constitute up to 70% of the dietary requirements of species in the nearshore along the Alaskan Beaufort Sea.

4.7 Conclusions

This study provides the first in-depth estimate of organic carbon content in coastal sediments of the Yukon Coastal Plain, and the first to specifically account for the volumes taken up by ground ice in those calculations. Soil organic carbon (SOC) is shown to constitute a large proportion of coastal bluffs. SOC accounted for between 0.5 and 49% by weight of the sediments sampled. This resulted in a mean carbon density of 41 kg C/m^3 in the top 1 metre of soil. Average values differed based on terrain units, being highest in fluvial sediments (58 kg C/m^3) and lowest in marine deposits (27 kg C/m^3), although differences between units were not considered significant in most cases. A considerable amount of SOC was also seen at depth, with the top meter accounting for only 43% of the total carbon in the soil column. In coastal flux studies, the entire soil column must therefore be considered, since failing to do so can result in underestimating carbon transfer by more than half. Terrain units with the lowest overall values of SOC were high bluffs with a high mineral content, while those with the highest SOC values were low bluffs with a thick organic cover. Wedge ice and massive ground ice constitute a significant portion of coastal sediments, with wedge ice accounting for up to 53% of the volume in some cases in the upper, carbon-rich soil layers. The variation of ground ice with depth is less important in low bluffs. If ground ice is not taken into consideration, flux measurements can be overestimated by 19% for SOC and 16% for sediment. Errors can be up to ten times that much in certain circumstances. The annual flux of organic carbon from coastal erosion along the Yukon Coastal Plain is 0.04Mt. Extrapolating these results to the area east of the Mackenzie Delta would result in a total coastal flux of organic carbon from the Canadian Beaufort Sea of 0.19 Mt/yr. This is approximately three times more than the values used to date in organic carbon budget calculations (Macdonald et al., 1998; Rachold et al., 2004). The sediment flux for the Yukon coast only is 2.66 Mt/yr, which is two thirds higher than previous estimates due to differences in the length of coastline considered and probable differences in cliff height estimates. A maximum of 11.5% of the organic carbon contributed to the nearshore by coastal erosion is sequestered in the shelf sediments. The rest is either metabolized in the nearshore or exported off the shelf by waves or ice action.

Table 4.1 Volume occupied by wedge ice at different depth ranges within the soil column. These are averages for the entire Yukon Coastal Plain. Values differ among different terrain units based on the size and spacing of wedges. Ice wedge depths for the region range from 3 to 7 m; ice wedge widths range from 1.5 to 2.3 m; and wedge spacings range from 7.5 to 20 m (Couture and Pollard, Chapter 3, this work). Since the depth and thickness of SOC measurements varied, actual corrections to SOC measurements were not made based on these averages, but rather on the specific percentage of wedge ice within the thickness of the sampled layer.

Depth range (m)	Wedge ice (%)
0 - 1	31
1 - 2	26
2 - 3	19
3 - 4	11
4 - 5	9
5 - 6	8
> 6	6

Table 4.2 Reduction in the measured values of soil organic carbon (M_C) and mineral sediment (M_S) once corrections are applied for wedge ice and massive ice. Corrections are needed because ice volumes were determined for the overall terrain unit, so are not accounted for within the individual samples. The volume of each ice type was calculated for every sampled layer of soil and a correction applied to the measured values of SOC and sediment. The results shown here are the summed values for all layers within a soil column.

Segment	Soil organic carbon			Mineral sediment		
	Before correction (kg)	After correction (kg)	Reduction (%)	Before correction (kg)	After correction (kg)	Reduction (%)
Roland Bay E	382	370	3	19533	19090	2
Running River	585	567	3	25469	25128	1
Sabine Point W	617	587	5	14464	14166	2
Komakuk Beach	145	135	7	956	868	9
King Point NW	674	616	9	49472	42848	13
Phillips Bay	159	143	10	5177	5039	3
Herschel Island N	641	575	10	68164	63476	7
Herschel Island W	1028	919	11	69280	62045	10
Komakuk Beach W2	221	195	12	3696	3496	5
Stokes Point W	527	466	12	29754	26576	11
Roland Bay W	456	402	12	25203	22620	10
Shingle Point E	315	277	12	24532	23359	5
Kay Point SE	507	443	13	33743	31179	8
Sabine Point	1009	864	14	47038	37944	19
Whale Cove W	51	44	15	662	579	13
Stokes Point SE	213	179	16	8749	8562	2
Herschel Island S	100	83	17	6790	5535	19
Roland Bay NW	112	93	17	679	570	16
Workboat Passage E	83	65	22	1603	1296	19
Kay Point	259	200	23	6940	5955	14
King Point	308	235	24	2619	1998	24
Workboat Passage W	157	118	25	2116	1601	24
Phillips Bay NW	275	204	26	15484	11384	27
Herschel Island E	437	307	30	30045	21519	28
Sabine Point E	617	424	31	14464	13034	10
King Point SE	188	116	38	15020	7558	50
Whale Cove E	81	50	38	4549	2606	43
Komakuk Beach W1	145	89	39	956	388	59
Shingle Point W	494	303	39	31378	27528	12
Clarence Lagoon W	218	116	47	3306	2568	22
Mean	**367**	**306**	**19**	**18728**	**16351**	**16**
Maximum	**1028**	**919**	**47**	**69280**	**63476**	**59**
Minimum	**51**	**44**	**3**	**662**	**388**	**1**

Table 4.3 Mass of soil organic carbon (M_C) and mineral sediment (M_S) for terrain units along the Yukon Coastal Plain. Values have been corrected for the presence of ground ice. Note that all sediment values are three orders of magnitude greater than organic carbon.

				Soil organic carbon					Sediment		
	Segment	Bluff height (m)	Erosion rate (m/yr)	M_C in 1 m^2 column (kg)	M_C in top 1 m (kg)	M_C > 1 m (kg)	M_C flux per m of coast (kg/yr)	M_C flux from unit (10^3 kg/yr)	M_S in 1 m^2 column (10^3 kg)	M_S flux per m of coast (10^3 kg/yr)	M_S flux from unit (10^6 kg/yr)
	Running River	23	0.7	567	59	508	390	1,535	25.1	17.3	68.0
	Shingle Point E	20	0.3	277	34	243	83	1,033	23.4	7.0	87.0
	Shingle Point W	26	0.4	303	35	267	115	1,029	27.5	10.4	93.6
	Sabine Point E	25	1.4	424	46	377	604	1,423	13.0	18.6	43.8
	Sabine Point	40	0.5	864	59	805	449	1,110	37.9	19.7	48.8
	Sabine Point W	25	0.8	587	46	541	477	1,267	14.2	11.5	30.6
	King Point SE	12	1.6	116	31	86	186	654	7.6	12.1	42.5
	King Point	7	2.4	235	40	195	574	541	2.0	4.9	4.6
*	King Point Lagoon	1	3.1	30	30	0	94	134	1.6	5.1	7.3
	King Point NW	40	0	616	40	576	0	0	42.8	0	0
	Kay Point SE	30	1.0	443	29	414	424	9,466	31.2	29.8	666.7
	Kay Point	7	2.7	200	63	138	531	1,518	6.0	15.8	45.1
*	Kay Point spit	1	0	30	30	0	0	0	1.6	0	0
	Babbage River Delta	3	0	157	72	86	0	0	2.4	0	0
	Phillips Bay	7	1.3	143	47	96	186	1,259	5.0	6.6	44.3
*	Phillips Bay W	1	0.6	34	34	0	19	86	1.6	0.9	4.2
	Phillips Bay NW	12	0	204	28	176	0	0	11.4	0	0
	Stokes Point SE	10	0.2	179	42	137	38	151	8.6	1.8	7.2
*	Stokes Point	2	1.4	57	24	33	78	246	3.1	4.3	13.4
	Stokes Point West	22	0.4	466	73	393	163	470	26.6	9.3	26.8
	Roland Bay East	15	0.3	370	24	347	107	200	19.1	5.5	10.3
	Roland Bay W	19	0.1	402	55	347	50	135	22.6	2.8	7.6
	Roland Bay NW	3	0.2	93	43	49	17	45	0.6	0.1	0.3
	Whale Cove E	5	0	50	18	32	0	0	2.6	0	0
*	Whale Cove	1	1.5	30	24	6	45	63	1.6	2.5	3.4

				Soil organic carbon					Sediment		
	Segment	Bluff height (m)	Erosion rate (m/yr)	M_C in 1 m^2 column (kg)	M_C in top 1 m (kg)	M_C > 1 m (kg)	M_C flux per m of coast (kg/yr)	M_C flux from unit (10^3 kg/yr)	M_S in 1 m^2 column (10^3 kg)	M_S flux per m of coast (10^3 kg/yr)	M_S flux from unit (10^6 kg/yr)
	Whale Cove W	2	0.1	44	36	8	3	17	0.6	0	0.2
*	Catton Point	1	0	42	24	18	0	0	2.3	0	0
	Workboat Passage E	3	0.4	65	33	32	25	255	1.3	0.5	5.1
	Workboat Passage W	5	0.5	118	42	77	62	111	1.6	0.8	1.5
	Herschel S	6	0	83	36	47	0	0	5.5	0	0
	Herschel E	25	0.8	307	34	273	230	2,423	21.5	16.1	170.0
*	Simpson Point	1	0	30	24	6	0	0	1.6	0	0
	Herschel N	60	0.7	575	30	545	408	6,721	63.5	45.1	741.7
	Herschel W	56	1.0	919	55	864	873	5,193	62.0	58.9	350.4
*	Avadlek Spit	1	0.8	30	24	6	23	219	1.6	1.3	12.0
*	Nunaluk Spit	1	1.0	36	24	12	34	902	2.0	1.9	49.2
*	Malcolm River fan w/ barriers	1	0	30	30	0	0	0	1.6	0	0
	Malcolm River fan	1	1.8	51	51	0	93	816	1.0	1.8	15.5
	Komakuk Beach	4	1.4	135	63	72	189	2,441	0.9	1.2	15.7
	Komakuk W1	4	0.7	89	64	26	60	97	0.4	0.3	0.4
	Komakuk W2	5	1.0	195	61	134	188	1,486	3.5	3.4	26.6
	Clarence Lagoon E	1	0.5	51	51	0	24	24	1.0	0.5	0.5
*	Clarence Lagoon	1	0.4	30	24	6	13	23	1.6	0.7	1.3
	Clarence Lagoon W	5	0.6	116	61	55	72	451	2.6	1.6	10.0
	Mean	12	0.7	223	41 ± 15	183	157	990	11.7	7.3	60.4
	Maximum	60	3.1	919	73	864	873	9466	63.5	58.9	741.7
	Minimum	1	0	30	18	0	0	0	0.4	0	0
	Total flux (Mt)							**0.04**			**2.66**

* Marine unit - TOC values from Smith et al. (1989) and Lawrence et al. (1984)

Table 4.4 Samples of marine sediments taken in the nearshore. The percentage of terrigenous organic carbon is based on a linear mixing model using $\delta^{13}C_{org}$ values from the samples and from known terrigenous and assumed marine end-members (see Equation 4.6). There are no significant trends in variations of terrigenous OC with water depth or distance from shore.

Sample	Distance from shore (m)	Water depth (m)	TOC (%)	C/N ratio	$\delta^{13}C_{org}$ (‰) vs. PDB	Terrigenous OC (%)
01-06	500	10.6	0.630	20.3	-26.86	95.9
03-06	100	3.7	0.979	11.9	-26.10	84.0
05-06	30	1.9	1.013	11.3	-26.21	85.7
06-06	500	14.5	0.829	18.0	-26.44	89.4
13-06	110	2.3	1.384	16.2	-26.91	96.7
15-06	500	2.7	1.375	20.1	-26.59	91.7
20-06	500	7.6	1.175	15.3	-27.00	98.1
27-06	250	1.2	1.014	18.6	-27.07	99.2
29-06	50	3.0	0.661 *	16.3 *	-27.19 *	> 100 *
30-06	30	2.0	15.317 *	45.1 *	-27.86 *	> 100 *
33-06	500	5.0	0.275	12.2	-26.69	93.2
38-06	30	3.8	0.861	13.4	-26.99	98.0
42-06	500	9.6	7.877	25.9	-26.72	93.7
45-06	250	5.2	1.142	14.0	-26.44	89.4
46-06	500	8.0	1.074	11.5	-26.52	90.5
47-06	30	2.3	1.853	13.5	-26.67	93.0
49-06	100	2.3	1.809	13.4	-26.37	88.3
51-06	500	2.5	1.944	13.1	-26.49	90.1
55-06	120	2.9	2.218	14.5	-26.58	91.4
57-06	500	2.7	1.435	15.0	-26.58	91.5
58-06	30	0.9	1.269	14.0	-26.31	87.3
62-06	500	6.7	0.801	12.4	-26.22	85.8
Mean			1.5	15.2	-26.6	91.7
Maximum		14.5	7.9	25.9	-26.1	99.2
Minimum		0.9	0.3	11.3	-27.0	84.0

* Samples omitted from calculation of means, maxima and minima because of unusually high terrigenous content.

Figure 4.1 Sampling sites within the 44 terrain units along the Yukon Coastal Plain. Samples of soil organic carbon (SOC) were collected at 26 onshore sites (▲) and 14 offshore sites («).

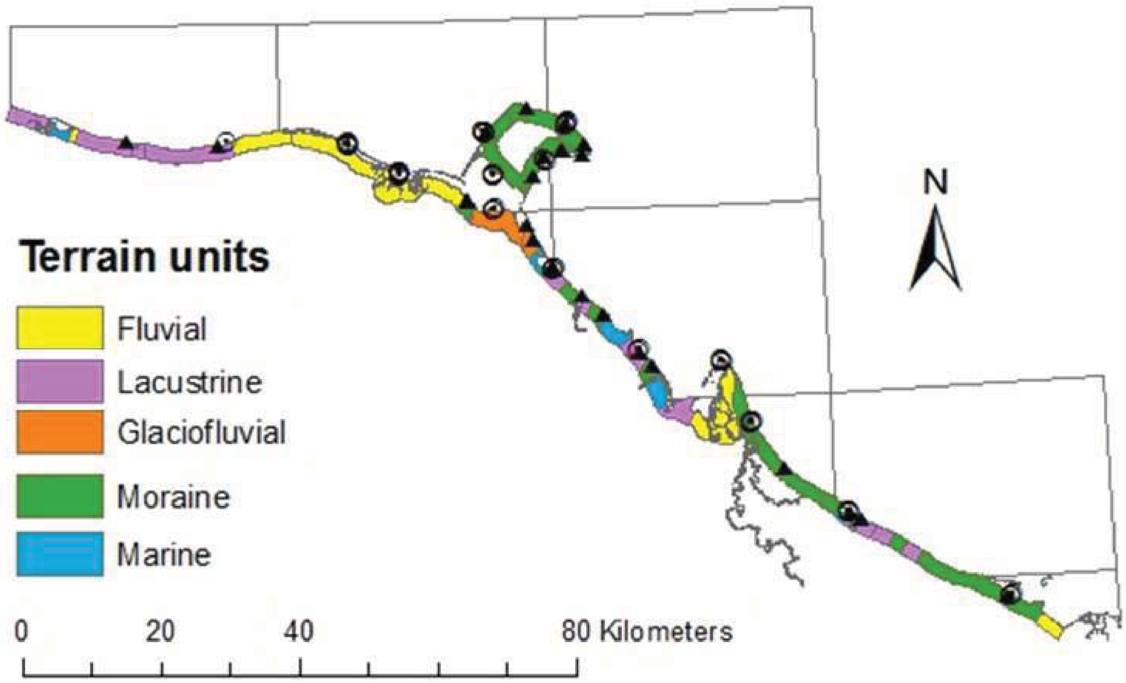

Figure 4.2 Relationship between measured bulk density and bulk density estimated from gravimetric ice contents (Equation 4.4).

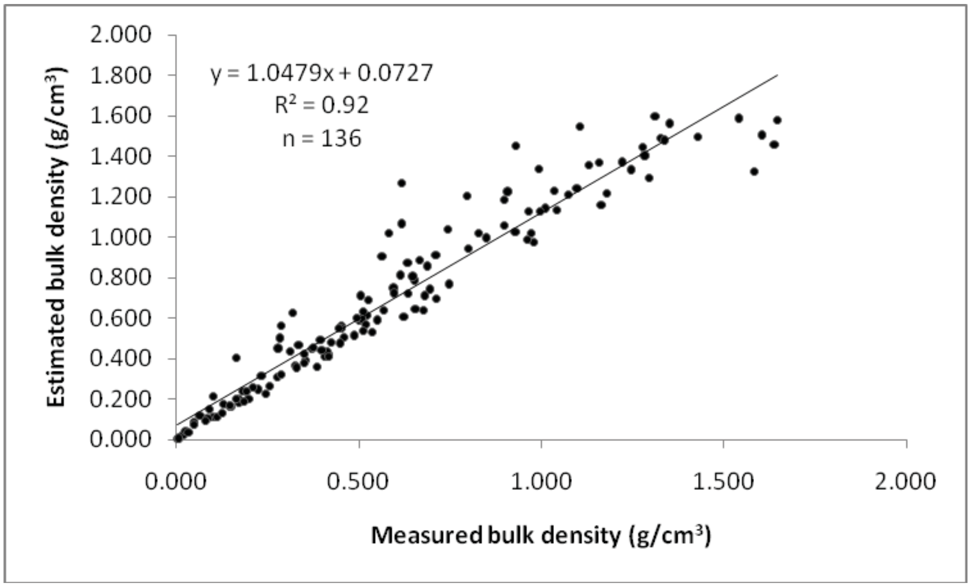

Figure 4.3 Variation in carbon density in top 1 m for terrain units with different surficial geologies (F = fluvial; G = glaciofluvial; L = lacustrine; M = morainal; Ma = marine). The line in the middle of boxes represents the median, with lower and upper part of the box representing 25% and 75% of the distribution, while the lower and upper whiskers represent the minimum and maximum of the distribution. Materials not sharing the same lower case letter above the box plots are significantly different from each other based on the Tukey-Kramer HSD comparison of means ($p < 0.05$).

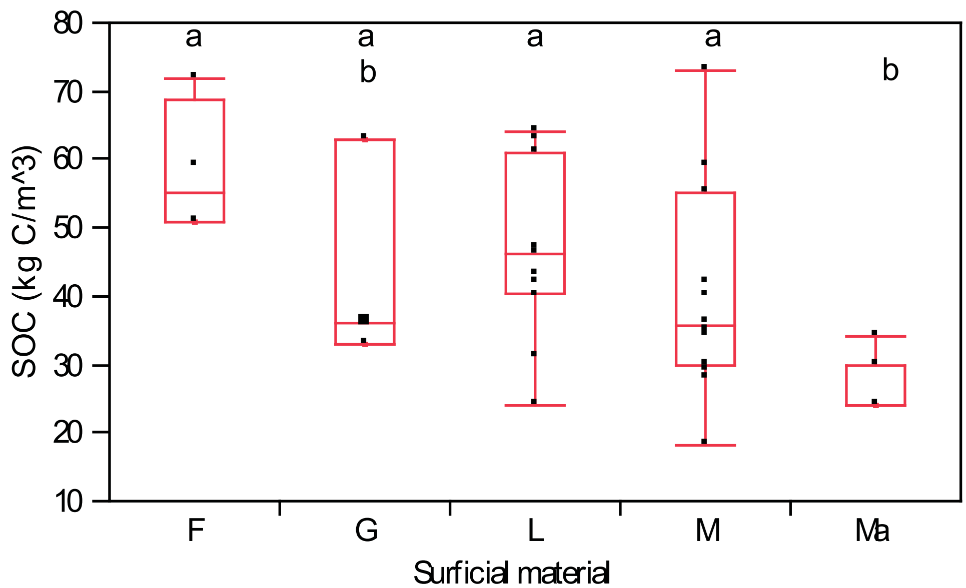

Figure 4.4 A plot displaying the relationship between C/N ratios and $\delta^{13}C_{org}$ for samples from the nearshore zone along the Yukon Coastal Plain. The proportion of marine vs. terrigenous organic matter can be inferred by assuming that organic carbon from a purely marine source will have a $\delta^{13}C$ value of approximately -20.75‰ (based on data from Naidu et al. (2000) and Belicka and Harvey (2009)) and a C/N = 6 to 7 (Macdonald et al., 2004). Samples from a purely terrigenous source are assumed to have a $\delta^{13}C$ value of -27.04‰ and C/N = 10 to 20, or even higher (Macdonald et al., 2004). Open triangles represent 3 samples that showed very little decomposition and appear to consist almost entirely of terrestrial organic matter. The dashed circle shows where a typical terrigenous end-member would be found, while the arrow indicates increasing marine organic matter content. The open circles are samples taken north of Herschel Island (see text for details).

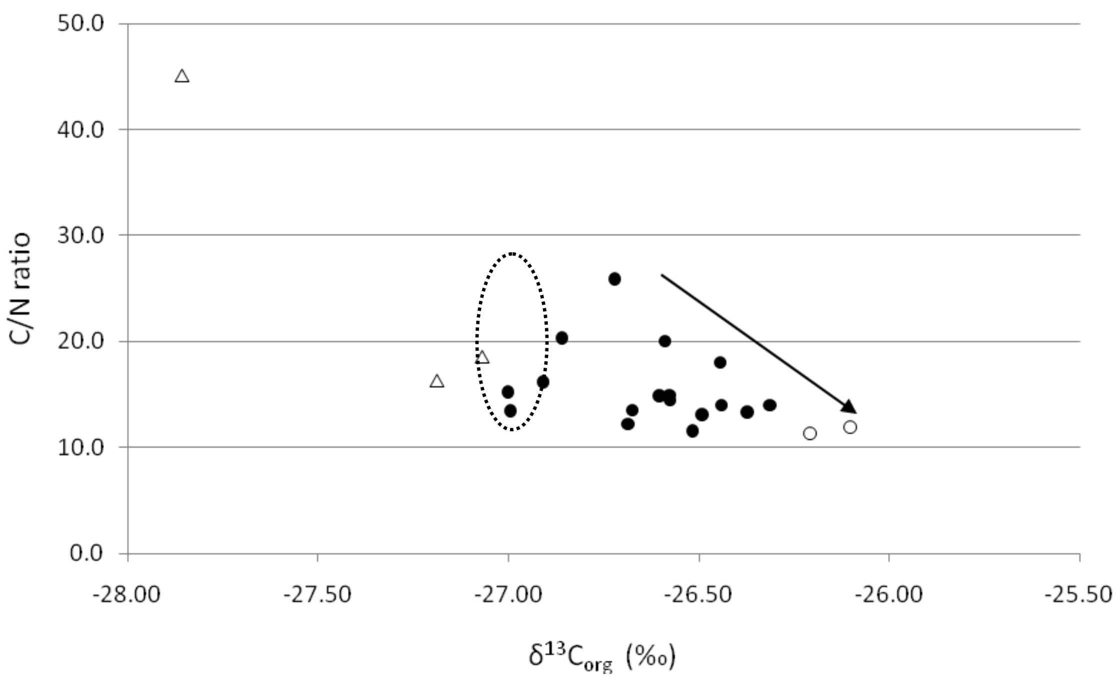

Figure 4.5 Distribution of $\delta^{13}C$ values in the sediments of the Beaufort Sea (from Macdonald et al., 2004 and based on data from Naidu et al., 2000). The heavier values farther from shore represent the increasing influence of marine organic carbon. Note the lighter values at the mouths of the Mackenzie and Colville Rivers, indicating a strong terrestrial signal. Blue dots correspond to samples from this study which conform to the contour lines shown. Yellow dots represent samples which do not match the contoured values and would suggest a slight modification of the lines to what is drawn here in yellow (Figure adapted from Macdonald et al., 2004).

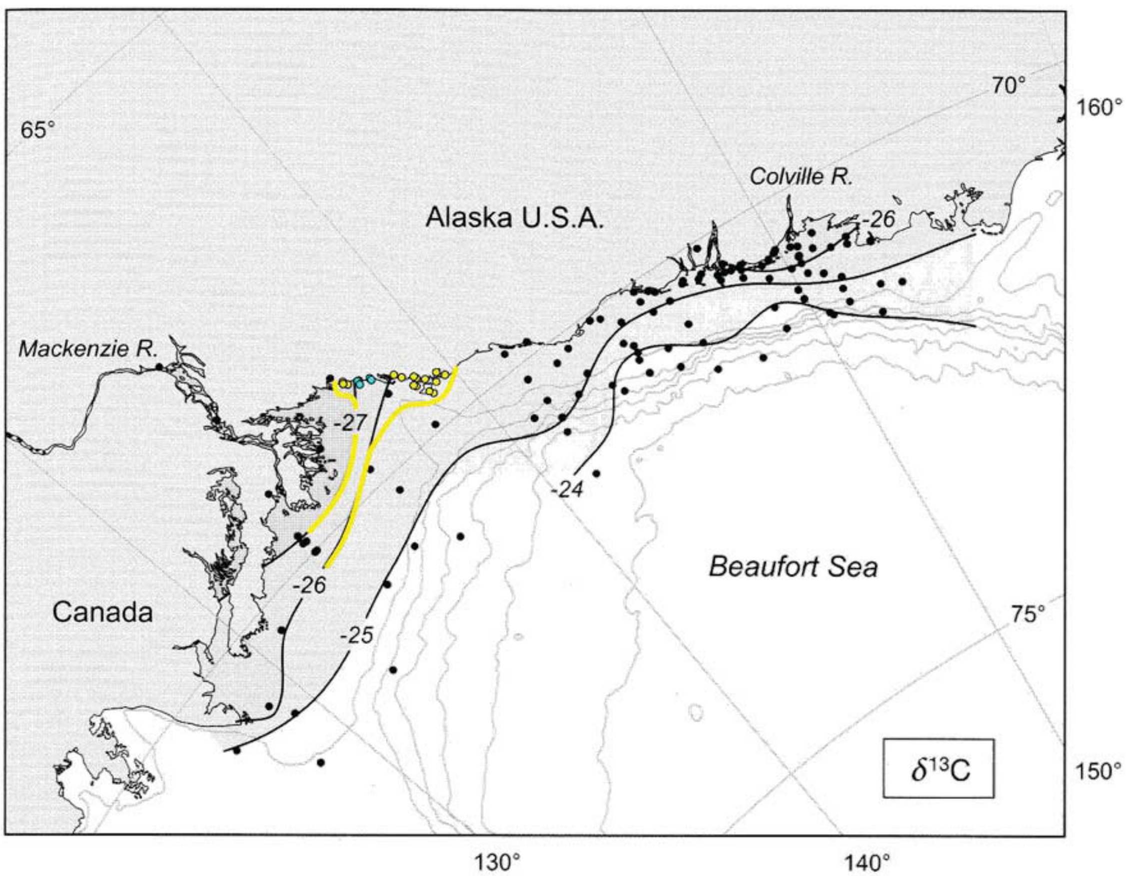

CHAPTER 5

PREDICTING FUTURE FLUXES OF ORGANIC CARBON FROM THE YUKON COASTAL PLAIN TO THE BEAUFORT SEA

5.1 Context within the thesis

Terrigenous organic carbon from coastal sources plays a significant role in the carbon cycle of the Arctic Ocean. As climate changes, the importance of this role is likely to change as well. The goal of this chapter is to assess how much the flux of SOC from the Yukon Coastal Plain is likely to increase in the coming decades. Current coastal erosion rates are examined in light of wave climate parameters and the ground ice contents calculated in Chapter 3. Future erosion is then established by examining how changing meteorological parameters will influence the potential wave climate. Finally, estimates of the future flux of soil organic carbon are determined using these predicted erosion rates and the organic carbon contents of the coastal sediments which were presented in Chapter 4. From this, we draw conclusions about the impact of future SOC fluxes.

5.2 Introduction and background

The oceans play a significant role in climatic change and understanding both positive and negative feedbacks to the system is crucial. Given the importance of the oceanic carbon cycle to these processes, an insight into changing carbon fluxes can help in anticipating the magnitude of feedbacks. The Arctic Ocean currently receives significant amounts of sediment and organic carbon from both riverine and coastal sources (Rachold et al., 2000; Rachold et al., 2004; Stein and Macdonald, 2004a; Vetrov and Romankevich, 2004) and this is likely to increase as a result of changing environmental forcings (McGuire et al., 2009).

In the Arctic, coastal erosion is both a mechanical and a thermal process and erosion rates are a function of wave energy, as well as the composition and morphology of coastal features (Are, 1988; Reimnitz et al., 1988; Kobayashi et al., 1999; Nairn et al., 1998; Wolfe et al., 1998). The Arctic Ocean's seasonal ice cover limits fetch, subdues wave action and paradoxically both reduces and enhances the erosion of coastal and nearshore sediments, making the coastal dynamics here distinctive from other parts of the world. In general, erosion in the region is limited to a three to four month ice-free period. During that time, fetch and wind are two of the most important meteorological variables governing wave behaviour. These variables are predicted to change in the coming decades (Manson and Solomon, 2007; McGillvray, 1993; Meehl et al., 2007) and are contributing factors to the Canadian Beaufort Sea coast's vulnerability to climate warming and sea-level rise (Shaw et al., 1998; Solomon et al., 1994). This coastline is of interest not only because erosion is likely to increase, but because its shores are especially rich in soil organic carbon (SOC) and, as such, the future flux of carbon will be affected.

Records from the Canadian Ice Service for 1979-2000 show that coastal areas of the Beaufort Sea are ice-covered for about nine months of the year, with break-up normally starting in the last week of June and freeze-up beginning in the first week of October. During the open-water season, ice-free fetches of more than 100 km are common, but the pack ice is usually within 200 to 300 km of the coast (McGillvray et al., 1993), however, it may remain within 20-50 km of shore in heavy ice years (Forbes et al., 1995). The southern Beaufort Sea is micro-tidal with astronomical tide heights less than 0.5 m, so it is storms which play the more important role in coastal dynamics because of their ability to generate large, high energy waves and to increase water levels due to surges. During the open water season, storm winds originate predominantly from the west and northwest, with a secondary mode from the east and northeast (Harper and Penland, 1982; Hill et al., 1991; Hudak and Young, 2002). Meteorological data from Distant Early Warning (DEW) line stations along the Yukon coast and near the Alaska border show general storm trends similar to those at Tuktoyaktuk (Solomon et al., 1994), but there are variations in wind direction and speed between coastal sites (Couture et al., 2008; Forbes, 1997; Harper and Penland, 1982).

Much of the coastal retreat in permafrost regions is known to occur as a result of storms (Dallimore et al., 1996; Héquette and Hill, 1993; Héquette et al., 2001; Solomon et al., 1994), but the link between storms and erosion rates is not fully understood. Two main erosional mechanisms are involved: the first is mechanical erosion due to higher energy wave action and increased water levels from storm surges, while the second is thermal erosion due to frozen sediments undergoing thaw from contact with warmer seawater (Are, 1988; Kobayashi et al., 1999). Thermal erosion occurs above the normal water line as a result of higher waves and water levels, but also below the waterline when any thawed material at the water-sediment interface is removed mechanically and the underlying frozen sediment is then subject to degradation. Commercial coastal erosion models cannot be applied in a permafrost setting because none of them can account for thermal erosion, or for ground ice as a shore material. A number of approaches have been used to explain and predict coastal recession in the Canadian Beaufort Sea region. Héquette and Barnes (1990) showed that coastal retreat was moderately correlated with several factors, including waves and coastal composition, but concluded that the action of sea ice in the nearshore was also important. Couture et al. (2008) compared actual retreat rates with potential retreat rates based on wave energy and longshore sediment transport. Several analytical and numerical models have been devised to help in explaining coastal processes (Hoque and Pollard, 2009; Kobayaski, 1985; Kobayashi et al., 1999; Nairn et al, 1998). Leont'yev (2003) developed a morphodynamic model to explain both short and long-term coastal evolution in terms of depth changes in the nearshore zone. He later adapted the model to account for thermally affected coasts (Leont'yev, 2004). Solomon et al. (1994) developed an index of storm intensity for the Canadian Beaufort Sea and demonstrated that shoreline recession at several points along the coast was strongly correlated with storm intensity. Manson and Solomon (2007) investigated the expected changes in a number of environmental forcings and developed a scenario of future conditions related to coastal evolution.

The goal of this paper is to examine the expected increase in material fluxes due to coastal erosion along the Yukon Coastal Plain of the Canadian Beaufort Sea. We hypothesize that future climatic changes will result in an increased rate of erosion and hence an increased flux. Current erosion rates are examined in light of the present-day wave climate. Expected changes in sea ice conditions and storminess for the mid-21st century are then outlined and used to predict a future wave climate and sediment transport scenario. Finally, the flux of material to the ocean is projected based on the morphology and composition of coastal bluffs. The focus will be on the action of waves in facilitating erosion, but the influence of other factors contributing to coastal retreat will be discussed as well. We emphasize that due to the uncertainties in climatic predictions and the incomplete understanding of erosional processes, particularly in permafrost environments, the present study attempts only an order of magnitude projection of future carbon flux.

5.3 Methods

5.3.1 Coastal profile model

Using expected changes in meteorological parameters, the morphodynamic model developed by Leont'yev (2003, 2004) is used to examine coastal profile evolution and coastal erosion along the Yukon Coastal Plain. Shoreline retreat occurs as water depths change. This can be due to removal of sediment in the nearshore, or due to changes in relative sea level (Figure 5.1). Although short-term changes in the nearshore zone may change the profile of a permafrost coast, it will eventually return to an equilibrium shape (Are et al, 2008). Leont'yev (2003, 2004) showed how changes in nearshore water depth, d, are related to short and long-term sediment transport according to the following equation:

$$[5.1] \qquad \frac{\partial d}{\partial t} = \frac{\partial q_x}{\partial x} + \frac{q_{aeol} + \Delta Q / \Delta y - q^*}{l^*} + w$$

where q_x is the short-term cross-shore sediment transport (i.e., at the scale of individual storm events), the second constituent on the right represents long-term transport (i.e., decadal scale), and the term w represents variations in relative sea level. The term q_{aeol} is aeolian sediment transport landward, $\Delta Q/\Delta y$ is the gradient in longshore sediment flux, q* is long-term seaward transport out of the active zone of the profile, and l* is the length of the active zone, defined as the distance between the upper limit of wave runup and the point where water depth is twice the mean wave height (Leont'yev, 2003). Maximum wave runup (R_{max}) is calculated following methods in the Coastal Engineering Manual (CEM, 2003) and is given by:

$$[5.2] \qquad R_{max} = 2.32\, H_s\, \xi_0^{0.77}$$

where H_s is the significant wave height (i.e., the highest one third of waves) and ξ_0 is the surf similarity parameter:

$$[5.3] \qquad \xi_0 = \tan \beta\, (H_s / L)^{-0.5}$$

where β is the beach and shoreface slope, and L is the wavelength.

Calculation of the short-term constituent in Equation 5.1 is beyond the scope of this study, and because the focus here is long-term coastal evolution, it is not considered further. In the Beaufort Sea region, aeolian sediment transport is negligible. Even though considerable amounts of sediment may be transported alongshore (Hoque et al., 2009), the flux is generally quite steady and the longshore gradient is therefore small and can be neglected (Leont'yev, 2003). Long-term seaward sediment transport can therefore be represented by q*/ l*. Leont'yev (2004) was able to develop an empirical relationship for q* by comparing observed and computed coastal retreat rates for a number of different Arctic sites having varying characteristics. For sites with ground ice, q* is represented by:

[5.4] $$|q^*| = 11.4\sqrt{h_{ce}\overline{H}}\,cos\Theta w - 11.1$$

where h_{ce} is the effective cliff height, $\overline{H}$ is the mean wave height for a once-per-year storm, and Θw is the angle of wave incidence relative to shore normal, which Leont'yev (2004) notes is more a measure of the direction of fetch area rather than storm winds, and can be represented by 0º as a result of waves refracting as they approach shore. The correlation coefficient for the relationship in Equation 5.4 is 0.90. The effective cliff height accounts for the presence of ground ice and is given by:

[5.5] $$h_{ce} = (1-n)\, h_c$$

where n is the percentage of ground ice and h_c is the actual height of the coastal cliff. Ground ice contents for terrain units along the Yukon Coastal Plain are taken from Couture and Pollard (Chapter 3, this work).

The long-term changes of depth will result in a shoreward translation of the coastal equilibrium profile. The equilibrium coastal profile is commonly represented by the Bruun rule, which can be written as:

[5.6] $$x = \sqrt[m]{\frac{d}{A}}$$

where x is distance between a given point and the shoreline, d is water depth, A is a dimensionless parameter related to sediment size, and m is a dimensionless coefficient that controls the profile shape. Although the Bruun rule is recognized as having a number of limitations (Komar, 1998, Masselink and Hughes, 2003; Pilkey and Cooper, 2004; Trenhaile, 1997), it has nevertheless been shown to provide a good fit for Arctic shoreface profiles (Are et al., 2008). Empirically determined values of the dimensionless variables for King Point and Komakuk Beach are provided in Are et al. (2008).

5.3.2 Current wave climate and erosion

Nearshore wave conditions along the Beaufort Sea coast were modelled by Hoque et al. (2009) for the 1985-2005 period. They used hourly deep water wave hindcast data from Environment Canada's Meteorological Service of Canada Beaufort (MSCB) project -- which in turn is based on NCEP/NCAR reanalysis wind data (Swail et al., 2007) -- and applied transformations to account for shoaling, refraction and incident wave angle. Two of the sites they examined were located along the Yukon Coastal Plain and are used in this study: Komakuk Beach (69.60ºN, 140.25ºW) in the western section of the coast, and King Point (69.15ºN, 138.00ºW) in the eastern section. The MSCB wind data was examined to isolate storm generating winds and waves from background values. Following several previous studies (Atkinson, 2005, Hudak and Young, 2002; Jones et al., 2009; Solomon et al., 1994), storms were defined as periods of 6 hours or more with a wind speed of at least 10m/s. Atkinson (2005) included lulls within his storm events, as well as the times leading up to and following the event itself. These were defined based on whether winds speeds crossed a "continuity threshold" of 7 m/s. An examination of longshore sediment transport and wave energy data from Hoque et al. (2009) shows that the rise and fall above background levels coincides closely with this same 7 m/s wind threshold, so we chose to include the periods above threshold level as part of the storm events. The mean wave height for once-per-year storm conditions was then extracted for input to the coastal profile model. Values of q* calculated from the model are compared with volumes of material currently eroding from the Yukon Coast to establish how well the model represents the long-term sediment flux. Current fluxes of organic carbon and sediment were determined by Couture and Pollard (Chapter 4, this work). The mean annual erosion rates used in the flux calculations cover different time intervals depending on the availability of data from published sources, but most span the period from the mid-1950's to the mid-1970's, with some extending into the 1990's and the 2000's. The assumption is made that the wave characteristics defined by the MSCB data are representative of the periods covered by the long-term erosion rates.

5.3.2 Changes in meteorological conditions

5.3.2.1 Sea ice

Satellite data show that since 1979, the annual extent of Arctic pack ice has declined by almost 10% per decade (Comiso et al., 2008; Serreze et al., 2007; Stroeve et al., 2007), with the decreases most pronounced in September. This trend is expected to continue (Dumas et al., 2005; Manson and Solomon, 2007; McGillvray et al., 1993; Walsh, 2008; Walsh et al., 2005), with some recent projections showing almost complete loss of summer sea ice by 2037 (Wang and Overland, 2009). Predictions from a suite of climate models used in the Fourth IPCC Assessment report which are based on the A1B climate forcing scenario (a "middle of the road" projection) show an increase in open water for the region of between 75 and 100 days by 2050 (Walsh, 2008). The current open water season along the Yukon Coastal Plain lasts approximately 104 days (last week of June to the first week of October), so using the average value from the IPCC models would results in a projected open water season of 191 days by 2050, an increase of 84%. Given that the greatest temperature increases are expected in the fall and winter (Serreze et al., 2007; Overland, 2009; Walsh, 2008), this implies that freeze-up will be delayed, providing for more open water during the stormier autumn months. In addition to increasing the time during which wave action can affect the coastline, an increase in open water will result in greater fetch and higher waves. McGillvray et al. (1993) estimated that under a $2xCO_2$ scenario, the average fetch length in the Beaufort Sea could increase to between 650 and 1100 km, with an associated increase in wave heights of 22 to 39%. We assume an average increase of 30.5%.

5.3.2.2 Storms

Studies documenting storm conditions in the southern Beaufort report storms counts of between 2 and 19 per year (Atkinson, 2005; Eid and Cardone, 1992; Hudak and Young, 2002; Manson et al, 2005). The difference in counts is due to slightly different criteria for storm definition, differing lengths of the storm season considered, and whether offshore or onshore winds were used in the assessment. Within a given year, however, as a rule both the number and the intensity of storms increased as the open water season progressed. There is a great deal of research examining future changes in cyclonic activity as a result of climate warming (Cassano et al., 2006; Ulbrich et al., 2009 and references therein). The overall consensus as stated in the IPCC's latest report is an increase in storminess at high latitudes (Meehl et al., 2007). How that translates into actual storm systems depends to a large extent on the methods used for identifying storms and quantifying the degree of their activity (Ulbrich et al., 2009 and references therein). A comprehensive review of climate projections which took into account these differences found that the total number of cyclones in the Northern Hemisphere is likely to decrease slightly under various climate warming scenarios in both winter and summer, but that the number of extreme cyclones (defined on the basis of core pressure) is likely to increase (Ulbrich et al., 2009). This is consistent with an earlier analysis by Lambert and Fyfe (2006) who examined 15 models for three different forcing scenarios from the 4^{th} IPCC Assesment Report (SRES B1, SRES A1B, and SRES A2) and one scenario where greenhouse gases were held constant at 2000 levels. Lambert and Fyfe (2006) provide measures of the degree of changes in storminess and, although their values are for winter conditions, we assume that the magnitude of change will be similar for open water conditions. Based on departures from 1961-2000 means, they estimate that by 2046-2065, there will be a decrease of 2% in the total number of storm events, and an increase of 7% in the number of intense events.

5.3.2.3 Water levels

Current changes in relative sea levels in the Beaufort Sea have been measured at 3.5 ± 1.1 mm/yr at Tuktoyaktuk due to subsidence, eustatic changes, or both (Manson et al., 2002). Assuming a further increase in steric sea level of 0.13 m by 2050 (Manson and Solomon 2007), total relative sea level in the region would rise by 0.31 m by mid-century. Positive storm surges are on the order of 1.6 m at Tuktoyaktuk (Kobayashi et al., 1999; Manson and Solomon, 2007; Solomon et al., 1994) and are generally higher than at other sites in the region (Harper et al., 1988). There are very few records of storm surges along the Yukon coast, however measurements from a storm in 2000 show a surge along the Yukon coast that was 0.7 times the height of the one at Tuktoyaktuk (S. Solomon, pers. comm.). Using this ratio gives a mean current surge value of 1.1 m for the Yukon coast. In his forecast of coastal recession in the Russian Arctic, Leont'yev (2004) anticipates an increase in surge levels of at least two-thirds. For the Beaufort Sea, Manson and Solomon (2007) showed that most of the variance in surge levels is explained by peak wind speeds, but they only project a slight increase in peak wind speeds. However, much of the increase in wind speeds is expected in the fall, which corresponds with periods of increased storm intensity and newly open water. We assume an increase in surge level for a storm-of-the-year to be 10%.

5.4 Results

5.4.1 Current wave climate and erosion

The storm characteristics for King Point and Komakuk Beach over the 1985-2005 period are shown in Table 5.1. The MSCB data show an average of 4 storms/year during the open-water period with a slight but statistically insignificant increase over the 20-year period. There were fewer storms at King Point than at Komakuk Beach, reflecting differences in wind direction and open water fetch length. Storm intensities are a function of the wind speed (which in turn affects wave height) and the duration of the storm. Intensities for the events in the MSCB database were determined by summing the hourly significant wave heights for each storm. The most intense storms for each year of the record were then averaged to ascertain the mean storm-of-the-year characteristics. The mean wave height for storm-of-the-year was 0.93 m for both sites, while the mean wave period was 6.0 m for King Point and 6.5 m for Komakuk Beach.

For those terrain units along the Yukon Coastal Plain that are actively eroding, initial values of the amount of material transported out of the active zone over the long-term (q*) were calculated using Equation 5.4 and are shown to be applicable for $11.4\sqrt{h_{ce}\overline{H}}\ cos\Theta w\ - 11.1\ >\ 0.97$. These values represent current day meteorological conditions. Figure 5.2 shows how this computed value compares with the volume of material eroded from the coastal bluffs that is determined from observed erosion rates and effective bluff heights. A 1:1 ratio between the two variables (the dashed line in Figure 5.2) indicates where eroded volumes are matched by long-term transport seaward. For points above the line, however, more material is being removed by long-term transport than is being added by bluff erosion. This implies that although some process is operating to transport material seaward over the long term, it does not result directly from bluff erosion. One possible explanation is that when large blocks of material are eroded from a bluff, there is a time lag before this material get transported seaward because of the time need for the blocks to be broken down by wave action. The effective cliff height appears to govern this process, with it being more prominent for higher bluffs (closed triangles in Figure 5.2) than for lower ones (open circles in Figure 5.2). The cliff height threshold separating the two cases lies between 4.1 and 4.4 m. The annual retreat rates for all the sites computed by the model was not correlated with observed retreat rates. Once the sites were divided into classes above and below the height threshold, however, the retreat rates showed significant correlation (Figure 5.3). Modelled erosion rates for the low cliff heights were of the same magnitude as observed rates, whereas modelled rates for the high cliff heights were close to one order of magnitude higher than the observed rates.

5.4.2 Future wave climate and erosion

The meteorological input parameters for the coastal profile model are shown in Table 5.2, as are their expected values for the year 2050. For simplicity, present day values are assumed to represent conditions in the year 2000. The model was run in 1-year time steps and parameter changes were considered to increase linearly by 1/50 of the total change each year. For each year, the resulting changes in water depth are computed by the model and converted to a coastline retreat based on Equation 5.6. Over the 50-year period, the total modelled retreat is up to 158 m for low cliffs , and up to 668 m for high cliffs (Table 5.3). Total erosion for the high cliffs is likely overestimated, however, due to the high retreat rates produced by the model. Because of these differences in the observed and the modelled retreat rates, it was decided that a more useful measure of how the coastline will evolve is the change in the erosion rates rather than absolute distances. Table 5.3 shows the percentage increase of the modelled erosion rates. The observed erosion rates are then multiplied by the percentage increase to arrive at projected values of annual erosion and of total retreat, both of which appear to better reflect actual conditions; these are the values used in the final flux analyses. For sites where cliffs were too low for the coastal profile model to be applicable, a 4% increase in erosion was assumed, which is the lowest percentage increase for low cliffs. The erosion rates of low cliffs increase over time (mean 1.1 to 1.4 m/yr), indicating a greater sensitivity to changes in meteorological parameters. High cliffs show a decreasing rate of erosion (mean 0.6 to 0.5 m/yr), except for one site (Stokes Point SE). So although the high cliffs continue to erode, the rate of retreat slows down, indicating that the changes in environmental forcings are not enough to keep pace with the increased input of sediment from the eroding cliffs.

5.4.3 Future fluxes of soil organic carbon

Current values of soil organic carbon fluxes are given by Couture and Pollard (Chapter 4, this work) and are shown in Table 5.4. The projected fluxes were obtained by multiplying carbon contents for each terrain unit by the projected erosion rates. Over the next 50 years, the mean SOC flux per meter of coastline will increase by 16% for low cliffs (from 120 to 139 kg C/m/yr), and decrease by 12% for high cliffs (from 315 to 278 kg C/m/yr). For all heights, this represents an average 2% decrease in flux (from 198 to 194 kg C/m/yr). A similar pattern is seen when considering the total annual flux: a 29% increase in the flux from low bluffs and a 13% decrease in the flux from high ones. The increase in total flux is greater for the low bluffs because more SOC is contained in the upper part of a soil profile, so SOC makes up a larger percentage of a low bluff. For the entire Yukon Coastal Plain, this results in an average overall decrease of 2% in the annual flux of organic carbon (from 0.044 Mt/yr to 0.042 Mt/yr).

5.5 Discussion

Despite the expectation that coastal erosion will increase uniformly under climate warming scenarios, results from this modelling exercise show that the response of a coastline depends to a large extent on its morphology and composition. Ice-thrusting and the deposit of glacial material have contributed to increasing the height of coastal bluffs along much of the Yukon Coastal Plain, so the region's geomorphic history influences coastal evolution. Leont'yev (2003, 2004) also noted variations in the response of coastal bluffs of different heights. Site-specific variables such as ground ice content and bed slope make it difficult to directly compare results, however. He posits that a slowing in the rate of erosion is due to a decrease in the slope of the shoreface as eroded sediment is added to the nearshore, and that this dissipates wave energy. In cases where he does not see a slowing of erosion, he expects that it would likely occur if the model were run for longer.

5.5.1 Model assumptions

The model outcomes need to be considered in light of a number of simplifying assumptions that were made. The first is that the empirical relationship for determining long-term flux (q*) is applicable in different regions. This appears to be a valid assumption since Leont'yev (2004) has demonstrated that the association holds well and shows little variance for a wide range of sites with different morphological and compositional characteristics in different parts of the Arctic. A second assumption is that this relationship will remain unchanged over time. This is not likely to be the case, however, since increases in the duration of both storms and the open water season imply an increase in q*. As such, the long-term fluxes and hence erosion rates calculated here are likely low estimates. Leont'yev (2004) presumes that q* for some sites in the Russian Arctic could increase by up to 66%. Another important assumption was the decision to ignore short-term sediment fluxes. Although overall losses from the system are still included within the long-term flux (q*), short-term fluxes change the nearshore morphological profile and affect slope and water depth. They also account for bottom currents generated by storm waves, and omitting such currents can result in an underestimate of coastal retreat (Héquette and Hill, 1993; Leont'yev, 2003). Because high bluffs add greater amounts of sediment to the nearshore than do low ones, errors associated with the omission of short-term flux and the related changes in nearshore morphology are likely more important for high bluffs. The model assumes that coastline evolution is the result of one high magnitude storm per year and that any other storms will simply result in shoreline oscillation or development of longshore bars. Although a decrease in storm numbers is predicted, the longer open water season means that, overall, more storms will likely impact the coasts. This would mean an increase in the ratio of low to high magnitude storms, so the impact of one single high magnitude storm may be lessened. It will thus become more important to ensure that short-term fluxes are considered. A final assumption is that the incident wave angle relative to shore normal is 0º. This is reflective of the orientation of the area of fetch rather than the origin of storm winds and although this may not currently be representative in regions where sea ice is close to shore, the expected increase of open water will make any errors associated with this assumption less important with time.

5.5.2 Environmental forcings

Several of the meteorological parameters used in the modelling exercise are conservative estimates. The increase in wave height was determined on the basis of greater fetch and did not explicitly account for greater storm intensity, due to the uncertainty of separating out the effects of increased fetch and of longer duration winds. The impact of more intense storms is therefore likely underestimated in future wave heights. Storm intensity was, however, accounted for to a certain extent by larger surge heights. However surge heights will also be affected by the amount of fetch available as well, a variable not explicitly factored in since it is also dependent on the direction of the storm. Manson and Solomon (2007) suggest that fetch might not have that important an effect on surge height in shallow areas with low shoreface slopes (i.e. depth limited areas), but this would not be the case along the Yukon coast where bed slopes are generally high. This study assumes a steady linear increase in the climatic factors, but this may not necessarily be the case since considerable year-to-year variability exists in such parameters as wave energy (Hoque et al., 2009; Manson and Solomon, 2007; Solomon et al., 1994), storminess (Atkinson, 2005; Hudak and Young, 2002), sea ice (Simmonds and Keay, 2009), and surge heights (Harper et al., 1988).

The assumption was made that the wave climate hindcast from the MSCB data (for the 1985-2005 period) is representative of the period when the erosion rates were measured (1950s-1970s in many cases). Although increases in erosion rates have been noted in Alaska in recent decades, (Jones et al., 2009; Mars and Houseknecht, 2007), there was a slight decrease in average erosion rates for Herschel Island between 1952 and 2000 (Lantuit and Pollard, 2008). The average retreat rate for the Yukon Coastal Plain used in this study is 0.7 m/yr and this value compares well with more recent measurements for the Mackenzie Delta region of 0.6 m/yr (Solomon, 2005). In that study, Solomon notes that although there is variability between sites, and some sites did see a slight decrease in retreat rates, average long-term rates remained constant over the 28-year period examined (from 1972 to 2000). The fact that changes in erosion rates are the focus of the modelling minimizes the importance of any errors in the starting values.

The spatial variability of meteorological parameters has been addressed to a certain extent by using different wave conditions for the eastern and western sectors of the Yukon coast. However, even though we consider the incident wave angle to be 0º at all sites, wave conditions will be slightly different for shorelines with different orientations. Solomon (2005) found coastal change rates were strongly influenced by exposure to northwest winds, with low retreat rates along east and south facing shorelines. The northwestern coast of Herschel Island shows much higher rates of erosion than other sites on the island (Lantuit and Pollard, 2008). The differences in shoreline orientation are reflected to a certain extent by differences in the observed erosion rates, but the model likely underestimates erosion on northwest facing coasts and overestimates it on coasts with other orientations. Shorelines may also be protected from wave attack by landmasses. Forbes (1997) notes that both Herschel Island and Kay Point exhibit strong sheltering effects from wind and waves and so the rates of change generated by the model may be too high for sites in this region.

The effects of sea ice are considerable in terms of coastal erosion. In addition to its impact on wave development, sea ice can gouge the sea floor, thrust sediments landward, and entrain and transport sediments seaward (Are, 1988; Forbes and Taylor, 1994; Héquette and Barnes, 1990; Héquette et al., 1995; Kovacs, 1983; Rearic et al., 1990; Reimnitz et al., 1990). All these factors influence both short-term and long-terms sediment fluxes. The model inherently accounts for seaward transport, but is not able to resolve the changes in nearshore morphology. There is speculation that offshore transport by sea ice will increase in coming decades (Eicken et al., 2005; Serreze et al, 2000), but there is a high degree of uncertainty in the magnitude of such changes. It was therefore assumed in the modelling process that there were no changes in sea ice transport or other sea ice-driven processes.

5.5.3 Coastal morphology and composition

Offshore and onshore morphology and composition influence coastal profile development and shoreline recession. Two different shoreface slopes are used in the model (east and west sectors) and the model is fairly sensitive to this parameter, so future estimates could be improved with the acquisition of bathymetric data for individual sites. Large scale bathymetry is known to play a role in coastal morphology (Ruz et al., 1992; Hill and Solomon, 1999), but is not considered in the model. For instance, submarine depressions can dissipate wave energy due to wave refraction and ridges can concentrate it and, as a result, wave action is often greater on headlands than in bays (Trenhaile, 1997). The Mackenzie Trough (a large cross-shelf canyon to the east of Herschel Island) and Herschel Basin (a depression to the southeast of the island) likely also influence wave behavior. Consideration of these bathymetric differences in a detailed analysis of short-term sediment transport would result in greater variability of wave inputs for the erosion model.

Although onshore ground ice is incorporated into calculations through the use of effective cliff heights, subsea ground ice is not. Changes in the shape of the shoreface profiles due to thawing of subsea ground ice were found to be minimal in Alaska (Reimnitz and Are, 2000; Reimnitz et al, 1988), but have been seen as important in furthering erosion in some cases (Wolfe et al., 1998). Because the subsidence from ground ice thaw on the shoreface is very slow when compared with erosion by waves (Are et al., 2008; Ostroumov et al., 2005), the omission of subsea ground ice in the model is not believed to affect the long-term results significantly. Onshore ground ice is a major control of mass movements such as thaw slumps or block failures along shorelines, and these episodic inputs of sediment to the coast will influence short-term development of the shoreface (Dallimore et al., 1996; Hill and Solomon, 1999; Hoque and Pollard, 2009; Lantuit and Pollard, 2008; Lewis and Forbes, 1974; Wolfe et al., 1998).

5.6 Conclusions

The incomplete understanding of erosional processes in the Arctic makes coastal modelling difficult (Harper et al., 1985; Héquette and Barnes, 1990; Pilkey and Cooper, 2004) and this study attempts only an order of magnitude projection of how changing climatic conditions may affect future fluxes of soil organic carbon. Using a morphodynamic model of coastal profile evolution fed by meteorological parameters, changes in water depth are used to determine coastal recession rates and how they are likely to change over time. The model accounts for both short-term and long-term sediment fluxes, but only the longer-term ones are considered in this study.

Important changes in environmental forcings are expected over the next half century. The current open water season along the Beaufort Sea coast lasts for approximately 104 days (last week of June to first week of October) during which an average of four storms per year occur. Significant wave heights for a storm-of-the-year are on the order of 1.47 m. In the coming decades, a reduction in summer sea ice which will increase the length of the open water season to 191 days. This could result in fetches of up to 1100 km and will increase wave heights by over 30%. The number of storms will decrease by 2%, but there will be a 7% increase in the number of intense ones. Sea levels will rise by 0.3 m over the next 50 years due to steric, eustatic and isostatic changes. A further rise in water levels will occur during storms, as surge levels increase by 10%.

The erosional response of coastal bluffs appears to be dependent on their composition and morphology. Effective bluff height in particular plays an important role, with a threshold of just over 4 m separating low from high bluffs. Modelled erosion rates for low cliffs are of the same magnitude as observed rates, whereas modelled rates for the high cliff heights are close to one order of magnitude higher than the observed rates. Long-term fluxes play a more important role in the retreat of high bluffs than of low ones. Future coastal recession rates are modelled based on the projected climatic conditions and changes in the rates are shown to depend on the height of the coastal bluffs. Results demonstrate that low bluffs erode more rapidly and that their rate of erosion will continue to grow over time. The increases in erosion rates for low bluffs range from 4 to 133%. High bluffs show lower overall erosion rates and almost all of them decrease with time; changes in erosion rates are between 3% and -21%. The decreases are likely due to the greater amount of sediment being input into the nearshore zone from the higher cliffs, which reduces the shoreface slope and diffuses wave energy. The total flux of soil organic carbon from low bluffs will increase by 29%, while that from high bluffs will decrease by 13%. This results in a slight overall decrease of 2% in the SOC flux for all height classes. Several of the assumptions made during the modelling process suggest that erosion rates are likely underestimated and that the values of SOC flux presented here are minimum values and may in fact be much higher. Variables such as the future effects of sea ice on nearshore morphodynamics remain unclear.

The modelling results from this study indicate that overall soil organic carbon fluxes from the Yukon Coastal Plain may remain close to current values, but could increase substantially, especially in areas where low coastal bluffs predominate. This has implications for the western part of the Canadian Beaufort Sea and regions such as the Alaska Coastal Plain where bluffs are approximately 2-6 m high (Reimnitz et al., 1988). Leont'yev (2003, 2004) found that erosion rates at some of the sites he examined in the East Siberian and Laptev Seas could increase by 40 to 50%. Even if there were to be no increase in the flux of organic carbon to the Arctic Ocean in the coming decades, changes in environmental forcings would still affect carbon cycling in the marine environment (McGuire et al., 2009). For instance, a reduction in sea ice resulting in longer periods of open water and greater mixing of water masses has implications for primary productivity (Belicka et al., 2009; Sakshaug, 2004), or an enhanced breakdown of refractory dissolved organic carbon due to greater exposure to UV radiation (Hernes and Benner, 2003; Miller and Zepp, 1995).

If there were to be a greater delivery of organic carbon to the ocean, there are a number of complex feedback processes that would accompany such movement (Lalande et al., 2007; McGuire et al., 2009). Any increases in the flux of SOC from coastal erosion could very well result in a greater flux of carbon dioxide to the atmosphere. New inputs of SOC to the ocean will most probably occur at the end of the summer when coastal permafrost is warmest and therefore weakest, or in the fall when storm activity is high. If spring phytoplankton blooms and continued production steadily reduce nutrient supply over the summer, inputs of terrestrial carbon and associated nutrients in the autumn will be more subject to microbial degradation and mineralization. Greater open water and storminess will promote resuspension, so burial in sediments will be less likely. Export from the continental shelf will also likely increase as convective mixing and shelf edge exchange are promoted. Partial pressure of CO_2 in surface waters will likely be kept higher, gas transfer will be greater, and these coastal areas could well become a source of CO_2 to the atmosphere. Although a number of uncertainties remain with regards to carbon dynamics in response to a changing climate, the results presented here contribute to an understanding of some of the changes in the Arctic carbon cycle that we can expect in the coming century.

Table 5.1 Storm characteristics for two sites along the Yukon coast for the period 1985-2005. Storms are defined as periods when winds are >10 m/s for 6 hours or more, but also include ramp-up and ramp-down periods (see text for details). The years when the maximum and minimum number of storms occurred are shown in parentheses.

	Total storms	Mean annual number of storms	St. dev.	Max. storms	Min. storms	Significant wave height for mean storm-of-the-year	Wave period for mean storm-of-the-year
King Point	83	4.0	2.1	8 (2003)	0 (2001)	1.47 m	6.0 sec.
Komakuk Beach	86	4.1	2.3	9 (2004)	0 (2001)	1.48 m	6.5 sec.

Table 5.2 Meteorological parameters used in coastal profile model. Present day values are shown as well as those projected for the year 2050.

	Significant wave height (m)	Wave period (s)	Change in water level (m)	Storm surge (m)
King Point	1.47 ---> 1.92	6.0 ---> 6.45	0 ---> 0.31	1.1 ---> 1.2
Komakuk Beach	1.48 ---> 1.93	6.5 ---> 6.99	0 ---> 0.31	1.1 ---> 1.2

Table 5.3 Variations in erosion rates for different cliff heights. For low cliffs, the rates produced by the model in Year 0 are of the same order of magnitude as the observed rates, whereas for high cliffs, differences between Year 0 and observed rates are much larger. The retreat rate for low cliffs increases over the 50 years, while it decreases over time for high cliffs. The projected values were obtained by multiplying the observed rates by the percentage increase. The coastal profile model was not applicable to sites with asterisks because q* was negative.

Low cliffs	Hc (m)	Model year 0 (m/yr)	Model year 50 (m/yr)	Δ (m/yr)	% increase	Total modelled retreat (m)	Observed (m/yr)	Projected (m/yr)	Total projected retreat (m)
Nunaluk Spit	1.2	0.2	0.5	0.3	133	19	1.0	2.2	81
Komakuk W1	1.2	0.2	0.5	0.3	122	20	0.7	1.5	55
Komakuk Beach	1.5	0.5	0.8	0.3	49	35	1.4	2.1	89
Stokes Point	1.8	1.1	1.4	0.3	31	62	1.4	1.8	80
Workboat Passage E	1.8	0.8	1.1	0.2	28	49	0.4	0.5	22
Clarence Lagoon W	2.1	1.1	1.3	0.2	20	61	0.6	0.7	35
Workboat Passage W	2.3	1.2	1.4	0.2	16	68	0.5	0.6	29
Komakuk W2	2.5	1.4	1.6	0.2	12	78	1.0	1.1	52
King Point SE	3.2	2.3	2.5	0.2	9	124	1.6	1.7	85
King Point	3.4	2.5	2.7	0.2	8	131	2.4	2.6	129
Phillips Bay	3.4	2.5	2.7	0.2	7	134	1.3	1.4	69
Kay Point	4.1	3.0	3.2	0.1	4	158	2.7	2.8	138
* Whale Cove W	0.6				4		0.1	0.1	4
* Roland Bay NW	0.9				4		0.2	0.2	9
* Clarence Lagoon	1.0				4		0.4	0.5	23
* Clarence Lagoon E	1.0				4		0.5	0.5	25
* Phillips Bay W	1.0				4		0.6	0.6	30
* Avadlek Spit	1.0				4		0.8	0.8	40
* Whale Cove	1.0				4		1.5	1.6	78
* Malcolm River fan	1.0				4		1.8	1.9	95
* King Point Lagoon	1.0				4		3.1	3.3	163
Mean for low cliffs		**1.4**	**1.6**	**0.2**	**23**	**78**	**1.1**	**1.4**	**63**
High cliffs									
Stokes Point SE	4.4	3.3	3.4	0.1	3	171	0.2	0.2	11
Roland Bay East	6.9	4.9	4.8	-0.1	-2	248	0.3	0.3	15
Roland Bay W	9.2	6.2	5.9	-0.3	-5	309	0.1	0.1	6
Stokes Point West	10.3	6.8	6.4	-0.4	-6	336	0.4	0.3	17
Herschel E	10.9	6.4	5.7	-0.7	-11	307	0.8	0.7	36
Shingle Point E	11.9	7.6	7.1	-0.5	-7	374	0.3	0.3	15
Shingle Point W	14.0	8.6	7.9	-0.7	-8	419	0.4	0.4	19
Running River	14.2	8.7	8.0	-0.7	-8	424	0.7	0.6	34
Sabine Point E	15.5	9.3	8.5	-0.8	-9	450	1.4	1.3	70
Sabine Point	16.1	9.6	8.7	-0.9	-9	464	0.5	0.5	25
Sabine Point W	17.4	10.1	9.2	-1.0	-10	489	0.8	0.7	40
Kay Point SE	18.5	10.61	9.6	-1.1	-10	511	1.0	0.9	46
Herschel W	27.3	13.8	11.0	-2.8	-20	622	1.0	0.8	44
Herschel N	29.9	14.9	11.8	-3.1	-21	668	0.7	0.6	32
Mean for high cliffs		**8.6**	**7.7**	**-0.9**	**-9**	**414**	**0.6**	**0.5**	**29**

Table 5.4 Current and projected fluxes of soil organic carbon (SOC) from terrain units along the Yukon coast.

	Erosion rate (m/yr)		**Mean SOC flux per m of coast (kg C/m/yr)**		**Total SOC flux (10^3 kg C/yr)**	
	Current	Projected	Current	Projected	Current	Projected
Low cliffs	1.1	1.4	120	139	11,388	14,637
High cliffs	0.6	0.5	315	278	32,155	27,858
All heights	0.7	0.8	198	194	43,544	42,495
St. dev.	0.7	0.8	216	193		
Total flux (Mt/yr)					0.044	0.042

Figure 5.1 Diagram showing a simplified version of the relationship between depth changes in the nearshore zone (Δd), and retreat of the coastline (Δr). The profiles depicted are equilibrium profiles which reflect long-term changes. Figure a) shows depth changes as a result of sediment transport out of the nearshore zone only, while b) depicts depth changes as a result of changing water level only. A combination of the two situations is expected as a result of changing meteorological conditions.

a)

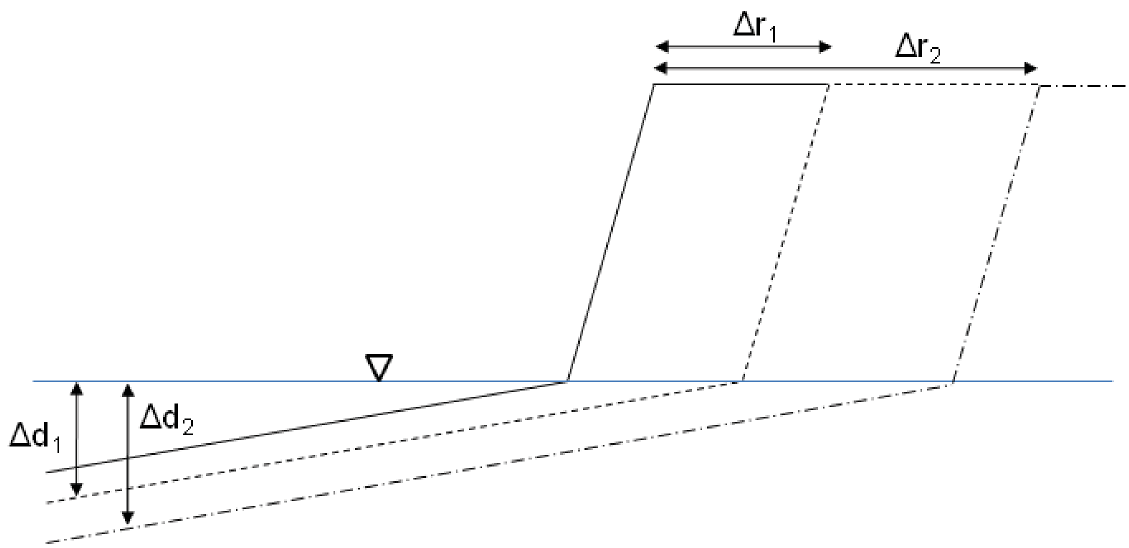

b)

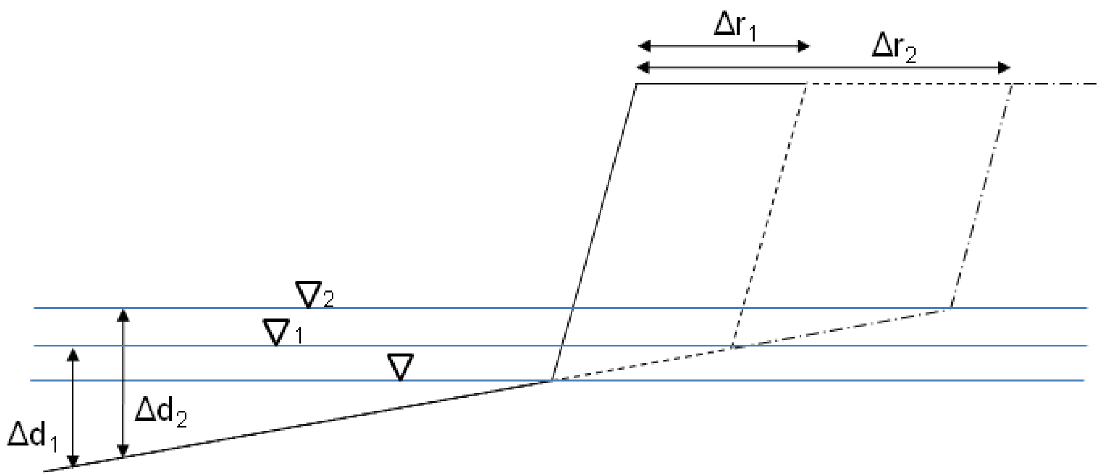

Figure 5.2 The relationship between computed long-term seaward sediment transport, q* (from Equation 5.4), and eroded volumes calculated from effective cliff heights and observed erosion rates for sites along the Yukon coast. The dashed line represents theoretical 1:1 values where sediment inputs from coastal erosion closely match long-term transport out of the system. Values above that line indicate that another process is involved, causing erosion rates to be out of sync with long term transport. This may be the result of the time lag between the erosion of large blocks of sediment from a bluff, and the time it takes for the blocks to be broken down by wave action and transported seaward. This lag effect is most pronounced with high cliffs. Open circles are bluffs with effective cliff heights < 4.1 m. Closed triangles are bluffs with effective cliff heights > 4.4 m.

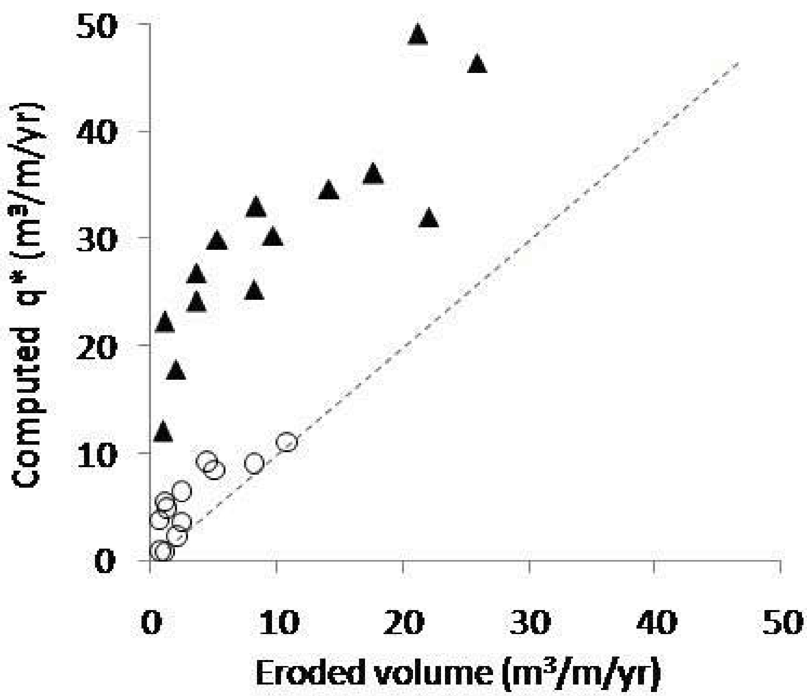

Figure 5.3 A comparison of observed and modelled annual erosion rates for different classes of effective cliff height. Note difference in vertical scale for the two figures.

a) Effective cliff height < 4.1 m.

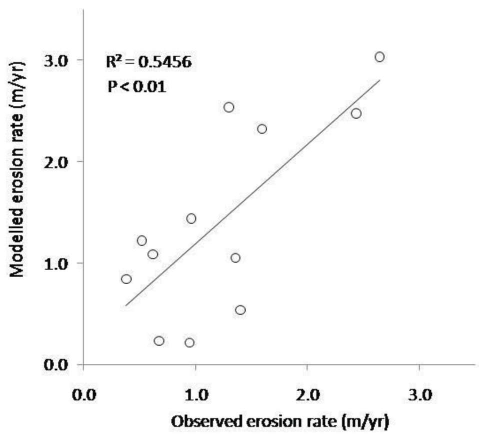

b) Effective cliff height > 4.4 m.

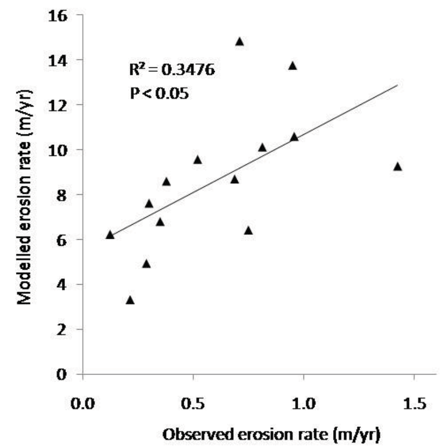

CHAPTER 6

THESIS SUMMARY AND CONCLUSIONS

Resolving uncertainties about the cycling of organic carbon in the world's oceans is crucial to understanding the effects and feedbacks of climatic warming. This is particularly so in the Arctic, because it is the locus of deep water formation, allowing carbon to be sequestered and isolated from the atmosphere for thousands of years. In addition, major environmental changes are occurring more rapidly at high latitudes. This thesis helps to fill gaps in our knowledge about organic carbon cycling in the Arctic Ocean. It is primarily a field-based, geomorphological study of permafrost and coastal processes. I contribute unique new knowledge by providing a comprehensive regional analysis of ground ice and the first detailed examination of how much soil organic carbon (SOC) is contained within the sediments along Canada's Yukon Coastal Plain. In addition, this work documents how much SOC is currently being eroded into the ocean from the area, how much of it is deposited in the nearshore and, finally, how the flux of organic carbon will change as climate warming proceeds.

A proper assessment of the volume of organic carbon and sediments in coastal bluffs in this permafrost environment could not be conducted without first determining the volume taken up by ground ice. In Chapter 3, a new method is developed for evaluating the volume of ground ice in the bluffs. Although ground ice assessments have been carried out in different regions using a variety of methods, to our knowledge this technique is the first that allows for site-specific differences in geomorphology and stratigraphic relationships between different types of ground ice, and for variations in the availability of data for different terrain units. This enables us to make a comprehensive, regional evaluation. The surficial geology of terrain units was seen to affect the ice content, as was the geomorphic history of the region. These are important in being able to extrapolate the results to wider regions where detailed ground ice data is lacking. In Chapter 4, SOC contents and fluxes were evaluated for the different terrain units. This is also the first systematic evaluation of soil organic carbon for the region and greatly expands the database of soil carbon measurements for the Canadian Arctic. The amount of ground ice is shown to be of consequence when evaluating material fluxes, and overlooking its presence can result in a significant overestimate of both the SOC and the mineral sediment in a terrain unit.

Values of organic carbon in the terrain units are related to the surficial material and to bluff height, with a considerable amount of carbon being found at depth. SOC fluxes along the Yukon coast are found to be higher than previously thought, but comparable to other parts of the Arctic. The organic carbon in nearshore sediments is overwhelmingly terrigenous, however, only a small proportion of the carbon eroded annually is buried in nearshore sediments. The rest is exported off-shelf or re-mineralized. This data fills a geographic gap where samples had been lacking. It is an important contribution to understanding regional carbon fluxes across the narrow continental shelf, and to constraining the influence of organic carbon contributions from the Mackenzie River to shelf sediments. In Chapter 5, a morphodynamic model of coastal evolution is used to evaluate how coastal retreat rates, and therefore fluxes of material, will change as a result of climate warming. Although there have been speculations about increasing carbon fluxes as a result of a changing environment, this study is the first to provide estimates of the magnitude of those fluxes for the Canadian Beaufort Sea. Results show that the response of terrain units is height-dependent, with lower bluffs retreating more rapidly than higher ones. The following specific conclusions can be drawn from this research:

1. Ground ice accounts for a significant portion of earth materials in coastal bluffs along the Yukon Coastal Plain and the amount of it is related to surficial material and geomorphic history. Coarse-grained marine deposits in bars and spits have the lowest ice contents (3%), followed by fluvial materials, glacial outwash, morainic deposits, and finally, lacustrine materials with the highest ground ice content (54%). None of the marine or fluvial terrain units contain excess ice. Ground ice makes up almost half of the soil volume in formerly glaciated areas where bluffs are generally high, but only one third of the volume in unglaciated portions of the coast which consist of low bluffs.

2. Not accounting for ground ice in coastal deposits can result in overestimates of SOC and mineral sediment of close to 20%. For some terrain units, errors can reach almost 50%. Correcting for ground ice is especially important in the upper soil layers, which are more ice-rich.

3. The average store of soil organic carbon is 223 kg C/m^2 for an entire soil column, which is four to six times higher than estimates that consider only the top meter of soil. At the terrain unit level, values of organic carbon are related to the surficial material and therefore the geomorphic history, being lowest in the marine units, and higher in the fluvial and lacustrine ones.

4. Although organic carbon contents decrease with depth, sampling only the top metre of soil can result in severe underestimates of SOC contents, since an average of 57% of the organic carbon in the soil column is located below that depth. This underlines the importance of deeper sampling. Although only the top layers of a soil column may be directly affected by a changing climate at inland sites, the deeper carbon is especially important to consider in coastal flux analyses because the entire soil column is mobilized by erosion.

5. The mean erosion rate for all terrain units along the Yukon coast is 0.7 m/yr. This results in an annual SOC flux of 157 kg per meter of coastline, which is intermediate to the results of studies for other Arctic Seas. It is higher than the annual fluxes for the Alaskan Beaufort Sea (149 kg C/m) and the Kara Sea (154 kg C/m), but lower than the average annual values for the Laptev Sea (263 kg C/m) and the East Siberian Sea (375 kg C/m).

6. The total annual flux of SOC from the Yukon Coastal Plain is 0.04 Mt, and extrapolation to the entire Canadian Beaufort Sea coast would result in a flux of 0.19 Mt/yr. This is over three times higher than the previous estimate for the region of 0.06 Mt/yr (MacDonald et al., 1998), and constitutes almost 10% of the organic carbon being added by the Mackenzie River (2.1 Mt/yr). Total annual SOC fluxes for other Arctic coasts range from 0.03 Mt for the Alaskan Beaufort Sea to 2.2 Mt for the East Siberian Sea (Rachold et al., 2004). Fluxes of sediment are two thirds higher than previous estimates.

7. Nearshore sediment samples have a mean $\delta^{13}C_{org}$ value of -26.6‰ and a C/N ratio of 15.2, indicating that 92% of the organic carbon in these sediments is from a terrigenous rather than

a marine source. Approximately 11% of the SOC eroded annually from the coast is sequestered in the nearshore, with the rest likely being exported off-shelf.

8. The effective cliff height of coastal bluffs appears to control the future erosional behaviour of coastal bluffs. Low bluffs show increasing erosion rates over the next 50 years (from 1.1 to 1.7 m/yr), whereas high bluffs show a slight decreasing trend (from 0.6 to 0.5 m/yr), likely because of the increased sediment input and its effect on short-term sediment transport in the nearshore. The threshold between the two height classes is just over 4 m. Ground ice contents affect the amount of sediment in coastal bluffs and therefore the modelled retreat rates, since bluffs with high ice contents have a lower effective cliff height.

9. Despite increases in environmental forcing factors that control coastal erosion, overall, SOC fluxes from the entire Yukon coast are not expected to change significantly within the next 50 years. This is because although fluxes from low coastal bluffs will increase by 29%, they will be offset by a 13% decrease in fluxes from high coastal bluffs. Model assumptions and conservative estimates of future climate forcings mean that retreat rates are somewhat underestimated, however, so the future flux of organic carbon could indeed increase somewhat.

10. Regions of low cliffs, where SOC fluxes are definitely expected to increase, could become sources of carbon flux to the atmosphere.

This study provides valuable input for both current and future studies of regional carbon dynamics. Regardless of whether fluxes remain steady or increase, by definitively quantifying the SOC in coastal and nearshore sediments, I have provided insight into the origins and fate of organic matter in a sensitive section of the Arctic coastal system. This is particularly relevant because changes in the sea ice regime will affect carbon cycling in shelf environments in the short-term. There is, however, a need to better incorporate short-term sediment fluxes in the nearshore to gain a better understanding of the evolution of the shoreface profile and its effect on coastal retreat rates. The erosion model used in this study is a simple one that does not account for many of the factors important in erosion modelling in a Arctic setting (i.e., it does not include variables such as changes in water temperature, or onshore processes such as thermal niching). It is also based on empirical relationships that are expected to change. Through groups such as the Arctic Coastal Dynamics project, efforts are underway to integrate several erosion models, including this one, in order to address the need for a better understanding of current and future processes. A specific focus is the need to better understand sea ice dynamics and its role in coastal erosion.

References

Are, F.E., 1988. Thermal abrasion of sea coasts. Polar Geography and Geology, **12**: 1-157.

Are, F.E., Reimnitz, E., Grigoriev, M., Hubberten, H. -W., and Rachold, V., 2008. The influence of cryogenic processes on the erosional Arctic shoreface. *Journal of Coastal Research*, **24**: 110-121.

Atkinson, D., 2005. Observed storminess patterns and trends in the circum-Arctic coastal regime. *Geo-Marine Letters*, **25**: 98-109.

Aylsworth, J.M., Duk-Rodkin, A., Robertson, T., and Traynor, J.A., 2000. Landslides of the Mackenzie Valley and adjacent mountainous and coastal regions. In: *The Physical Environment of the Mackenzie Valley: A Baseline for the Assessment of Environmental Change*, L.D. Dyke and G.R. Brooks (eds.). Geological Survey of Canada Bulletin 547, 167-176.

Batjes, N. H., 1996. Total carbon and nitrogen in the soils of the world. *European Journal of Soil Science*, **47**: 151–163.

Belicka, L.L. and Harvey, H.R., 2009. The sequestration of terrestrial organic carbon in Arctic Ocean sediments: a comparison of methods and implications for regional carbon budgets. *Geochimica et Cosmochimica Acta*, **73**: 6231-6248.

Belicka, L.L., MacDonald, R.W., and Harvey, H.R., 2002. Sources and transport of organic carbon to shelf, slope, and basin surface sediments of the Arctic Ocean. *Deep-Sea Research*, **I49**: 1463-1483.

Belicka, L.L., MacDonald, R.W., and Harvey, H.R., 2009. Trace element and molecular markers of organic carbon dynamics along a shelf–basin continuum in sediments of the western Arctic Ocean. *Marine Chemistry*, **115:** 72-85.

Berner, R.A., 1982. Burial of organic carbon and pyrite sulfur in the modern ocean: Its geochemical and environmental significance. *American Journal of Science*, **282**: 451-473.

Bitz, C.M., Fyfe, J.C., and Flato, G.M., 2002. Sea ice response to wind forcing from AMIP models. *Journal of Climate*, **15**: 522-536.

Blair, N.E., Leithold, E.L., Aller, R.C., 2004. From bedrock to burial: the evolution of particulate organic carbon across coupled watershed-continental margin systems. *Marine Chemistry*, **92**: 141-156.

Bockheim, J. G., 2007. Importance of cryoturbation in redistributing organic carbon in permafrost-affected soils. *Soil Science Society of America Journal*, **71:** 1335–1342.

Bockheim, J. G. and Hinkel, K.M., 2007. The importance of "deep" organic carbon in permafrost-affected soils of Arctic Alaska. *Soil Science Society of America Journal*, **71**: 1889-1892.

Bockheim, J.G., Everett, L.R., Hinkel, K.M., Nelson, F.E., and Brown, J., 1999. Soil organic carbon storage and distribution in arctic tundra, Barrow, Alaska. *Soil Science Society of America Journal*, **63**: 934-940.

Bockheim, J.G., Hinkel, K.M., Eisner, W.R., and Dai, X.Y., 2004. Carbon pools and accumulation rates in an age-series of soils in drained thaw-lake basins, Arctic Alaska. *Soil Science Society of America Journal*, **68:** 697-704.

Bockheim, J.G., Hinkel, K.M. and Nelson, F.E., 2003. Predicting carbon storage in tundra soils of arctic Alaska. *Soil Science Society of America Journal*, **67**: 648–650.

Bockheim, J. G., and Tarnocai, C., 1998a. Nature, occurrence and origin of dry permafrost. Proceedings of *Seventh International Permafrost Conference*, Yellowknife, N.W.T., 57-63.

Bockheim, J. G., and Tarnocai, C., 1998b. Recognition of cryoturbation for classifying permafrost-affected soils. *Geoderma,* **81**: 281–293.

Bockheim, J.G., Walker, D.A. and Everett, L.R., 1998. Soil carbon distribution in nonacidic and acidic tundra of arctic Alaska. P. 143–155. In: *Soil processes and the Carbon Cycle*, R. Lal et al. (ed.). CRC Press, Boca Raton, FL.

Brown, J., 1968. An estimation of the volume of ground ice, coastal plain, northern Alaska. *U.S. Army CRREL* Technical Note, 22 pp.

Brown, R. J. E., 1974. Distribution and environmental relationships of permafrost. Proceedings of *Workshop Seminar on Permafrost-Hydrology and Geophysics*, Calgary, Alberta, 1-17.

Brown, J., Jorgenson, M.T., Smith, O.P., and Lee, W., 2003. Long-term rates of coastal erosion and carbon input, Elson Lagoon, Barrow, Alaska. Proceedings *8th International Conference on Permafrost*, Zurich, Switzerland, 101-106.

Burn, C.R., 1997. Cryostratigraphy, paleogeography, and climate change during the early Holocene warm interval, western Arctic coast, Canada. *Canadian Journal of Earth Sciences*, **34**: 912-925.

Canfield, D., 1994. Factors influencing organic carbon preservation in marine sediments. *Chemical Geology*, **114**: 315-329.

Carmack, E. C., and Kulikov, E. A., 1998. Wind-forced upwelling and internal Kelvin wave generation in Mackenzie Canyon, Beaufort Sea, *Journal of Geophysical Research*, **103**:, 18,447–18,458.

Carmack, E. C., and Macdonald, R.W., 2002. Oceanography of the Canadian Shelf of the Beaufort Sea: A setting for marine life. *Arctic*, **55**, SUPP. 1, 29–45.

Cassano, J.J., Uotila, P., and Lynch, A., 2006. Changes in synoptic weather patterns in the polar regions in the twentieth and twenty-first centuries, Part 1: Arctic. *International Journal of Climatology*, Published online, doi: 10.1002/joc.1306.

CEM (*Coastal Engineering Manual)*, 2003. U.S. Army Corps of Engineers, Washington, D.C.

Chen, C.-T.A., Liu, K.-K., and MacDonald, R.W., 2003. Continental margin exchanges. In: *Ocean Biogeochemistry: The Role of the Ocean Carbon Cycle in Global Change*, M.J.R. Fasham (ed.). Springer-Verlag, Berlin, Germany, 53-98.

Chester, R. 2000. *Marine Geochemistry*. Blackwell Science, Oxford, UK, 506 pp.

Church, J.A., Gregory, J.M., Huybrechts, P., Kuhn, M., Lambeck, K., Nhuan, M.T., Qin, D., and Woodworth, P.L., 2001. Changes in sea level. In: *Climate Change 2001, The Scientific Basis. Contribution of Working Group I to the Third Assessment Report of the Intergovernmental Panel on Climate Change.* Cambridge University Press, Cambridge, UK.

Comiso,J.C., Parkinson, C.L., Gersten, T., and Stock, L., 2008. Accelerated decline in the Arctic sea ice cover. *Geophysical Research Letters*, **35**: L01703, doi: 10.1029/2007GL031972.

Couture, N.J. and Pollard W.H., 1998. An assessment of ground ice volume near Eureka, Northwest Territories. *Permafrost, Seventh International Conference*, Yellowknife, Canada. A.G. Lewkowicz and M. Allard (eds.). Université Laval, Centre d'études nordiques, Collection Nordicana, 195-200.

Couture, N.J., Hoque, A.Md., and Pollard W.H., 2008. Modelling the erosion of ice-rich deposits along the Yukon Coastal Plain. Proceedings *Ninth International Conference on Permafrost*, Fairbanks, Alaska, 303-308.

Dallimore, S.R., Kurfurst, J.J. and Hunter, J.A.M. 1988. Geotechnical and geothermal conditions of near-shore sediments, southern Beaufort Sea, Northwest Territories, Canada. Proceedings of *5th International Permafrost Conference*, Trondheim, Norway, 127-131.

Dallimore, S.R., Wolfe, S.A., and Solomon, S.M., 1996. Influence of ground ice and permafrost on coastal evolution, Richards Island, Beaufort Sea coast, N.W.T. *Canadian Journal of Earth Sciences*, **33**: 664-675.

de Haas, H., van Weering, T.C.E., and de Stigter, H., 2002. Organic carbon in shelf seas: sinks or sources, processes and products. *Continental Shelf Research*, **22**: 691–717.

de Krom, V., 1990. Retrogressive thaw slumps and active layer slides on Herschel Island, Yukon. Unpublished M.Sc. Thesis, McGill University, Montréal, Quebec, 157 pp.

Dittmar, T., and Kattner, G., 2003. The biogeochemistry of the river and shelf ecosystem of the Arctic Ocean: a review. *Marine Chemistry*, **83**: 103-120.

Dostovalov, B.N., and Popov, A.I., 1963. Polygonal systems of ice-wedges and conditions of their development. Proceedings of *First International Permafrost Conference*, Lafayette, Indiana, 102-105.

Drenzek, N.J., Montluçon, D.B., Yunker, M.B., Macdonald, R.W., and Eglinton, T.I., 2007. Constraints on the origin of sedimentary organic carbon in the Beaufort Sea from coupled molecular 13C and 14C measurements. *Marine Chemistry,* **103**: 146–162.

Ducklow, H.W. and McCallister, S.L., 2004. The biogeochemistry of carbon dioxide in the coastal oceans. In: *The* Sea, Volume 13, A.R. Robinson and K.H. Brink (eds.), Harvard University Press, Cambridge, U.S., 269-315.

Duk-Rodkin, A., Barendregt, R. W., Froese, F. G., Weber, F., Enkin, R., Smith, I., Zazula, G. D., Waters, P., and Klassen, R., 2004. Timing and extent of Plio-Pleistocene glaciations in north-western Canada and east-central Alaska. In: *Quaternary Glaciations - Extent and Chronology, Part II: North America*. J. Ehlers and P.L. Gibbard, (eds.), Amsterdam.

Dumas, J., Carmack, E., and Melling, H., 2005. Climate change impacts on the Beaufort shelf landfast ice. *Cold Regions Science and Technology*, **42**: 41-51.

Dunton, K.H., Weingartner, T., and Carmack, E.C., 2006. The nearshore western Beaufort Sea ecosystem: Circulation and importance of terrestrial carbon in arctic coastal food webs. *Progress in Oceanography*, **71**: 362–378.

Dyke, L.D. 1991. Temperature changes and thaw of permafrost adjacent to Richards Island, Mackenzie Delta, N.W.T. *Canadian Journal of Earth Sciences*, **28**: 1834-1842.

Dyke, A.S., and Savelle, J.M., 2000. Major end moraines of Younger Dryas age on Wollaston Peninsula, Victoria Island, Canadian Arctic: implications for paleoclimate and for formation of hummocky moraine. *Canadian Journal of Earth Sciences,* **37**: 601–619.

Dyke, A.S., and Prest, W.K., 1987. Late Wisconsinan and Holocene history of the Laurentide Ice Sheet. *Géographie Physique et Quaternaire*, **41**: 237-263.

Eicken, H., 2004. The role of Arctic sea ice in transporting and cycling terrigenous organic matter. In: *The Organic Carbon Cycle in the Arctic Ocean*, R. Stein and R.W. Macdonald (eds.), Springer, Berlin, 45-53.

Eicken H., Gradinger, R., Gaylord A., Mahoney A., Rigor I., and Melling H., 2005. Sediment transport by sea ice in the Chukchi and Beaufort Seas: Increasing importance due to changing ice conditions? *Deep-Sea Research Part II: Topical Studies in Oceanography*, **52** (24-26), 3281-3302.

Eid, B.M. and Cardone, V.J. 1992. *Beaufort Sea extreme waves study*. Environmental Studies Research Funds, Calgary, Alberta. Report Series No. 114, 143 pp.

Forbes, D.L., 1980. Late Quaternary sea level in the Beaufort Sea. Geological Survey of Canada Paper 80-1B, 75-87.

Forbes, D.L. 1989. Discussion - Maximum storm surge elevations in the Tuktoyaktuk region of the Canadian Beaufort Sea. Letter to the Editor, *Arctic*, **42**: 182.

Forbes, D.L. 1997. *Coastal erosion and nearshore profile variability in the southern Beaufort Sea, Ivvavik National Park, Yukon Territory*. Geological Survey of Canada Open File 3531, 28 pp.

Forbes, D.L. and Frobel, D. 1985. Coastal erosion and sedimentation in the Canadian Beaufort Sea. *Current Research*, Geological Survey of Canada Paper 85-1B, 69-80.

Forbes, D.L., Solomon, S.M. and Frobel, D. 1995. *Report of the 1992 coastal surveys in the Beaufort Sea*. Geological Survey of Canada Open File 3053, 39 pp.

Forbes, D.L., and Taylor, R.B., 1994. Ice in the shore zone and the geomorphology of cold coasts. *Progress in Physical Geography*, **18**(1): 59-89.

French, H. M., 1996. *The Periglacial Environment*, 2nd ed., Longman, London, 341 pp.

French, H. M., Bennett, L., and Hayley, D. W., 1986. Ground ice conditions near Rea Point and on Sabine Peninsula, eastern Melville Island. *Canadian Journal of Earth Sciences*, **23**: 1389-1400.

French, H. M., and Harry, D. G., 1990. Observations of buried glacier ice and massive segregated ice, western Arctic coast, Canada. *Permafrost and Periglacial Processes*, **1**: 31-43.

Friedlingstein, P., Bopp, L., Ciais, P., Dufresne, J.-L., Fairhead, L., LeTreut, H., Monfray, P. and Orr, J., 2001. Positive feedback between future climate change and the carbon cycle. *Geophysical Research Letters*, **28**: 1543-1546.

Gillie, R.D., 1987. Shore profile surveys, Canadian Beaufort Sea coast. Geological Survey of Canada Open File 1826, 21 pp.

.

Goñi, M.A., Yunker, M.B., Marcdonald, R.W., and Eglinton, T.I., 2000. Distribution and sources of organic biomarkers in arctic sediments from the Mackenzie River and Beaufort Shelf. *Marine Chemistry*, **71**: 23-51.

Grigoriev, M.N., and Rachold, V., 2003. The degradation of coastal permafrost and the organic carbon balance of the Laptev and East Siberian Seas. Proceedings *8th International Conference on Permafrost*, Zurich, Switzerland, 319-324.

Harper, J.R. 1990. Morphology of the Canadian Beaufort Sea Coast. *Marine Geology*, **91**: 75-91.

Harper, J.R., Henry, R.F. and Stewart, G.G. 1988. Maximum storm surge elevations in the Tuktoyaktuk region of the Canadian Beaufort Sea. *Arctic*, **41**: 48-52.

Harper, J.R., and Penland, P.S., 1982. *Beaufort Sea sediment dynamics.* Contract report to Atlantic Geoscience Centre, Geological Survey of Canada.

Harper, J.R., Reimer, P.D., and Collins, A.D., 1985. Canadian Beaufort Sea physical shore zone analysis. Geological Survey of Canada Open File Report 1689, 105 pp.

Harris, C., and Murton, J.B., 2005. Interactions between glaciers and permafrost: an introduction. In: *Cryospheric Systems: Glaciers and Permafrost, C.* Harris and J.B. Murton, (eds.). Geological Society, London, Special Publications, 242, 1-9.

Harry, D.G., and Dallimore, S.R., 1989. Permafrost, ground ice and global change in the Beaufort Sea coastlands. *Geos*, **18**: 48–53.

Harry, D.G., French, H.M., and Pollard, W.H., 1985. Ice wedges and permafrost conditions near King Point, Beaufort Sea coast, Yukon Territory. Geological Survey of Canada Paper 85-1A, 111-116.

Harry, D.G., French, H.M. and Pollard, W.H., 1988. Massive ground ice and ice-cored terrain near Sabine Point, Yukon coastal Plain. Canadian Journal of Earth Sciences, **25**: 1846-1856.

Hedges, J.I., Keil, R.J., and Benner, R., 1997. What happens to terrestrial organic matter in the ocean? *Organic Geochemistry*, **27**: 195-212.

Hedges, J.I., Clark, W.A., Quay, P.D., Richey, J.E., Devol, A.H. and Santos, U.D.M., 1986. Composition and fluxes of particulate organic material in the Amazon River. *Limnology and Oceanography*, **31**: 717-738.

Héquette, A. and Barnes, P.W., 1990. Coastal retreat and shoreface profile variations in the Canadian Beaufort Sea. *Marine Geology,* **91**: 113-132.

Héquette, A., Desroisiers, M. and Barnes, P.W. 1995. Sea ice scouring on the inner shelf of the southeastern Canadian Beaufort Sea. *Marine Geology*, **128**: 201-219.

Héquette, A., Desrosiers, M., Hill, P.R., and Forbes, D.L., 2001. The influence of coastal morphology on shoreface sediment transport under storm-combined flows, Canadian Beaufort Sea. *Journal of Coastal Research*, **17**: 507-516.

Héquette, A. and Hill, P.R., 1993. Storm-generated currents and offshore sediment transport on a sandy shoreface, Tibjak Beach, Canadian Beaufort Sea. *Marine Geology,* **113**: 283-304.

Hernes, P.J. and Benner, R., 2003. Photochemical and microbial degradation of dissolved lignin phenols: Implications for the fate of terrigenous dissolved organic matter in marine environments. *Journal of Geophysical Research*, **108** (C9), 3291, doi:10.1029/2002JC001421: C9, 7-1 - 7-9.

Hill, P.R., Blasco, S.M., Harper, J.R. and Fissel, D.B. 1991. Sedimentation on the Canadian Beaufort Shelf. *Continental Shelf Research*, **11**: 821-842.

Hill, P.R., Lewis, C.P., Desmarais, S., Kauppaymuthoo, V. and Rais, H., 2001. The Mackenzie Delta: sedimentary processes and facies of a high-latitude, fine-grained delta. *Sedimentology*, **48**: 1047-1078.

Hill, P.R. and Solomon, S.M., 1999. Geomorphologic and sedimentary evolution of a transgressive thermokarst coast, Mackenzie Delta region, Canadian Beaufort Sea. *Journal of Coastal Research*, **15**: 1011-1029.

Hinzman L., Bettez, N.D., Bolton, W.R., Chapin, F.S., Dyurgerov, M.B., Fastie, C.L., Griffith, B., Hollister, R.D., Hope, A., Huntington, H.P., Jensen, A.M., Jia, G.J., Jorgenson, T., Kane, D.L., Klein, D.R., Kofinas, G., Lynch, A.H., Lloyd, A.H., McGuire, A.D., Nelson, F.E., Oechel, W.C., Osterkamp, T.E., Racine, C.H., Romanovsky, V.E., Stone, R.S., Stow, D.A., Sturm, M., Tweedie, C.E., Vourlitis, G.L., Walker, M.D., Walker, D.A., Webber, P.J., Welker, J.M., Winker, K.S., and Yoshikawa, K., 2005. Evidence and implications of recent climate change in terrestrial regions of the Arctic. *Climatic Change*, **72**: 251-298.

Hobbie, S.E., Schimel, J.P., Trumbore, S.E., and Randerson, J.R., 2000. Controls over carbon storage and turnover in high-latitude soils. *Global Change Biology*, **6** (Suppl. 1), 196–210.

Hoque, Md.A., and Pollard, W.H., 2009. Arctic coastal retreat through block failure. *Canadian Geotechnical Journal,* **46**: 1103–1115, doi:10.1139/T09-058.

Hoque, Md.A., Solomon, S., and Perrie, W., 2009. Modeling nearshore transport along the Canadian Beaufort Sea coast. *GeoHalifax 2009*. Proceedings of the 62nd Canadian Geotechnical Conference and 10th Joint CGS/ IAH-CNC Groundwater Specialty Conference, Halifax, N.S., 954-961.

Hudak, D.R. and Young, J.M.C. 2002. Storm climatology of the southern Beaufort Sea. *Atmosphere-Ocean*, **40**: 145-158.

Hume, J.D. and Schalk, M., 1976. The effects of ice on the beach and nearshore, Point Barrow, Alaska. *Revue géographique de Montréal*, **30**: 105-114.

International Permafrost Association, 1998. *Multi-Language Glossary of Permafrost and Related Ground-Ice Terms*, R.O. van Everdingen (ed.), The Arctic Institute of North America, University of Calgary, Calgary.

Ittekott, V., 1988. Global trends in the nature of organic matter in river suspensions. *Nature*, **332**: 436-438.

Jobbágy, E.G., Jackson, R.B., 2000. The vertical distribution of soil organic carbon and its relation to climate and vegetation. *Ecological Applications*, **10**: 423–436.

Johannessen, O.M., Bengtsson, L., Miles, M.W., Kuzmina, S.I., Semenov, V.A., Alekseev, G.V., Nagurnyi, A.P., Zakharov, V.F., Bobylev, L., Pettersson, L.H., Hasselmann, K., and Cattle, H.P., 2002. *Arctic climate change - observed and modeled temperature and sea ice variability*. Nansen Environmental and Remote Sensing Centre Technical Report 218, 22 pp.

Johnson, K., Solomon, S.M., Berry, D. and Graham, P., 2003. Erosion progression and adaptation strategy in a northern coastal community. Proceedings *8th International Conference on Permafrost*, Zurich, Switzerland, 489-494.

Jones, B.M., Arp, C.D., Jorgenson, M.T., Hinkel, K.M., Schmutz, J.A. and Flint, P.L., 2009. Increase in the rate and uniformity of coastline erosion in Arctic Alaska, *Geophysical Research Letters*, **36**: L03503, doi:10.1029/2008GL036205.

Jorgenson, M.T., and Brown, J., 2005. Classification of the Alaskan Beaufort Sea Coast and estimation of carbon and sediment inputs from coastal erosion. *Geo-Marine Letters*, **25**: 69–80.

Kobayashi, N., 1985. Formation of thermoerosional niches into frozen bluffs due to storm surges on the Beaufort Sea coast. *Journal of Geophysical Research*, **90**(C6): 11983-11988.

Kobayashi, N., Vidrine, J.C., Nairn, R.B. and Solomon, S.M. 1999. Erosion of frozen cliffs due to storm surge on Beaufort Sea coast. *Journal of Coastal Research*. **15**: 332-344.

Kokelj, S.V., Smith, C.A.S., and Burn, C.R., 2002. Physical and chemical characteristics of the active layer and permafrost, Herschel Island, western Arctic coast, Canada. *Permafrost and Periglacial Processes*, **13**: 171–185. doi: 10.1002/ppp.417

Komar, Paul, D., 1998. *Beach Processes and Sedimentation*. 2nd ed., Prentice Hall, Upper Saddle River, N.J., 544 pp.

Kovacs, A., 1983. Shore ice ride-up and pile-up features. Part 1: Alaska's Beaufort Sea coast. CRREL Report 83-9, 50 pp.

Lachenbruch, A. H., 1962. Mechanics of thermal contraction cracks and ice-wedge polygons in permafrost. Geological Society of America Special Paper No. 70, 69 pp.

Lalande, C., Grebmeier, J.M., Wassmann, P., Cooper, L.W., Flint, M.V., and Sergeeava, V.M., 2007. Export fluxes of biogenic matter in the presence and absence of seasonal sea ice cover in the Chukchi Sea. *Continental Shelf Research*, **27**: 2051–2065.

Lambert, S.J., 1995. The effect of enhanced greenhouse warming on winter cyclone frequencies and strengths. *Journal of Climate*, **8**: 1447-1452.

Lambert S.J., and Fyfe, J.C., 2006. Changes in winter cyclone frequencies and strengths simulated in enhanced greenhouse warming experiments: results from the models participating in the IPCC diagnostic exercise. *Climate Dynamics*, **26**: 713–728.

Lantuit, H., Rachold, V., Pollard, W.H., Steenhuisen, F., Ødegård, R., Hubberten, H.-W., 2009. Towards a calculation of organic carbon release from erosion of Arctic coasts using non-fractal coastline datasets, *Marine Geology*, **257**, 1-10., doi: 10.1016/j.margeo.2008.10.004.

Lantuit, H. and Pollard, W.H., 2008. Fifty years of coastal erosion and retrogressive thaw slump activity on Herschel Island, southern Beaufort Sea, Yukon Territory, Canada. *Geomorphology*, doi:10.1016/j.geomorph.2006.07.040

Lawrence, M., Pelletier. B.R.. and Lacho, G., 1984. Sediment sampling of beaches along the Mackenzie Delta and Tuktoyaktuk Peninsula, Beaufort Sea. Geological Survey of Canada. Paper 84-l A, 633-640.

Leffingwell, E. d. K., 1915. Ground ice-wedges. The dominant form of ground ice on the north coast of Alaska. *Journal of Geology*, **23**: 635-654.

Leont'yev, I.O., 2003. Modeling erosion of sedimentary coasts in the western Russian Arctic. *Coastal Engineering,* **47**: 413–429.

Leont'yev, I.O., 2004. Coastal profile modeling along the Russian Arctic coast. *Coastal Engineering*, **51**: 779-794.

Lewis, C.P. and Forbes, D.L., 1974. Sediments and sedimentary processes, Yukon Beaufort Sea Coast. Task Force on Northern Oil Development, Report No. 74-29, 40 pp.

Macdonald, R.W., Naidu, A.S., Yunker, M.B., and Gobeil, C. 2004. The Beaufort Sea: Distribution, sources, fluxes and burial of organic carbon. In: *The Organic Carbon Cycle in the Arctic Ocean*, R. Stein and R.W. Macdonald (eds.), Springer, Berlin, 177-193.

Macdonald, R.W., Solomon, S.M., Cranston, R.E., Welch, H.E., Yunker, M.B., and Gobeil, C., 1998. A sediment and organic carbon budget for the Canadian Beaufort Shelf. *Marine Geology*, **144**: 255-273.

Mackay, J.R., 1959. Glacier ice-thrust features of the Yukon Coast. *Geographical Bulletin,* **13**: 5-21.

Mackay, J. R., 1963a. Notes on the shoreline recession along the coast of the Yukon Territory. *Arctic*, **16**: 195-197.

Mackay, J. R., 1963b. The Mackenzie Delta area, N.W.T. *Memoir* 8, Geographical Branch, Department of Mines and Technical Surveys, Ottawa, Ontario, 202 pp.

Mackay, J. R., 1970. Disturbances to the tundra and forest tundra environment of the western Arctic. *Canadian Geotechnical Journal*, **7**: 420-432.

Mackay, J. R., 1971. The origin of massive icy beds in permafrost, western Arctic coast, Canada. *Canadian Journal of Earth Sciences*, **8**: 397-422.

Mackay, J. R., 1972. The world of underground ice. *Annals of the American Association of Geographers*, **62**: 1-22.

Mackay, J. R., 1973. Problems in the origin of massive ice beds, western Arctic, Canada. Proceedings of *Second International Permafrost Conference*, Yakutsk, USSR, 223-228.

Mackay, J. R., 1974. Ice-wedge cracks, Garry Island, Northwest Territories. *Canadian Journal of Earth Sciences*, **11**: 1366-1383.

Mackay, J.R. 1977. The widths of ice wedges. Geological Survey of Canada Paper 77-1A, 43–44.

Mackay, J.R., 1979. Pingos of the Tuktoyaktuk Peninsula area, Northwest Territories. *Géographie Physique et Quaternaire,* **33**: 3-61.

Mackay, J.R., 1985. Pingo ice of the western Arctic coast, Canada. *Canadian Journal of Earth Sciences*, **22**: 1452-1464.

Mackay, J. R., 1986. Fifty years (1935-1985) of coastal retreat west of Tuktoyaktuk, District of Mackenzie. Geological Survey of Canada Paper 86-1A, 727-735.

Mackay, J. R., 1988. Ice wedge growth in newly aggrading permafrost, western Arctic Coast, Canada. Proceedings of *Fifth International Conference on Permafrost*, Trondheim, Norway, 809-814.

Mackay, J. R. 1989. Massive ice: Some field criteria for the identification of ice types. Geological Survey of Canada Paper 89-1G, 5–11.

Mackay, J. R., 1990. Some observations on the growth and deformation of epigenetic, syngenetic and anti-syngenetic ice wedges. *Permafrost and Periglacial Processes*, **1**: 15-29.

Mackay, J. R. and Dallimore, S. R. 1992. Massive ice of the Tuktoyaktuk area, western Arctic coast, Canada. *Canadian Journal of Earth Sciences,* **29**: 1235–1249.

Mahoney, A., Eicken, H., Shapiro, L., and Grenfell, T.C., 2004. Ice motion and driving forces during a spring ice shove on the Alaska Chukchi coast. *Journal of Glaciology*, **50**: 195-207.

Mandelbrot, B. 1967. How long is the coast of Britain? Statistical self-similarity and fractional dimension. *Science*, **155**: 636-638.

Manson, G.K. and Solomon, S.M., 2007. Past and future forcing of Beaufort Sea coastal change. *Atmosphere-Oceans,* **45**: 107-122, doi: 10.3137/ao.450204.

Manson, G.K., Solomon, S.M., and MacDonald, A., 2002. Describing Beaufort Sea coastal climate variability. *Reports on Polar and Marine Research*, **413**: 31-33.

Manson, G.K., Solomon, S.M., Forbes, D.L., Atkinson, D.E. and Craymer, M. 2005. Spatial variability of factors influencing coastal change in the western Canadian Arctic. *Geo-Marine Letters*, **25**: 138-145.

Marinov, I. and Sarmiento J.L., 2004. The role of the oceans in the global carbon cycle: An overview. In: *The Ocean Carbon Cycle and Climate*, M. Follows and T. Oguz, (eds.). Kluwer Academic Publishers, Dordrecht, The Netherlands, 251-295.

Mars, J.C. and Houseknecht, D.W., 2007. Quantitative remote sensing study indicates doubling of coastal erosion rate in past 50 yr along a segment of the Arctic coast of Alaska. *Geology,* **35**: 583-586. doi: 10.1130/G23672A.1

Masselink, G., and Hughes, M.G., 2003. *Introduction to Coastal Processes and Geomorphology*, Oxford University Press, New York, 354 pp.

McCabe, G.J., Clark, M.P., and Serreze, M.C., 2001. Trends in Northern Hemisphere surface cyclone frequency and intensity. *Journal of Climate*, **14**: 2763-2768.

McDonald, B.C. and Lewis, C.P. 1973. *Geomorphologic and sedimentologic processes of rivers and coasts, Yukon Coastal Plain*. Environmental-Social Committee, Northern Pipelines, Report 73-39, 245 pp.

McGillvray, D.G., Agnew, T.A., McKay, G.A., Pilkington, G.R., and Hill, M.C., 1993. *Report summary of impacts of climatic change on the Beaufort sea-ice regime: Implications for the Arctic petroleum industry*. Prepared for Climate Change Digest, Atmospheric Environment Service, CCD93-01, 17 pp.

McGuire, A.D., Anderson, L.G., Christensen, T.R., Dallimore, S., Guo, L., Hayes, D.J., Heimann, M., Lorenson, T.D., Macdonald, R.W., and Roulet, N. 2009. Sensitivity of the carbon cycle in the Arctic to climate change. *Ecological Monographs*, **79**: 523-555. doi: 10.1890/08-2025.1.

Meehl, G.A., Stocker, T.F., Collins, W.D., Friedlingstein, P., Gaye, A.T., Gregory. J.M., Kitoh, A., Knutti, R., Murphy, J.M., Noda, A., Raper, S.C.B., Watterson, I.G., Weaver, A.J., and Zhao, Z.-C., 2007. Global climate projections. In: *Climate change 2007: the physical science basis. Contribution of working group I to the fourth assessment report of the intergovernmental panel on climate change.* Solomon S, Qin D, Manning M, Chen Z, Marquis M, Averyt KB, Tignor M, Miller HL (eds). Cambridge University Press, Cambridge.

Meyers, P.A., 1997. Organic geochemical proxies of paleoceanographic, paleolimnologic, and paleoclimatic processes. *Organic Geochemistry,* **27**: 213-250.

Meyers, P.A., 1994. Preservation of elemental and isotopic source identification of sedimentary organic matter. *Chemical Geology*, **114**: 289-302.

Michaelson, G.J., Ping, C.L., and Kimble, J.M., 1996. Carbon storage and distribution in tundra soils of arctic Alaska, U.S.A. *Arctic and Alpine Research*, **28**: 414-424.

Miller, W.L. and Zepp, R.G., 1995. Photochemical production of dissolved inorganic carbon from terrestrial organic matter: Significance to the oceanic organic carbon cycle. *Geophysical Research Letters*, **22**: 417-420.

Murton, J.B., Whiteman, C.A., Waller, R.I., Pollard, W.H., Clark, I.D., Dallimore, S.R., 2005. Basal ice facies and supraglacial melt-out till of the Laurentide Ice Sheet, Tuktoyaktuk Coastlands, western Arctic Canada. *Quaternary Science Reviews*, **24**: 681-708.

Naidu, A.S., Cooper, S.W., Finney, B.P., Macdonald, R.W., Alexander, C., and Semiletov, I.P., 2000. Organic carbon isotope ratios ($\delta^{13}C$) of Amerasion continental shelf sediments. *International Journal of Earth Sciences*, **89**: 522-532.

Nairn, R.B., Solomon, S., Kobayashi, N., and Virdrine, J., 1998. Development and testing of a thermal-mechanical numerical model for predicting Arctic shore erosion process. Proceedings of the *7th International Permafrost Conference*, Yellowknife, N.W.T., 789-796.

O'Brien, M.C., Macdonald, R.W., Melling, H., and Iseki, K., 2006. Particle fluxes and geochemistry on the Canadian Beaufort Shelf: Implications for sediment transport and deposition. *Continental Shelf Research*, **26**: 41-81.

O'Connor, M.J. and Associates, 1986. *Investigations of subsurface conditions at King Point, Yukon Territory*. Technical Report for Indian and Northern Affairs Canada, Calgary, Alberta, 163 pp.

Ogorodov, S.A., 2003. The role of sea ice in the coastal zone dynamics of the Arctic Seas. *Water Resources*, **30**: 509-518.

Ogorodov, S.A., Kamalov, A., Zubakin, G., and Gudoshnikov, Y.P., 2005. The role of sea ice in coastal and bottom dynamics in the Pechora Sea. *Geo-Marine Letters*, **25**: 146-152.

Ostroumov, V., Rachold. V. Vasiliev, A., and Sorokovikov, V., 2005. An application of a Markov-chain model of shore erosion for describing the dynamics of sediment flux. *Geo-Marine Letters*, **25**: 196-203.

Overduin, P.P., and Couture, N., (eds.), 2008. The 6th Annual Arctic Coastal Dynamics (ACD) workshop, October 22-26, 2006, Groningen, Netherlands. *Berichte zur Polar- und Meeresforschung*, **576**: 1–105.

Overland, J. E., 2009. Meteorology of the Beaufort Sea, *Journal of Geophysical Research*, **114**: C00A07, doi:10.1029/2008JC004861.

Péwé, T.L., 1963. Ice-wedges in Alaska - classification, distribution, and climatic significance. Proceedings *1st International Conference on Permafrost*, Lafeyette, Indiana, 76-81.

Pihlainen, J. A., and Johnston, G. H., 1963. Guide to a field description of permafrost. *Technical memorandum* 79, National Research Council, Ottawa, Ontario.

Pilkey, O.H. and Cooper, A.G., 2004. Society and sea level rise. *Science*, **303**: 1781-1782

Ping, C.-L., Michaelson, G.J., Jorgenson. M.T., Kimble, J.M., Epstein, H., Romanovsky, V.E., and D.A. Walker., 2008. High stocks of soil organic carbon in the North American Arctic region. *Nature Geoscience,* **1**: 615 - 619. doi:10.1038/ngeo284.

Pollard, W. H., 1990. The nature and origin of ground ice in the Herschel Island area, Yukon Territory. *Permafrost Canada* - Proceedings of the *Fifth Canadian Permafrost Conference*, Québec City, Québec, 23-30.

Pollard, W.H., 1991. The investigation of buried snowbank ice in ice-rich permafrost in central and northern Yukon, Canada. *Bulletin of Glacier Research*, **9**: 1-7.

Pollard, W.H., 2000. Distribution and characterization of ground ice on Fosheim Peninsula, Ellesmere Island, Nunavut. In: *Environmental Response to Climate Change in the Canadian High Arctic,* M**.** Garneau and B.T. Alt (eds.), Geological Survey of Canada Bulletin 529, 207-233.

Pollard, W.H. and Couture, N.J., 1999. *The use of morphological methods to estimate ground ice volumes along the Canadian Beaufort Sea coast*. Report for the Geological Survey of Canada (Atlantic), 30 pp.

Pollard, W.H. and Dallimore, S.R., 1988. Petrographic characteristics of massive ground ice, Yukon Coastal Plain, Canada. Proceedings *5th International Permafrost Conference*, Trondheim, Norway, 224-229.

Pollard, W. H., and French, H. M., 1980. A first approximation of the volume of ground ice, Richards Island, Pleistocene Mackenzie Delta, NWT. *Canadian Geotechnical Journal*, **17**: 509-516.

Post, W.M., Emanuel, W.R., Zinke, P.J., and Stangenberger, A.G., 1982. Soil carbon pools and world life zones. *Nature*, **298**: 156-159.

Prentice, I.C., Farquhar, G.D., Fasham, M.J.R., Goulden, M.L., Heimann, M., Jaramillo, V.J., Kheshgi, H.S., Le Quéré, C., Scholes, R.J., and Wallace, D.W.R. 2001. The carbon cycle and atmospheric carbon dioxide. In: *Climate Change 2001: The Scientific Basis. Contribution of Working Group I to the Third Assessment Report of the Intergovernmental Panel on Climate Change,* J.T. Houghton, Y. Ding, D.J. Griggs, M. Noguer, P.J. van der Linden, X. Dai, K. Maskell, and C.A. Johnson (eds.). Cambridge University Press, Cambridge, United Kingdom and New York, NY, USA, 881 pp.

Rachold. V., Are, F.E., Atkinson, D.E., Cherkashov, G., and Solomon, S.M., 2005. Arctic Coastal Dynamics (ACD): an introduction. *Geo-Marine Letters*, **25**: 63-68.

Rachold, V., Brown, J., and Solomon, S. (eds.), 2002. Arctic Coastal Dynamics. Report of the 2nd International Workshop. November 26-30, 2001, Potsdam, Germany. *Berichte zur Polar- und Meeresforschung*, **413**: 1–103.

Rachold, V., Brown, J., Solomon, S., and Sollid, J. L. (eds.), 2003. Arctic Coastal Dynamics. Report of the 3rd International Workshop. December 2-5, 2002, University of Oslo, Norway. *Berichte zur Polar- und Meeresforschung*, **443**: 1–127.

Rachold V., and Cherkashov, G. (eds.), 2004. Arctic Coastal Dynamics. Report of the 4th International Workshop. November 10-13, 2003, VNIIOkeangeologia, St. Petersburg, Russia. *Berichte zur Polar- und Meeresforschung*, **429**: 1–229.

Rachold, V., Eicken, H., Gordeev., V.V., Grigoriev, M.N., Hubberten, H.-W., Lisitzin, A.P., Shevchenko, V.P., and Schirrmeister, L., 2004. Modern terrigenous organic carbon input to the Arctic Ocean. In: *The Organic Carbon Cycle in the Arctic Ocean*, R. Stein and R.W. Macdonald (eds.), Springer, Berlin, 33-55.

Rachold. V., Grigoriev, M.N., Are, F.E., Solomon, S., Reimnitz, E., Kassens, H., and Antonow, M., 2000 Coastal erosion vs. riverine sediment discharge in Arctic shelf seas. *International Journal of Earth Sciences*, **89**: 450-460.

Rachold, V., Lantuit, H., Couture, N., and Pollard, W.H. (eds.), 2005. Arctic Coastal Dynamics. Report of the 5th International Workshop, October 13-16, 2004, McGill University, Montreal, Canada. *Berichte zur Polar- und Meeresforschung*, **506**: 1–143.

Rampton, V. N., 1974. The influence of ground ice and thermokarst upon the geomorphology of the Mackenzie-Beaufort region. Proceedings of *3rd Guelph Symposium on Geomorphology*, Guelph, Ontario, 43-59.

Rampton, V.N., 1982. Quaternary Geology of the Yukon Coastal Plain. Geological Survey of Canada Bulletin 317, 49 pp.

Rampton, V. N. 1991. Observations on buried glacier ice and massive segregated ice, western Arctic coast, Canada: Discussion. *Permafrost and Periglacial Processes,* **2**: 163–165.

Rampton, V.N. and Mackay, J.R., 1971. Massive ice and icy sediments throughout the Tuktoyaktuk Peninsula, Richards Island, and nearby areas, District of Mackenzie. Geological Survey of Canada Paper, 71-21.

Rearic, D.M.; Barnes, P.W., and Reimnitz, E., 1990. Bulldozing and resuspension of shallow-shelf sediment by ice keels: implications for Arctic sediment transport trajectories. *Marine Geology,* **91**: 133–147.

Reimnitz, E. and Are, F., 2000. Coastal bluff and shoreface comparison over 34 years indicates large supply of erosion products to Arctic seas. *Polarforschung,* **68**(1–9): 231–235.

Reimnitz, E., and Barnes, P.W., 1974. Sea ice as a geologic agent on the Beaufort Sea shelf of Alaska. In: *The Coast and Shelf of the Beaufort Sea*. J. Reed and J. Sater (eds.). Arctic Institute of North America, Arlington, VA, 301-353.

Reimnitz, E. and Barnes, P. W., 1987. Sea-ice influence on arctic coastal retreat. Proceedings *Coastal Sediments 87*, New Orleans, LA, 1578-1591.

Reimnitz, E., Barnes, P.W., and Harper, J.R., 1990. A review of beach nourishment from ice transport of shoreface materials, Beaufort Sea, Alaska. *Journal of Coastal Research,* **8**: 439–470.

Reimnitz, E., Barnes, P.W., Toimil, L.J., and Melchior, J., 1977. Ice gouge recurrence and rates of sediment reworking, Beaufort Sea, Alaska. *Geology*, **5**: 405-408.

Reimnitz, E., Dethleff, D., and Nürnberg, D., 1994. Contrasts in Arctic shelf sea-ice regimes and some implications: Beaufort Sea versus Laptev Sea. *Marine Geology*, **119**: 215-225.

Reimnitz, E., Graves, S.M., and Barnes, P.W., 1988. Map showing Beaufort Sea coastal erosion, sediment flux, shoreline evolution, and the erosional shelf profile. Menlo Park, California: U.S. Geological Survey, Map I-1182-G, scale 1:82,000, 22 pp.

Robinson, S.D., Moorman, B.J., Judge, A.S., and Dallimore, S.R., 1993. The characterization of massive ground ice at Yaya Lake, Northwest Territories using radar stratigraphy techniques. Geological Survey of Canada Paper 93-1B, 23-32.

Romanovskii, N.N., 1985. Distribution of recently active ice and soil wedges in the U.S.S.R. In: *Field and Theory; Lectures in Geocryology*, M. Church and O. Slaymaker (eds.). University of British Colombia Press, 154-165.

Ruz, M.-H., Héquette, A. and Hill, P.R. 1992. A model of coastal evolution in a transgressed thermokarst topography, Canadian Beaufort Sea. *Marine Geology*, **106**: 251-278.

Sakshaug, E., 2004. Primary and secondary production in the Arctic seas. In: *The Organic Carbon Cycle in the Arctic Ocean*, R. Stein and R.W. Macdonald (eds.). Springer, Berlin, 57-81.

Schlesinger, W.H., 1997. *Biogeochemistry: An Analysis of Global Change*. Academic Press, San Diego, 588 pp.

Schuur, E.A.G., Bockheim, J., Canadell, J.G., Euskirchen, E., Field, C.B., Goryachkin, S. V., Hagemann, S., Kuhry, P., Lafleur, P.M., Lee, H., Mazhitova, G., Nelson, F.E., Rinke, A., Romanovsky, V.E., Shiklomanov, N., Tarnocai, C., Venevsky, S., Vogel, J.G., and Zimov, S.A., 2008. Vulnerability of permafrost carbon to climate change: Implications for the global carbon cycle. *BioScience*, **58**: 701–714.

Serreze, M.C., Holland, M.M., and Stroeve, J., 2007. Perspectives on the Arctic's Shrinking Sea-Ice, *Science*, **315**: 1533-1536. doi: 10.1126/science.1139426

Serreze, M. C., Maslanik, J. A., Scambos, T. A., Fetterer, F., Stroeve, J., Knowles, K., Fowler, C., Drobot, S., Barry, R. G., and Haran,, T.M., 2003. A record minimum arctic sea ice extent and area in 2002. *Geophysical Research Letters*, **30**: 1110, doi:10.1029/2002GL016406.

Serreze, M.C., Walsh, J. E., Chapin, F. S., Osterkamp, T., Dyurgerov, M., Romanovsky, V., Oechel, W. C., Morison, J., Zhang, T., and Barry, R. G., 2000. Observational evidence of recent change in the northern high-latitude environment. *Climatic Change*, **46**: 159-207.

Sharpe, D.R., 1992. Quaternary geology of Wollaston Peninsula, Victoria Island, Northwest territories. Geological Survey of Canada Memoir 434, 84 pp.

Shaver, G.R., Billings, W.D., Chapin, F.S., Giblin, A.E., Nadelhoffer, K.J., Oechel, W.C., and Rastetter, E.B., 1992. Global change and the carbon balance of Arctic ecosystems. *BioScience*, **42**: 433-441.

Shaw, J., Taylor, R.B., Forbes, D.L., Ruz, M.-H. and Solomon, S. 1998. Sensitivity of the coasts of Canada to sea-level rise. GSC Bulletin 505, 79 pp.

Short, A.D., 1976. Observations on ice deposited by waves on Alaskan Arctic beaches. *Revue géographique de Montréal*, **30**: 115-122.

Simmonds, I., and Keay, K., 2009. Extraordinary September Arctic sea ice reductions and their relationships with storm behavior over 1979–2008, *Geophysical Research Letters*, **36**: L19715, doi:10.1029/2009GL03981.

Smith, C.A.S., Kennedy, C.E., Hargrave, A.E., and McKenna, K.M., 1989. *Soil and vegetation of Herschel Island, Yukon Territory*. Yukon Soil Survey Report No. 1. Land Resource Research Centre, Agriculture Canada, Ottawa, 101 pp.

Smith, S.L., and Burgess, M.M., 2000. Ground temperature database for northern Canada. Geological Survey of Canada Open File 3954, 28 pp.

Smith, S.L., Burgess, M.M., Chartrand, J. and Lawrence, D.E. 2005. Digital borehole geotechnical database for the Mackenzie Valley/Delta region. Geological Survey of Canada Open File 4924.

Smith, S.V. and Hollibaugh, J.T., 1993. Coastal metabolism and the oceanic organic carbon cycle. *Reviews of Geophysics*, **31**: 75-89.

Solomon, S.M. 2005. Spatial and temporal variability of shoreline change in the Beaufort-Mackenzie region, Northwest Territories, Canada. *Geo-Marine Letters*, **25**: 127-137.

Solomon, S.M., Forbes, D.L. and Keirstead, B. 1994. Coastal impacts of climate change: Beaufort Sea erosion study. Geological Survey of Canada Open File 2890.

Stein, R., 1991. *Accumulation of Organic Carbon in Marine Sediments.* Springer-Verlag, Berlin, 217 pp.

Stein, R. and Macdonald, R.W. (eds.), 2004a. *The Organic Carbon Cycle in the Arctic Ocean*, Springer, Berlin, 363 pp.

Stein, R. and Macdonald, R.W., 2004b. Geochemical proxies used for organic carbon source identification in Arctic Ocean sediments. In: *The Organic Carbon Cycle in the Arctic Ocean*, R. Stein and R.W. Macdonald (eds.), Springer, Berlin, 24-32.

Stein, R., and MacDonald, R.W. 2004c. Organic carbon budget: Arctic Ocean vs. global ocean. In: *The Organic Carbon Cycle in the Arctic Ocean*, R. Stein and R.W. Macdonald (eds.), Springer, Berlin, 315-322.

Streletskaya, I.D., Vasiliev, A.A., and Vanstein, B.G., 2009. Erosion of sediment and organic carbon from the Kara Sea coast. *Arctic, Antarctic, and Alpine Research*, **41**: 79–87.

Stroeve,J., Holland, M.M., Meier, W., Scambos, T., and Serreze, M. 2007. Arctic sea ice decline: Faster than forecast. *Geophysical Research Letters*, **34**: L09501, doi: 10.1029/2007GL029703.

Swail, V.R., Cardone, V.J., Ferguson, M., Gummer, D.J., and Cox, A.T., 2007. *MSC Beaufort Sea Wind and Wave Reanalysis*, 10th International Wind and Wave Workshop, Oahu, Hawaii, 22 pp.

Tarnocai, C., 1998. The amount of organic carbon in various soil orders and ecological provinces in Canada. In: *Soil Processes and the Carbon Cycle*, R. Lal, J.M. Kimble, R.F. Follett and B.A. Stewart (eds). CRC Press, Boca Raton, FL, 81-92.

Tarnocai, C., Canadell, J. G., Schuur, E. A. G., Kuhry, P., Mazhitova, G., and Zimov, S., 2009. Soil organic carbon pools in the northern circumpolar permafrost region. *Global Biogeochemical Cycles*, **23:** GB2023, doi:10.1029/2008GB003327, 2009.

Tarnocai, C., J. Kimble and G. Broll. 2003. Determining carbon stocks in cryosols using the northern and mid latitudes soil database. Proceedings *8th International Conference on Permafrost*, Zurich, Switzerland, 1129–1134.

Tarnocai, C. and B. Lacelle, 1996. *The Soil Organic Carbon Digital Database of Canada*. Research Branch, Agriculture Canada, Ottawa, Canada.

Tarnocai, C., Ping, C.-L. and Kimble, J. , 2007. Carbon Cycles in the Permafrost Region of North America. In: *The First State of the Carbon Cycle Report (SOCCR): The North American Carbon Budget and Implications for the Global Carbon Cycle*, A.W. King, L. Dilling, G.P. Zimmerman, D.M. Fairman, R.A. Houghton, G. Marland, A.Z. Rose, and T.J. Wilbanks (eds.). National Oceanic and Atmospheric Administration, National Climatic Data Center, Asheville, NC, 127-138.

Taylor, R.B., and McCann, B., 1976. The effect of sea and nearshore ice on coastal processes in Canadian Arctic Archipelago. *Revue géographique de Montréal*, **30**: 123-132.

Teeri, J.A. and Stowe, L.G., 1976. Climatic pattern and the distribution of C_4 grasses in North America. *Oecologica*, **23**: 1-12.

Trenhaile, A.S., 1997. *Coastal Dynamics and Landforms*, Clarendon Press, Oxford, 366 pp.

Ulbrich, U., Leckebusch, G.C., and Pinto, J.G., 2009. Extra-tropical cyclones in the present and future climate: a review. *Theoretical and Applied Climatology,* **96**: 117–131, doi 10.1007/s00704-008-0083-8

van Everdingen, Robert, (ed.), 1998 revised May 2005. *Multi-language glossary of permafrost and related ground-ice terms*. Boulder, CO, National Snow and Ice Data Center/World Data Center for Glaciology.

Vetrov, A.A., and Romankevich, E.A. (eds.), 2004. *Carbon cycle in the Russian Arctic seas*. Springer, Berlin, 331 pp.

Walsh, J., 2008. Climate of the Arctic marine environment. *Ecological Applications*, **18**: Supplement, 3–S22.

Walsh, J.E., Anisimov, O., Hagen, J.O.M., Jakobsson, T., Oerlemans, J., Prowse,T.D., Romanovsky, V., Savelieva, N., Serreze, M., Shiklomanov, A., Shiklomanov, I., Solomon, S., Arendt, A., Atkinson, D., Demuth, M.N., Dowdeswell, J., Dyurgerov, M., Glazovsky, A., Koerner, R.M., Meier, M., Reeh, N., Sigurðsson, O., Steffen, K., and Truffer, M., 2005. Cryosphere and Hydrology. In: *Arctic Climate Impact Assessment*, C. Symon, L. Arris and B. Heal (Eds), Cambridge University Press, Cambridge, UK, 184-242.

Wang, M. and Overland, J.E., 2009. A sea ice free summer Arctic within 30 years? *Geophysical Research Letters*, **36**: L07502, doi:10.1029/2009GL037820

Weisse, R., von Storch, H., and Feser, F., 2005. Northeast Atlantic and North Sea storminess as simulated by a reigonal climate model during 1958-2001 and comparison with observations. *Journal of Climate*, **18**: 465-479.

Williams, P.J., and M.W. Smith. 1989. *The Frozen Earth: Fundamentals of Geocryology.* Cambridge, UK: Cambridge University Press, 306 pp.

Wolfe, S.A., Dallimore, S.R., Solomon, S.M., 1998. Coastal permafrost investigations along a rapidly eroding shoreline, Tuktoyaktuk, N.W.T. Proceedings of the *7th International Permafrost Conference*, Yellowknife, N.W.T., 1125-1131.

Wolfe, S.A., Kotler, E., Dallimore, S.R., 2001. Surficial characteristics and the distribution of thaw landforms (1970-1999), Shingle Point to Kay Point, Yukon Territory. Geological Survey of Canada Open File 4115, 18 pp.

Yunker, M.B., Macdonald, R.W., Cretney, W.J., Fowler, B.R., and McLaughlin, F.A., 1993. Alkane, terpene, and polycyclic aromatic hydrocarbon geochemistry of the Mackenzie River and Mackenzie shelf: Riverine contributions to Beaufort Sea coastal sediment. *Geochimica et Cosmochima Acta*, **57**: 3041-3061.

Yunker, M.B., Macdonald,R.W., Fowler, B. R., Cretney, W.J., Dallimore, S.R. and Mclaughlin, F.A., 1991. Geochemistry and fluxes of hydrocarbons to the Beaufort Sea shelf: A multivariate comparison of fluvial inputs and coastal erosion of peat using principal components analysis. *Geochimica et Cosmochimica Acta*, **55**: 255-213.

Yunker., M.B., McLaughlin, F.A., Fowler, B.R., Smyth, T.A., Cretney, W.J., Macdonald, R..W. and McCullough, D. 1990. NOGAP B6; Volume 7: *Hydrocarbon Determinations; Mackenzie River and Beaufort, Sea Shoreline Peat Samples*. Canadian Data Report of Hydrography and Ocean Sciences, **60**: 81 pp.

Zhang, T., Chen, W., Smith, S., Riseborough, D., and Cihlar, J., 2005. Soil temperature in Canada during the twentieth century: Complex responses to atmospheric climate change. *Journal of Geophysical Research*, **110**: D03112, doi: 10.1029/2004JD004910.

Zimov, S.A., Schuur, E.A.G., and F.S. Chapin III, 2006. Permafrost and the global carbon budget, *Science*, **312**: 1612 – 1613, doi:10.1126/ science.1128908.

APPENDICES

Appendix A - Definition of symbols used

Input variables

Symbol	Definition
A	total surface area of a terrain unit
AL	thickness of the active layer
D_1	thickness of the uppermost layer of soil
D_{BM}	depth to the bottom of massive ice
D_M	depth to the top of massive ice
D_W	depth of ice wedge
e	soil porosity
H_C	height of coastal segment
N_G	number of pingos
P_G	volumetric ice content of pingo ice
P_M	volumetric ice content of massive ice
P_{P1}	volumetric ice content due to pore ice and thin segregated lenses in layer 1
P_{P2}	volumetric ice content due to pore ice and thin segregated lenses in layer 2
P_W	volumetric ice content of wedge ice
R	mean pingo radius
W_S	mean ice wedge spacing
W_T	mean ice wedge width

Derived variables and volumes

Symbol	Description
D_2	thickness of the lower layer of soil
D_{W2}	height of ice wedge in layer 2
D_{WM1}	height of ice wedge from top of massive ice in layer 1
D_{WM2}	height of ice wedge from top of massive ice in layer 2
D_{WT}	depth of ice wedge above sea level
Lw	total length of ice wedge troughs
PEI	percentage of excess ice
PIV	percentage ice volume
TIV	total ice volume
V_G	volume of pingo ice
V_{M1}	volume occupied by massive ice in layer 1
V_{M2}	volume occupied by massive ice in layer 2
V_{MT}	total volume of massive ice
V_{P1}	volume of soil containing pore ice and thin segregated lenses in layer 1
V_{P2}	volume of soil containing pore ice and thin segregated lenses in layer 2
V_{T1}	total potential volume of frozen material in layer 1
V_{T2}	total potential volume of frozen material in layer 2
V_{WT}	total volume of ice wedges in a terrain unit

V_{W1}	volume of ice wedges in layer 1 of a terrain unit
V_{W2}	volume of ice wedges in layer 2 of a terrain unit
V_{WM1}	volume of ice wedges in massive ice in layer 1
V_{WM2}	volume of ice wedges in massive ice in layer 2
W_2	mean ice wedge width at the top of layer 2
W_{M1}	mean ice wedge width at the top of massive ice in layer 1
W_{M2}	mean ice wedge width at the top of massive ice in layer 2

Sources of input data for input variables

Segment name	Area (m^2)	AL (m)	D_1 (m)	e	D_{BM} (m)	D_M (m)	D_W (m)	H_C (m)	N_G	P_G	P_M (%)	P_{P1} (%)	P_{P2} (%)	P_W (%)	R	W_S (m)	W_T (m)
Avadlek Spit	944854	0.80	1.0	0.355	0	0	0	1.0	0	0	0.00	0.10	0.10	0	0	0	0
Catton Point	372942	0.80	1.4	0.355	0	0	0	1.4	0	0	0.00	0.10	0.10	0	0	0	0
Whale Cove	139247	0.80	1.0	0.355	0	0	0	1.0	0	0	0.00	0.10	0.10	0	0	0	0
Stokes Point	315723	0.80	1.9	0.355	0	0	0	1.9	0	0	0.00	0.10	0.10	0	0	0	0
Phillips Bay	675996	0.50	3.5	0.463	0	0	4.1	6.5	0	0	0.00	0.60	0.38	0.875	0	16.0	1.7
Kay Point spit	435240	0.80	0.9	0.355	0	0	0	0.9	0	0	0.00	0.10	0.10	0	0	0	0
Babbage River Delta	1456240	1.50	2.5	0.540	0	0	0	3.0	0	0	0.00	0.35	0.95	0	0	0	0
King Point lagoon	141715	0.80	1.0	0.355	0	0	0	1.0	0	0	0.00	0.10	0.10	0	0	0	0
King Point SE	352324	0.42	5.5	0.524	11.5	7.0	6.0	12.0	0	0	0.95	0.65	0.45	0.875	0	9.0	2.3
Running River	393573	1.00	1.0	0.461	0	0	4.1	23.3	0	0	0.00	0.50	0.40	0.875	0	18.0	1.7
Malcolm River fan	874547	1.00	1.0	0.520	0	0	4.1	1.0	0	0	0.00	0.59	0.40	0.875	0	14.5	1.7
Clarence Lagoon	220209	0.80	1.0	0.355	0	0	0	1.0	0	0	0.00	0.10	0.10	0	0	0	0
Clarence Lagoon W	628090	0.50	3.0	0.440	3.0	1.0	4.1	5.0	0	0	0.80	0.72	0.44	0.875	0	16.0	1.7
Malcolm River fan with barrier islands	3853500	1.00	1.0	0.330	0	0	4.1	1.0	0	0	0.00	0.40	0.40	0.875	0	18.0	1.7
Workboat Passage W	180421	0.34	2.0	0.371	0	0	6.0	5.0	0	0	0.00	0.79	0.37	0.875	0	7.5	2.0
Stokes Point W	288274	0.35	5.0	0.526	7.0	5.0	6.0	22.0	0	0	0.80	0.67	0.45	0.875	0	12.0	2.3
Roland Bay W	271282	0.50	5.0	0.515	5.0	3.0	6.0	19.0	0	0	0.80	0.67	0.45	0.875	0	12.0	2.3
Stokes Point SE	392833	0.28	4.0	0.447	0	0	4.1	10.0	0	0	0.00	0.84	0.40	0.875	0	8.0	1.7
Phillips Bay NW	254100	0.83	3.0	0.419	6.0	3.0	6.0	12.0	0	0	0.80	0.65	0.57	0.875	0	12.0	2.3
Kay Point	285887	0.50	1.0	0.404	0	0	6.0	7.0	0	0	0.00	0.50	0.35	0.875	0	12.0	2.3
Kay Point SE	2233460	0.37	6.1	0.413	12.0	10.0	6.0	30.0	0	0	0.80	0.50	0.30	0.875	0	12.0	2.3
King Point NW	292141	0.50	10.0	0.470	15.0	10.0	6.0	40.0	0	0	0.80	0.33	0.45	0.875	0	12.0	2.3
Komakuk Beach W2	791088	0.50	2.5	0.440	0	0	4.1	5.3	0	0	0.00	0.72	0.44	0.875	0	16.0	1.7
Komakuk Beach W1	160314	0.50	2.0	0.440	3.5	2.0	4.1	3.5	0	0	0.80	0.72	0.44	0.875	0	16.0	1.7
Komakuk Beach	1293380	0.39	2.5	0.440	0	0	4.1	3.5	0	0	0.00	0.72	0.44	0.875	0	16.0	1.7
Herschel Island W	594524	0.60	10.0	0.470	16.0	10.0	7.0	56.0	0	0	0.77	0.52	0.47	0.875	0	12.0	2.1
Herschel Island N	1645770	0.69	2.5	0.470	8.5	2.5	7.0	60.0	0	0	0.77	0.59	0.47	0.875	0	12.0	2.1
Herschel Island E	1053250	0.45	2.5	0.470	11.5	2.5	7.0	24.5	0	0	0.69	0.44	0.47	0.875	0	12.0	2.1
Workboat Passage E	1028160	0.38	0.6	0.366	0	0	6.0	3.0	0	0	0.00	0.40	0.35	0.875	0	12.0	2.3
Shingle Point W	897492	0.50	6.0	0.443	6.0	1.0	6.0	26.0	0	0	0.70	0.57	0.40	0.875	0	12.0	2.3
Shingle Point E	1241680	0.42	1.0	0.389	0	0	6.0	20.0	0	0	0.00	0.57	0.38	0.875	0	12.0	2.3
Roland Bay E	187568	0.35	10.0	0.513	0	0	4.1	15.0	0	0	0.00	0.59	0.45	0.875	0	16.0	1.7
Herschel Island S	1330580	0.50	5.5	0.412	0.0	0.0	7.0	5.5	0	0	0.00	0.65	0.65	0.875	0	12.0	2.1
Whale Cove E	82882	0.52	1.0	0.430	3.5	1.5	6.0	5.0	0	0	0.70	0.47	0.40	0.875	0	12.0	2.3
Roland Bay NW	270776	0.31	0.8	0.595	0	0	6.0	2.5	0	0	0.00	0.81	0.70	0.875	0	15.0	2.3
Phillips Bay W	445736	0.80	1.0	0.355	0	0	0	1.0	0	0	0.00	0.10	0.10	0	0	0	0
Nunaluk Spit	2625290	0.80	1.2	0.355	0	0	0	1.2	0	0	0.00	0.10	0.10	0	0	0	0
Clarence Lagoon E	99640	1.00	1.0	0.330	0	0	4.1	1.0	0	0	0.00	0.40	0.40	0.875	0	18.0	1.7
Simpson Point	311249	0.80	1.0	0.355	0	0	0	1.0	0	0	0.00	0.10	0.10	0	0	0	0
Whale Cove W	480986	0.32	1.5	0.470	0	0	6.0	1.5	0	0	0.00	0.71	0.40	0.875	0	20.0	2.3
Sabine Point E	235582	0.50	3.0	0.470	6.0	2.0	3.0	25.0	0	0	0.80	0.30	0.30	0.875	0	12.0	1.7
Sabine Point	247250	0.50	14.0	0.478	14.0	7.0	5.0	40.0	0	0	0.97	0.60	0.50	0.875	0	12.0	1.5
Sabine Point W	265431	0.50	3.0	0.470	0	0	3.0	25.0	0	0	0.00	0.30	0.30	0.875	0	12.0	1.7
King Point	94182	0.34	5.5	0.524	0	0	6.0	7.0	0	0	0.00	0.49	0.45	0.875	0	12.0	2.3

Calculated from GIS | This study | Forbes, 1997 | Forbes et al., 1995 | Gillie, 1987 | Harry et al., 1985 | Harry et al., 1988 | Lewis and Forbes, 1974

McDonald and Lewis, 1973 | Pollard, 1990 | Rampton, 1982 | Solomon et al, 1994/M.J. O'Connor and Associates 1986

Appendix B1 - Equations for all derived variables and volumes

[B1] Thickness of the lower layer of soil

$D_2 = H_C - D_1$

[B2] Check that height of ice wedges does not exceed cliff height

if $Dw + AL > Hc$ set $D_{WT} = Hc - AL$

[B3] Height of ice wedge in layer 2:

$D_{W2} = D_{WT} + AL - D_1$ set to 0 if < 0

[B4] Height of ice wedge from top of massive ice in layer 1:

$D_{WM1} = D_{WT} + AL - D_M$ set to 0 if $D_M = 0$
or $D_M > D_1$
or $D_M > D_{WT} + AL$

[B5] Height of ice wedge from top of massive ice in layer 2:

$D_{WM2} = D_{WT} + AL - D_1$ set to 0 if $D_M = 0$
or $D_{BM} <= D_1$
or $D_1 > D_{WT} + AL$
or $D_M > D_{WT} + AL$

but set to $D_{WM2} = D_{WT} + AL - D_M$ if $D_M > D_1$

[B6] Total potential volume of frozen material in layer 1:

$V_{T1} = (D_1 - AL)\ A$

[B7] Total potential volume of frozen material in layer 2:

$V_{T2} = D_2\ A$

[B8] Mean ice wedge width at the top of layer 2:

$W_2 = \frac{D_{W2}\ W_T}{D_{WT}}$ set to 0 if $D_{WT} = 0$

[B9] Mean ice wedge width at the top of massive ice in layer 1:

$W_{M1} = \frac{D_{WM1}\ W_T}{D_{WT}}$ set to 0 if $D_{WT} = 0$

[B10] Mean ice wedge width at the top of massive ice in layer 2:

$W_{M2} = \frac{D_{WM2}\ W_T}{D_{WT}}$ set to 0 if $D_{WT} = 0$

[B11] Total length of ice wedge troughs

$Lw = (A * 2) / Ws$ set to 0 if $W_S = 0$

[B12] Total volume of ice wedges in a terrain unit:

$V_{WT} = 0.5 \; W_T \, D_{WT} \, L_W$

[B13] Total volume of ice wedges in layer 2 of a terrain unit:

$V_{W2} = 0.5 \; W_2 \, D_{W2} \, L_W$

[B14] Total volume of ice wedges in layer 1 of a terrain unit:

$V_{W1} = V_{WT} - V_{W2}$

[B15] Volume of ice wedges in massive ice in layer 1:

$V_{WM1} = (0.5 \; W_{M1} \, D_{WM1} \, L_W) - V_{W2}$ set to 0 if $D_{WM1} = 0$

[B16] Volume of ice wedges in massive ice in layer 2:

$V_{WM2} = 0.5 \; W_{M2} \, D_{WM2} \, L_W$

[B17] Volume occupied by massive ice in layer 1:

$V_{M1} = [(D_1 - D_M) \; A] - V_{WM1}$ set to 0 if $D_M = 0$ or $D_M > D_1$

[B18] Volume occupied by massive ice in layer 2:

$V_{M2} = [(D_{BM} - D_M) \; A] - V_{WM2}$ set to 0 if $D_M = 0$ or $D_M < D_1$

[B19] Volume of soil containing pore ice and thin segregated lenses in layer 1:

$V_{P1} = V_{T1} - V_{W1} - V_{M1}$

[B20] Volume of soil containing pore ice and thin segregated lenses in layer 2:

$V_{P2} = V_{T2} - V_{W2} - V_{M2}$

[B21] Total volume of massive ice:

$V_{MT} = V_{M1} + V_{M2}$

[B22] Volume of pingo ice:

$$V_G = N_G \; 0.5 \left(\frac{4}{3} \pi R^3 \right)$$

[B23] Total ice volume:

$TIV = P_{P1} V_{P1} + P_{P2} V_{P2} + P_W V_{WT} + P_M V_{MT} + P_G V_G$

[B24] Percentage ice volume:

$$PIV = \frac{TIV}{V_{T1} + V_{T2} + (AL*A) + V_G}$$ set to 0 if denominator = 0

[B25] Percentage of excess ice:

$$PEI = \frac{PIV - [\,1.09e\,(1\text{-}PIV) / (1\text{-}e)\,]}{PIV - [\,1.09e\,(1\text{-}PIV) / (1\text{-}e)\,] + [\,(1\text{-}PIV) / (1\text{-}e)\,]}$$ set to 0 if < 0

Appendix B2 – R code for equations for all derived variables and volumes

```
#
# Nicole Couture
#
# This script derives variables for my ground ice model using
# a series of input variables, then write the derived variables to
# the same table that the inputs come from, but save it as a separate file
#
# September 24 2009
#

##################################################
# Parameters for this script
# In R Change Dir to where files are located

  setwd('g:/PhD/Data/GIS data/Work from Sept 2009')

  filename = paste("CBS_project_inputs", ".csv", sep="")

# read in the data...
# Here I'm creating a data frame called groundice
  groundice = read.table(filename, header=TRUE, sep=",", dec=".", na.strings="NA",
strip.white=TRUE)

###################################################
# DERIVED VARIABLES
###################################################

# D2  thickness of the lower layer of soil
# D2 = Hc - D1
  D2 = groundice$Hc - groundice$D1
  groundice = data.frame(groundice, D2)

# This is to ensure that if the height of ice wedges is greater than the cliff height, only the part of
the wedges above sea level is included in the calculations
Dwt = rep(NaN, length(groundice$AL))
  for (i in 1:length(groundice$AL)) {
        if (groundice$Dw[i] + groundice$AL[i] > groundice$Hc[i] )
   {Dwt[i] = groundice$Hc[i] - groundice$AL[i]}
  else
   {Dwt[i] = groundice$Dw[i]}
 } # end for loop
  groundice = data.frame(groundice, Dwt)
```

```
# Dw2           height of ice wedge in layer 2
# Dw2 = Dwt + AL - D1
# set to 0 if less than 0
  Dw2 = rep(NaN, length(groundice$AL))
  for (i in 1:length(groundice$AL)) {
          if (groundice$Dwt[i] + groundice$AL[i] - groundice$D1[i] >=0)
   {Dw2[i] = groundice$Dwt[i] + groundice$AL[i] - groundice$D1[i]}
  else
   {Dw2[i] = 0}
 } # end for loop
  groundice = data.frame(groundice, Dw2)


# Dwm1                height of ice wedge from top of massive ice in layer 1
# Dwm1 = Dwt + AL - Dm
# set to 0 if Dm = 0 or Dm > D1 or Dm > Dwt + AL
  Dwm1 = rep(NaN, length(groundice$AL))
  for (i in 1:length(groundice$AL)) {
          if (groundice$Dm[i] == 0 || groundice$Dm[i] > groundice$D1[i] || groundice$Dm[i] >
groundice$Dwt[i] + groundice$AL[i])
   {Dwm1[i] = 0}
  else
   {Dwm1[i] = groundice$Dwt[i] + groundice$AL[i] - groundice$Dm[i]}
  } # end for loop
  groundice = data.frame(groundice, Dwm1)


# Dwm2                height of ice wedge from top of massive ice in layer 2
# Dwm2 = Dwt + AL - D1
# set to 0 if Dm = 0 or Dbm <= D1 or D1 > (Dwt + AL) or Dm > (Dwt + AL)
# set to (Dwt + AL - Dm) if Dm > D1
  Dwm2 = rep(NaN, length(groundice$AL))
  for (i in 1:length(groundice$AL)) {
  if (groundice$Dm[i] == 0 || groundice$Dbm[i] <= groundice$D1[i] || groundice$D1[i] >
(groundice$Dwt[i] + groundice$AL[i]) || groundice$Dm[i] > (groundice$Dwt[i] +
groundice$AL[i]))
        {Dwm2[i] = 0} else
  if(groundice$Dm[i] > groundice$D1[i])
   {Dwm2[i] = groundice$Dwt[i] + groundice$AL[i] - groundice$Dm[i]}
  else
   {Dwm2[i] = groundice$Dwt[i] + groundice$AL[i] - groundice$D1[i]}

  } # end for loop
    groundice = data.frame(groundice, Dwm2)
```

```
# Vt1           total potential volume of frozen material in layer 1
# Vt1 = (D1  - AL) * A
  Vt1 = (groundice$D1  - groundice$AL) * groundice$A
  groundice = data.frame(groundice, Vt1)


# Vt2           total potential volume of frozen material in layer 2
# Vt2 = D2 * A
  Vt2 = groundice$D2 * groundice$A
  groundice = data.frame(groundice, Vt2)


# W2            mean ice wedge width at the top of layer 2
# W2  =   (Dw2 / Dwt) * Wt
# set to 0 if Dwt =0
  W2 = rep(NaN, length(groundice$AL))
  for (i in 1:length(groundice$AL)) {
          if (groundice$Dwt[i] == 0)
   {W2[i] = 0}
  else
   {W2[i] = (groundice$Dw2[i] / groundice$Dwt[i]) * groundice$Wt[i]}
 } # end for loop
  groundice = data.frame(groundice, W2)


# Wm1           mean ice wedge width at the top of massive ice in layer 1
# Wm1  = (Dwm1 / Dwt)  * Wt
# set to 0 if Dwt =0
  Wm1 = rep(NaN, length(groundice$AL))
  for (i in 1:length(groundice$AL)) {
          if (groundice$Dwt[i] == 0)
   {Wm1[i] = 0}
  else
   {Wm1[i] = (groundice$Dwm1[i] / groundice$Dwt[i])  * groundice$Wt[i]}
 } # end for loop
  groundice = data.frame(groundice, Wm1)


# Wm2           mean ice wedge width at the top of massive ice in layer 2
# Wm2  = (Dwm2 / Dwt) * Wt
# set to 0 if Dwt =0
  Wm2 = rep(NaN, length(groundice$AL))
  for (i in 1:length(groundice$AL)) {
          if (groundice$Dwt[i] == 0)
   {Wm2[i] = 0}
```

```
  else
   {Wm2[i] = (groundice$Dwm2[i] / groundice$Dwt[i]) * groundice$Wt[i]}
 } # end for loop
  groundice = data.frame(groundice, Wm2)


# Lw    total length of ice wedge troughs
# Lw  =  (A * 2) / Ws
# set to 0 if Ws =0
  Lw = rep(NaN, length(groundice$AL))
  for (i in 1:length(groundice$AL)) {
          if (groundice$Ws[i] == 0)
   {Lw[i] = 0}
  else
   {Lw[i] = (groundice$A[i] * 2) / groundice$Ws[i]}
 } # end for loop
groundice = data.frame(groundice, Lw)


# Vwt             total volume of ice wedges in a terrain unit
# Vwt  = 0.5 * Wt * Dwt * Lw
  Vwt  = 0.5 * groundice$Wt * groundice$Dwt * groundice$Lw
  groundice = data.frame(groundice, Vwt)


# Vw2                       volume of ice wedges in layer 2 of a terrain unit
# Vw2  = 0.5 * W2 * Dw2 * Lw
  Vw2  = 0.5 * groundice$W2 * groundice$Dw2 * groundice$Lw
  groundice = data.frame(groundice, Vw2)


# Vw1                       volume of ice wedges in layer 1 of a terrain unit
# Vw1 = Vwt - Vw2
  Vw1 = groundice$Vwt - groundice$Vw2
  groundice = data.frame(groundice, Vw1)


# Vwm1                      volume of ice wedges in massive ice in layer 1
# Vwm1  =  ( 0.5 * Wm1 * Dwm1 * Lw ) - Vw2
# set to 0 if Dwm1 = 0
  Vwm1 = rep(NaN, length(groundice$AL))
  for (i in 1:length(groundice$AL)) {
          if (groundice$Dwm1[i] == 0)
   {Vwm1[i]  = 0}
  else
```

```
  {Vwm1[i]   =    ( 0.5  *  groundice$Wm1[i]  *  groundice$Dwm1[i]  *  groundice$Lw[i]  )  -
groundice$Vw2[i]}
  } # end for loop
  groundice = data.frame(groundice, Vwm1)


# Vwm2                    volume of ice wedges in massive ice in layer 2
# Vwm2  =   0.5 * Wm2 * Dwm2 * Lw
  Vwm2  =   0.5 * groundice$Wm2 * groundice$Dwm2 * groundice$Lw
  groundice = data.frame(groundice, Vwm2)


# Vm1            volume occupied by massive ice in layer 1
# Vm1   =  ((D1 - Dm) * A) - Vwm1
# set to 0 if Dm = 0 or Dm > D1
  Vm1 = rep(NaN, length(groundice$AL))
  for (i in 1:length(groundice$AL)) {
          if (groundice$Dm[i] == 0 | groundice$Dm[i] > groundice$D1[i])
   {Vm1[i] = 0}
  else
   {Vm1[i]   =  ((groundice$D1[i] - groundice$Dm[i]) * groundice$A[i]) - groundice$Vwm1[i]}
  } # end for loop
  groundice = data.frame(groundice, Vm1)


# Vm2            volume occupied by massive ice in layer 2
# set to 0 if  Dm = 0  or Dm < D1
# set to Vm2 = ((Dbm - Dm) * A) - Vwm2      if Dm >= D1
   Vm2 = rep(NaN, length(groundice$AL))
  for (i in 1:length(groundice$AL)) {
          if (groundice$Dm[i] == 0 | groundice$Dm[i] < groundice$D1[i])
   {Vm2[i] = 0}
  else
   {Vm2[i] = ((groundice$Dbm[i] - groundice$Dm[i]) * groundice$A[i]) - groundice$Vwm2[i]}
  } # end for loop
  groundice = data.frame(groundice, Vm2)


# Vp1            volume of soil containing pore ice and thin segregated lenses in layer 1
# Vp1 = Vt1 - Vw1 - Vm1
  Vp1 = groundice$Vt1 - groundice$Vw1 - groundice$Vm1
  groundice = data.frame(groundice, Vp1)


# Vp2  volume of soil containing pore ice and thin segregated lenses in layer 2
# Vp2 = Vt2 - Vw2 - Vm2
```

```
  Vp2 = groundice$Vt2 - groundice$Vw2 - groundice$Vm2
  groundice = data.frame(groundice, Vp2)


# Vmt             total volume of massive ice
# Vmt = Vm1 + Vm2
  Vmt = groundice$Vm1 + groundice$Vm2
  groundice = data.frame(groundice, Vmt)


# Vg              volume of pingo ice
# Vg =  Ng * 0.5 * ((4/3) * pi * R^3)
  Vg =  groundice$Ng * 0.5 * ((4/3) * pi * groundice$R^3)
  groundice = data.frame(groundice, Vg)


# TIV             total ice volume
# TIV =  Pp1 * Vp1   +  Pp2 * Vp2  +  Pw * Vwt  + Pm * Vmt  + Pg * Vg
 TIV  =   groundice$Pp1  *  groundice$Vp1     +    groundice$Pp2  *  groundice$Vp2    +
groundice$Pw  *  groundice$Vwt   +  groundice$Pm  *  groundice$Vmt   +  groundice$Pg  *
groundice$Vg
  groundice = data.frame(groundice, TIV)


# PIV             percentage ice volume
# PIV  =          TIV / (Vt1 + Vt2 + AL*A + Vg)
# set to 0 if  Vt1 + Vt2 + AL*A + Vg = 0
  PIV = rep(NaN, length(groundice$AL))
  for (i in 1:length(groundice$AL)) {
        if  ((groundice$Vt1[i]  +  groundice$Vt2[i]  +  (groundice$AL[i]  *  groundice$A[i])  +
groundice$Vg[i]) == 0)
   {PIV[i] = 0}
  else
   {PIV[i]  =    groundice$TIV[i]  /  (groundice$Vt1[i]  +  groundice$Vt2[i]  +  (groundice$AL[i]  *
groundice$A[i]) + groundice$Vg[i])}
  } # end for loop
    groundice = data.frame(groundice, PIV)


# PEI             percentage of excess ice
# PEI =  (PIV - (1.09*e*(1-PIV))/(1-e)) / ((PIV - ((1.09*e*(1-PIV)) / (1-e)) + ((1-PIV) / (1-e)))
# set to 0 if  < 0
  PEI = rep(NaN, length(groundice$AL))
  for (i in 1:length(groundice$AL)) {
```

```
  if ((groundice$PIV[i] - (1.09*groundice$e[i]*(1-groundice$PIV[i]))/(1-groundice$e[i])) / (groundice$PIV[i] - ((1.09*groundice$e[i]*(1-groundice$PIV[i])) / (1-groundice$e[i])) + ((1-groundice$PIV[i]) / (1-groundice$e[i]))) <0)
   {  PEI[i] = 0}
   else
   {PEI[i] = (groundice$PIV[i] - (1.09*groundice$e[i]*(1-groundice$PIV[i]))/(1-groundice$e[i])) / ((groundice$PIV[i] - (1.09*groundice$e[i]*(1-groundice$PIV[i])) / (1-groundice$e[i])) + ((1-groundice$PIV[i]) / (1-groundice$e[i])))}
   } # end for loop
  groundice = data.frame(groundice, PEI)


##########################################################

# modify the dataframe by adding a new column
# groundice = data.frame(groundice, A, Dw2, ..., PIV, PEI)

# output data to a csv for safekeeping (and/or further processing)
  write.table(groundice, file = "CBS_project_derived_variables.csv", sep = ",", col.names = NA)

##########################################################
```

Appendix C - Possible scenarios of stratigraphic relationships between ground ice types and illustrative equations for total ground ice volume

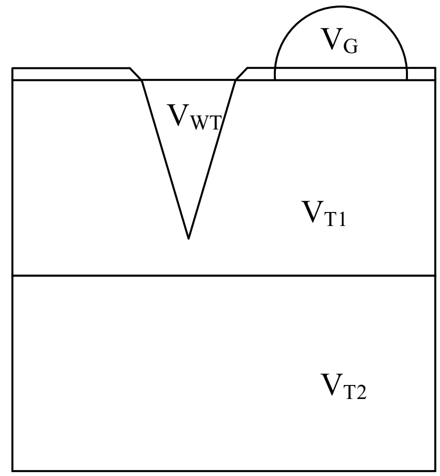

Case 1: Pore ice and thin lenses of segregated ice, plus ice wedges which do not penetrate into layer 2.

$$TIV = P_{P1}(V_{T1} - V_{WT}) + P_{P2}V_{T2} + P_W V_{WT} + P_G V_G$$

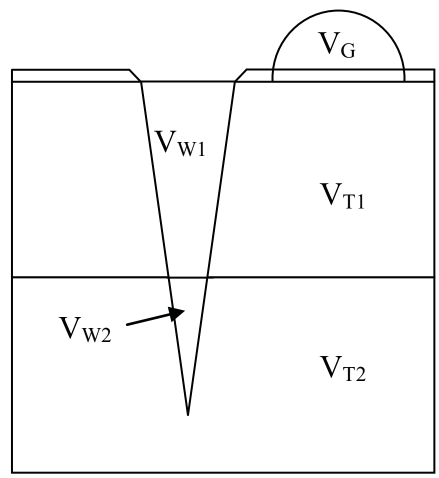

Case 2: Pore ice and thin lenses of segregated ice, plus ice wedges which penetrate into layer 2.

$$TIV = P_{P1}(V_{T1} - V_{W1}) + P_{P2}(V_{T2} - V_{W2}) + P_W V_{WT} + P_G V_G$$

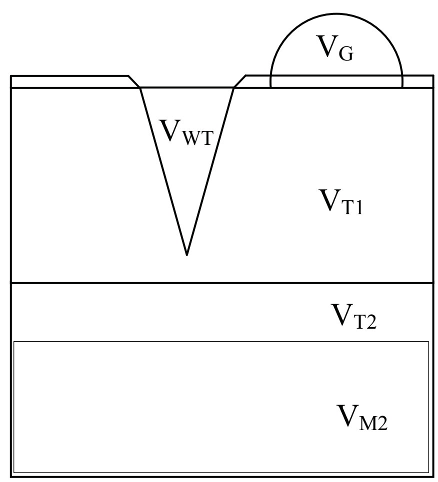

Case 3: Pore ice and thin lenses of segregated ice, plus massive ice in layer 2 only, plus ice wedges which do not penetrate into layer 2.

$$TIV = P_{P1}(V_{T1} - V_{WT}) + P_{P2}(V_{T2} - V_{M2}) + P_W V_{WT} + P_M V_{M2} + P_G V_G$$

Case 4: Pore ice and thin lenses of segregated ice, plus massive ice in layer 2 only, plus ice wedges which penetrate into layer 2, but not into the massive ice.

$$TIV = P_{P1}(V_{T1} - V_{W1}) + P_{P2}(V_{T2} - V_{W2} - V_{M2})$$

$$+ P_W V_{WT} + P_M V_{M2} + P_G V_G$$

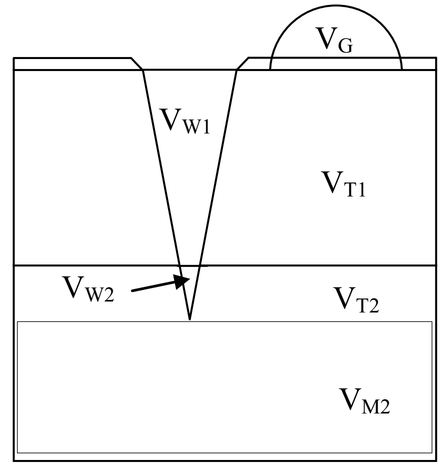

Case 5: Pore ice and thin lenses of segregated ice, plus massive ice in layers 1 and 2, plus ice wedges which do not penetrate into the massive ice.

$$TIV = P_{P1}(V_{T1} - V_{WT} - V_{M1}) + P_W V_{WT} + P_M (V_{M1} + V_{M2})$$

$$+ P_G V_G$$

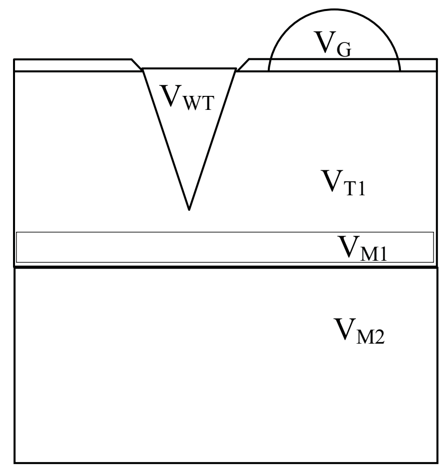

Case 6: Pore ice and thin lenses of segregated ice, plus massive ice in layers 1 and 2, plus ice wedges which penetrate into the massive ice.

$$TIV = P_{P1}(V_{T1} - V_{W1} - V_{M1}) + P_W V_{WT}$$

$$+ P_M (V_{M1} - V_{WM1} + V_{M2} - V_{W2}) + P_G V_G$$

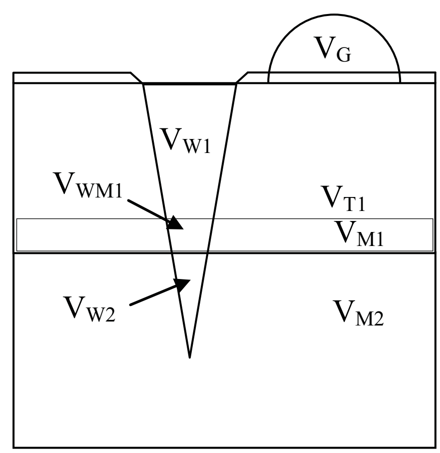

Modelling the erosion of ice-rich deposits along the Yukon Coastal Plain

Nicole J. Couture
Geography Department, McGill University, Montreal, Canada
Md. Azharul Hoque
Geography Departmen, McGill University, Montreal, Canada
Wayne H. Pollard
Geography Department, McGill University, Montreal, Canada

Abstract

The Yukon Coastal Plain is an area of ice-rich deposits along the Canadian Beaufort Sea and has been identified as highly vulnerable to the effects of sea-level rise and climate warming. Erosion is a function of the composition and morphology of coastal features, as well as wave energy. This paper outlines a simple model that considers these factors. Variations in ground ice contents and onshore and nearshore morphology are examined, as is their effect on the coastal dynamics of the region. Ice volumes are variable, ranging 52 to 61% by volume. A wave climate for the region is hindcast from historical climate records with offshore significant wave heights averaging between 0.32 and 0.45 m. Modelled wave energy shows that cross shore energy is up to 4 times greater than longshore. Net longshore sediment transport is westward at all sites although the magnitude varies. Potential erosion is appraised.

Keywords: Beaufort Sea; coastal erosion; erosion model; ground ice; wave climate; Yukon Coastal Plain.

Introduction

Climate changes in the Arctic will have profound impacts on the permafrost coastline of Canada's Beaufort Sea. In addition to warmer air and sea temperatures, changes are expected in several other primary environmental forcings on permafrost coastal systems such as relative sea level (RSL), storminess, and the duration and extent of the open water season. The Yukon Coastal Plain is considered to be in a submergent area (Forbes 1980), with current rates of RSL rise estimated to be approximately 3.5mm/a (Manson et al., 2002). These increases in sea level will be magnified by oceanic thermal expansion, which will contribute to the region's sensitivity to erosion (Shaw et al. 1998). Lambert (1995) suggested an increase in the frequency of storms under a warming climate and Solomon et al. (1994) have shown that there is a strong correlation between storm intensity and coastal erosion along the Beaufort Sea. The coast of the Beaufort Sea is micro-tidal with astronomical tide heights less than 0.5 m, so waves play a strong role in coastal change. This is particularly true during the open water season, when sea ice does not dampen wave development. Impacts of climate change along the Yukon Coastal Plain go beyond a physical response. The oil and gas industry are concerned about the effect of shoreline changes on infrastructure and exploration activities. Erosion and changes in the nearshore ecology also have the potential to directly affect local communities since hunting, fishing and trapping are economic and cultural mainstays for many aboriginal communities along the coast. Numerous historical and archeological sites in the region have already been destroyed by erosion and a number of others are threatened.

The goal of this paper is to outline a simple erosion model to predict how ice-rich coastlines along the Beaufort Sea will respond to changes in climate. A wave climate is generated based on historical climate data and is then used to calculate the wave energy available for erosion and sediment transport. The properties of the coastal bluffs are considered in determining spatial variability in erosion potential. The future susceptibility of the different coastline types is considered, based on predicted changes in environmental forcings for the region.

Study Area

Canada's Yukon Coastal Plain, located along the Beaufort Sea west of the Mackenzie Delta (Figure 1), is a lowland of dissected and hilly tundra about 250 km long and 10-30 km wide. Offshore, the continental shelf slopes gently to the shelf break located at about 80 m water depth (Hill et al., 1991). The shelf is relatively narrow, ranging from 40 km

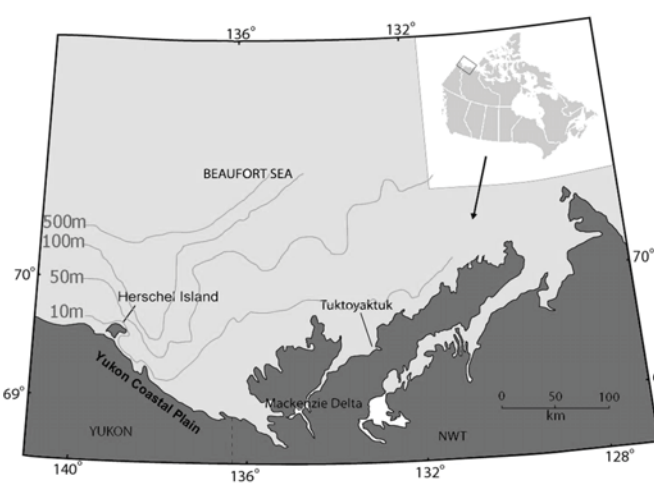

Figure 1. Location map showing the study region along Canada's Yukon Coastal Plain.

wide in the western area to over 150 km wide at the Mackenzie Delta. This region is classified as having a low arctic climate, with a mean annual temperature of –11°C and mean annual precipitation between 200 and 300 mm. The coastal plain is largely an erosion surface cut into Tertiary sandstone and shale. Most of it was covered by a lobe of the Laurentide ice sheet known as the Buckland Glaciation in the early Wisconsin, as well as by a later stillstand or re-advance known as the Sabine Phase. Surficial deposits reflect this history, with the coast east of Herschel Island being covered by glacial outwash plains and fans, moraines, and fine-grained lacustrine sediment. Moraines make up ice-pushed ridges, or else blanket rolling to hummocky topography likely resulting from thermokrast activity (Rampton, 1982). West of Herschel Island, the plain was unaffected by the Buckland Glaciation and is made up of coastal lagoons, coalesced deltas and alluvial fans (Rampton, 1982). Most of the flat or gently sloping landscape is covered by organic deposits and peat beds are common, particularly in lacustrine basins (Rampton, 1982). Beaches along the coast are generally narrow and are backed by coastal bluffs up to 90 m high. Permafrost along the Yukon coast is continuous and reaches depths of approximately 300 m (Smith and Burgess, 2000). The ice content of these soils is high due to the presence of pore ice and thin ice lenses, abundant ice wedges, and beds of massive ice. Subsea ice-bonded permafrost is present below the Beaufort Sea in water depths up to 100 m (Mackay, 1972, Dallimore et al., 1988, Dyke, 1991). Three sites along the coastal plain were selected for study: Komakuk Beach, King Point,and Shingle Point.

Methods

Coastal composition and morphology

The ground ice content of coastal soils governs the sediment content and influences the coast's susceptibility to erosion. To assess ice content along the Yukon Coastal Plain, a morphological model was developed based on a method first presented by Pollard and Couture (1999). The model calculates the total volume of ground ice for different terrain units along the coast by determining how much of each different type of ground ice is contained within that segment. Three types of ground ice are considered in the calculations: 1) pore ice and thin lenses of segregated ice, 2) wedge ice, and 3) beds of massive ice. As part of the Arctic Coastal Dynamics (ACD), a detailed segmentation of the Canadian Beaufort Sea coastline was conducted based on predominant landforms, surficial materials, permafrost conditions, and coastal processes. This initial segmentation was then refined using direct field observations, as well as data from Rampton (1982). Wolfe et al. (2001), and Harper et al. (1985). The percentage of ice content for each ice type of ground ice was first established, then the volume of each ice type in a terrain unit is determined. Finally, the percentages of ice content by volume for each terrain unit are calculated.

Wave hindcasting

Meteorological data was obtained from Environment Canada weather observing stations at Komakuk Beach and Shingle Point, and from a Campbell Scientific automatic weather station set up at King Point in 2004. Average hourly wind speed and direction were considered for the open water period for the years 2004-2006. The open water period is based on normals of median sea-ice concentration data from the Canadian Ice Service for the period 1971-2000. For the Yukon coast, ice concentrations fall below 5/10 during the last week of June, and open water lasts until the first week of October. Data from the King Point observing station was first adjusted to the10 m level. Wind speed measurements from the three overland stations were then converted to overwater values to account for differences in roughness between the two surfaces, using commonly used empirical coefficients (Resio and Vincent 1977, cited in Kamphuis). The wind data were then used to model deepwater waves, following the Jonswap method:

$$H_s = \frac{\lambda u^2}{g} \qquad (1)$$

H_s = significant wave height for a fully developed sea (m)
λ = dimensionless coefficient (approx. equal to 0.243)
u = wind speed (m/s)
g = gravitational acceleration (9.8 m/s^2)

In the above calculations, shoreline orientation at each site was accounted for, and only offshore winds were considered to be capable of wave generation; winds blowing from a landward direction were set to 0. The waves are not considered to be fetch-limited, so the values are for a fully developed sea.

Wave energy and material transport

As waves approach shore, the bottom of the wave begins to interact with the sea bed and shoaling begins. The wave is slowed, the wavelength becomes shorter, successive waves begin to pile up, and the height of the waves increase until they steepen to the point that they break on the shore. The energy they contain is thereby liberated to effect sediment transport and erosion. If a wave approaches the shore at an angle, the portion of the wave closer to shore will slow first, while the deeper portion remains unaffected. As a result, the wave is refracted, or bent, so that the wave crest more closely parallels the shore. Standard equations based on linear wave theory were used to converty the deepwater waves to nearshore ones and determine the height of the breaking wave. Wave energy was then calculated based on the following equation:

$$E = \frac{\rho g H_b^2}{8} \qquad (2)$$

where g is as noted above and
E = energy per area (N/m^2)
ρ = density of seawater (1025 kg/m^3)
H_b = breaking wave height

The energy term was separated into its component vectors to give longshore and crossshore values. Sediment transport in the longshore direction is given by the CERC expression (Kamphuis 2000):

$$Q = 330\, H_b^{5/2} \sin 2\,\alpha_b \qquad (3)$$

Q = volume of transported material (m^3/hr)
α_b = incident angle of breaking wave

Results

Wind data for the three-year period under consideration is shown in Figure 1. The coastal plain is narrowest in the west, and at Komakuk Beach, the close proximity of the British mountain likely contribute to channeling the winds in an east-west direction. Offshore waves were hindcast from these winds producing average significant wave heights ranging up to 0.45 m. Details of the significant wave heights for the three sites are given in Table 1.

Table 1. Modelled significant wave heights

Site	Average offshore height (m)	Maximum offshore height (m)	Average breaking height (m)	Maximum breaking height (m)
Komakuk	0.32	8.94	0.40	6.55
King Pt.	0.37	4.51	0.39	3.28
Shingle Pt	0.45	4.51	0.48	3.43

The breaking wave heights are used to generate a wave energy for each modeled wave, which is then broken down into a cross shore component (X) and a longshore one (Y) (Table 2). The proportion of energy going into each component is dependent on the incident angle of the nearshore wave which is, in turn, a factor of the original wind direction and the degree of wave refraction that occurs. This angle also governs which direction the longshore current will take (overall east or west, in the cases examined here). Net annual longshore energy is obtained by subtracting the total longshore in one direction from the total in the opposite direction. Using Equation 3, the potential net volume of sediment transported by the longshore wave energy can be calculated for the three-year period examined (Table 3). In order to assess how this potential sediment transport might affect coastal retreat at the study sites, the actual volume of material in the bluff needs to be considered. At Komakuk Beach, coastal bluffs are approximately 3 m high and consist of fine-grained lacustrine material. Ground ice comprises 61% by volume of the coastline. At King Point, cliffs up to 30 m high are made up of morainic material. The presence of beds of massive ice contribute to a very high ice content of 84%. At

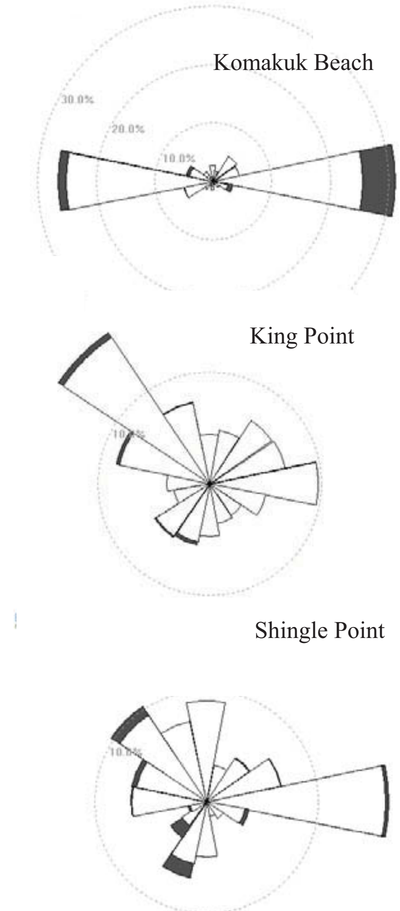

Figure 1. Wind roses showing frequency and magnitude of winds. Shaded areas indicate winds in excess of 37 km/hr.

Table 3.Modelled longshore sediment transport for 2004-06

Site	Q (m^3)
Komakuk	3.19×10^5 towards the west
King Pt.	0.54×10^5 towards the west
Shingle Pt	0.10×10^5 towards the west

Table 2. Cross shore (X) and longshore (Y) components of modeled wave energy

Site	Total X (N/m^2)	Total Y (N/m^2)	Eastward Y* (N/m^2)	Westward Y* (N/m^2)	Ratio X/Y
Komakuk	15.7×10^5	5.23×10^5	0.65×10^5	4.58×10^5	3.0
King Pt.	13.39	3.38×10^5	1.28×10^5	2.10×10^5	4.0
Shingle Pt.	15.97	4.45×10^5	2.22×10^5	2.23×10^5	3.6

* These represent only general direction of Y component. Actual movement of material is parallel to the shore at each site.

Shingle Point, the 10 m high bluffs are also morainic in origin, but their ice content is only 52%. Figure 2 provides an indication of how these values compare to other sites along the Yukon coast.

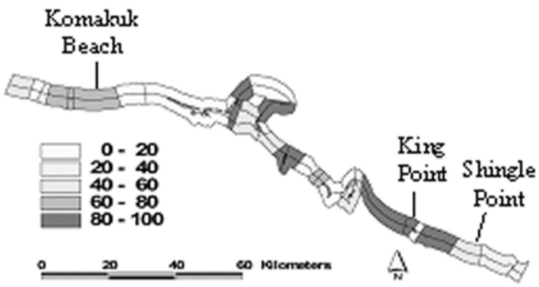

Figure 2. Ground ice volumes (by percentage) for different terrain units along the Yukon Coastal Plain

Based on cliff heights and the percentage of ice they contain, the volume of actual sediments per metre of coastline can be calculated. Because incoming waves affect a larger area, however, it is more realistic to consider a longer length of coastline so 10 m sections of coast have been selected for the purposes of this study. Table 4 shows the volume of sediments in 10 m sections that is potentially available for transport. Based on the modelled transport, an annual retreat rater is calculated.

Table 4. Volume of sediments and erosion rates for 10 m sections of coast

Site	Volume (m^3)	Modelled transport (m^3)	Annual transport (m^3)	Potential retreat (m/yr)
Komakuk	0.70 X 10^5	3.19 X 10^5	1.06 X 10^5	1.51
King Pt.	1.43 X 10^5	0.54 X 10^5	0.18 X 10^5	0.13
Shingle Pt	4.23 X 10^5	0.10 X 10^5	0.03 X 10^5	0

Discussion and Conclusions

This study examines nearshore wave energy generated through hindcasting. Previous studies have modeled potential erosion through wave climate analysis (Solomon et al. 1994, Hequette & Barnes 1990), but used offshore waves only so the results cannot be directly compared. Different techniques for nearshore wave transformation produce varying results (Pinchin & Nairn 1987) and the results of this study will need to be validated using measured nearshore waves. Previous work usually considers only storm winds and waves in their evaluation of erosion. We chose to examine all waves because several processes unique to Arctic coasts can provide material for erosion between storms. Figure 3 shows two types of failures along coastal bluffs – retrogressive thaw slumps and block failures -- that are common in ice-rich environments such as the Yukon Coastal Plain. In both cases, material is available close to the waterline and so is potentially subject to erosion by even moderate wave action.

The modelled results can be considered acceptable given that the annual erosion rates are of the same order of magnitude as measured rates for the region (e.g., Harper 1990, Solomon 2005). Improvements can be made by, however, by extending the length of the data set (preferably to at least 15 years), by validating the hindcast wave climate, and by incorporating grain size into the sediment transport equation since the one used for this study assumes that all transported material is sand. Fetch length was considered to be unlimited as soon as ice concentrations fell below 5/10, but its variability with time and direction should be part of future work. An examination of cross shore sediment transport is also planned. The model could be used to examine future erosion rates, but several factors would need to be considered including changes to sea ice extent.

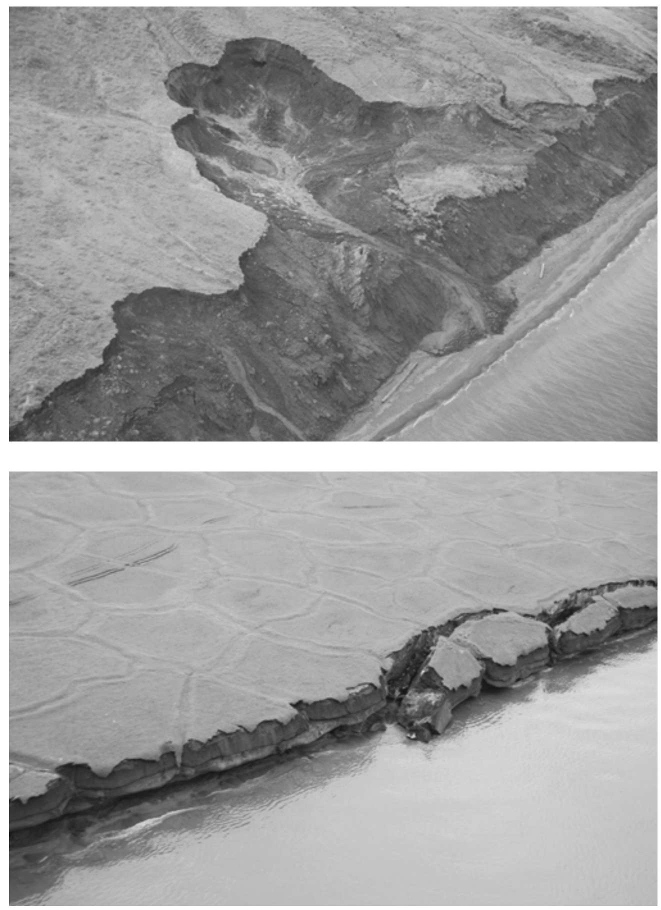

Figure 3. A retrogressive thaw slump near King Point and a block failure near Komakuk Beach.

Acknowledgments

Financial assistance was provided by ArcticNet NCE, the Natural Science and Engineering Research Council of Canada, and Fond québécois de la recherche sur la nature et les technologies. Fieldwork was made possible by the Polar Continental Shelf Project and the Northern Scientific Training Program. We would also like to thank the Alfred Wegener Institute for Polar and Marine Science (Potsdam), Herschel Island Territoral Park, Ivvavik National Park, the Aurora Research Institute, S. Solomon, H. Lantuit, G. DePascale, T. Haltigin, and D. Leitch.

References

Dallimore, S.R., Kurfurst, J.J. and Hunter, J.A.M. 1988. Geotechnical and geothermal conditions of near-shore sediments, southern Beaufort Sea, Northwest Territories, Canada. *Proceedings of 5th International Permafrost Conference*, Trondheim, Norway, 127-131.

Dyke, L.D. 1991. Temperature changes and thaw of permafrost adjacent to Richards Island, Mackenzie Delta, N.W.T. *Canadian Journal of Earth Sciences*, 28: 1834-1842.

Forbes, D.L., 1980. Late Quaternary sea level in the Beaufort Sea. *GSC Paper 80 (1B*), 75-87.

Harper, J.R. 1990. Morphology of the Canadian Beaufort Sea Coast. *Marine Geology*, 91, 75-91.

Harper, J.R., Reimer, P.D., and Collins, A.D., 1985. Canadian Beaufort Sea physical shore zone analysis. *Geological Survey of Canada Open File Report 1689*, 105 pp.

Héquette, A. and Barnes, P.W. 1990. Coastal retreat and shoreface profile variations in the Canadian Beaufort Sea. *Marine Geology,* **91**: 113-132.

Hill, P.R., Blasco, S.M., Harper, J.R. and Fissel, D.B. 1991. Sedimentation on the Canadian Beaufort Shelf. *Continental Shelf Research*, 11: 821-842.

Kamphuis, J.W., 2000. *Introduction to Coastal Engineering and Management*. Singpore: World Scientific Publishing, 437 pp.

Lambert, S.J., 1995. The effect of enhanced greenhouse warming on winter cyclone frequencies and strengths. *Journal of Climate*, 8: 1447-1452.

Mackay, J. R., 1972. The world of underground ice. *Annals of the American Association of Geographers*, 62: 1-22.

Manson, G.K., Solomon, S.M., and MacDonald, A., 2002. Describing Beaufort Sea coastal climate variability. *Reports on Polar and Marine Research*, 413: 31-33.

Pinchin, B.M. and Nairn, R.B. 1987. *Beaufort Sea coastal sediment study: evaluation of inshore wave climate and coastal sediment transport techniques at King Point, Yukon*. Keith Philpott Consulting Limited, Toronto, Ontario.

Pollard, W.H. and Couture, N.J., 1999. The use of morphological methods to estimate ground ice volumes along the Canadian Beaufort Sea coast. *Report for the Geological Survey of Canada (Atlantic)*, 30 pp.

Rampton, V.N., 1982. Quaternary Geology of the Yukon Coastal Plain. *Geological Survey of Canada Bulletin 317*. 49 pp.

Shaw, J., Taylor, R.B., Forbes, D.L., Ruz, M.-H. and Solomon, S. 1998. Sensitivity of the coasts of Canada to sea-level rise. *Geological Survey of Canada Bulletin 505*. 79 pp.

Smith, S., and Burgess, M., 2000. Ground temperature database for northern Canada. *Geological Survey of Canada Open File 3954*, 28 pp.

Solomon, S.M. 2005. Spatial and temporal variability of shoreline change in the Beaufort-Mackenzie region, Northwest Territories, Canada. *Geo-Marine Letters*, 25: 127-137.

Solomon, S.M., Forbes, D.L. and Keirstead, B. 1994. Coastal impacts of climate change: Beaufort Sea erosion study. *Geological Survey of Canada Open-File 2890.*Wolfe, S. A., Kotler, E., Dallimore, S. R., 2001. Surficial characteristics and the distribution of thaw landforms (1970-1999), Shingle Point to Kay Point, Yukon Territory. Geological Survey of Canada, *Open File 4115*, 18 pp.